DESIGN AND CHARACTERIZATION OF SALICYLIC ACID-BASED HYDROGELS FOR PROTEIN DELIVERY APPLICATIONS

By

BAHAR DEMIRDIREK

A dissertation submitted to the

Graduate School-New Brunswick

Rutgers, The State University of New Jersey

In partial fulfillment of the requirements

For the degree of

Doctor of Philosophy

Graduate Program in Chemistry & Chemical Biology

Written under the direction of

Dr. Kathryn E. Uhrich

And approved by

_____

_____

_____

_____

New Brunswick, New Jersey

January, 2016

ABSTRACT OF THE DISSERTATION

Design and characterization of salicylic acid-based hydrogels for protein delivery applications

by BAHAR DEMIRDIREK

Dissertation Director:

Kathryn E. Uhrich

Combination drug delivery has received much attention in the pharmaceutical industry to meet the need for increased efficacy and improved patient compliance. Hydrogels are cross-linked networks of hydrophilic polymers that resembles natural tissue and thus successfully developed for drug delivery applications. In three separate chapters, this dissertation describes novel salicylic acid-based hydrogel systems that concurrently deliver salicylic acid as well as the encapsulated protein. The hydrogels systems described herein are formed via physically and chemically cross-linking techniques.

First, salicylic acid-based poly(anhydride-esters) were physically cross-linked with poly(N-isopropylacrylamide-*co*-acrylic acid) via a solvent-casting technique to form injectable hydrogel systems. The physical interactions between these polymer systems were characterized by Fourier transform infrared spectroscopy. Bovine serum albumin, a representative protein, was successfully incorporated into the hydrogel systems. The

release profiles of both salicylic acid and bovine serum albumin were ascertained.

Second, salicylic acid-based poly(anhydride-esters) were physically cross-linked with poly(acrylic acid) to develop pH-sensitive hydrogels for oral protein delivery. These systems were characterized using spectroscopic techniques such as Fourier transform infrared spectroscopy. Insulin was incorporated into these systems, release of both insulin and salicylic acid was determined to be pH-dependent. The physical and chemical stability of insulin was characterized following release from the hydrogel system. In addition, these systems displayed mucoadhesive behavior which may further enable insulin bioavailability. The results suggest that these systems may be useful for oral administration of insulin and salicylic acid.

Third, salicylic acid was chemically incorporated into hydrogel systems via attachment of salicylic acid to an itaconate moiety followed by cross-linking using acrylic acid and poly(ethylene glycol)-diacrylate via UV. The structure, swelling behavior, pore structure, salicylic acid release, rheological, and mucoadhesion behavior of these hydrogels were studied. These hydrogels systems showed pH-responsive behavior: collapsing at acidic pH levels and leading to slower salicylic acid release, and swelling at higher pH conditions leading to salicylic acid release within 24 hours. Pore structure analysis showed a promising pore size for physically encapsulating of proteins.

In conclusion, these results suggested that these systems can potentially be used in combination delivery of proteins and salicylic acid.

DEDICATION

To my beautiful family.....

ACKNOWLEDGEMENTS

I would like to thank everyone who helped me during this journey.

I would like to specially thank Kathryn Uhrich for being a great mentor and offering her guidance. I would like to specially thank my committee members: Professors Larry Romsted, Deirdre O'Carroll, and Charlie Roth.

I would like to specially thank Holger Heumann for being there for me in every moment of this journey. I couldn't finish this dissertation without you. Thank you so much. I am a lucky woman to have you in my life, you are the best!!!!

Words are not enough to thank my beautiful, smart mom, Zeliha Demirdirek, I love you mom, thank you for everything.

Dad, Haluk Demirdirek, thank you for your support and being there for me all the time, love you....

My beautiful, smart sister, Basak Demirdirek, you are my sunshine... Thank you for being there no matter what. Love you.

I would like to thank Uhrich group members: Jonathan Faig, Nicholas Stebbins, Allison Faig, Weiling (Connie) Yu, Yingyue (Joanna) Zhang, Jennifer Chan, Alysha Moretti, Stephan Bien-Aime, Ruslan Guliyev, Dania Aguero Davie, and Ning Wang.

I would like to specially thank Bristol-Myers Squibb Company for providing funding for my tuition and would like to thank the following colleagues for being a good friend and for scientific discussions: Madhavi Srikoti, Elizabeth Galella, Scott Jennings, Pankaj Shah, John Fiske, Patricia Bercik, Judith Niederman, Elizabeth Borgeson, Megerle Escotet, Steve Pafiakis, Skylar Wolfe, Anuji Abraham, Duohai Pan, Regina Black, Eugene Guo, Sarah

Deleon, Dolapo Olusanmi, Vildan Kortan, Erinc Sahin, Aastha Puri, Mary Krause and Jade Trinh.

I would like to thank all my friends in USA, Turkey and all over Europe. Thank you for your calls and messages.

I do apologize if I missed anyone. I am grateful for everyone in my life. Thank you for your support.

TABLE OF CONTENTS

ABSTRACT OF THE DISSERTATION ii

DEDICATION iv

ACKNOWLEDGEMENTS v

TABLE OF CONTENTS vii

LIST OF FIGURES xiii

LIST OF SCHEMES xix

LIST OF TABLES xx

ABBREVIATIONS xxi

1. INTRODUCTION 1

1.1. Drug Administration Routes 1

1.2. Drug and Protein Delivery Systems 3

1.3. Hydrogels 6

1.3.1. Smart hydrogels 7

1.3.1.1. pH-sensitive hydrogels 8

1.3.1.2. Temperature-sensitive hydrogels 9

1.3.2. Hydrogels for drug/protein delivery 10

1.4. Polyanhydrides 11

1.4.1. Salicylic acid-based poly(anhydride-esters) 12

1.4.1.1. Salicylic acid 13

1.5. Diabetes 14

1.6. Research Projects 14

1.6.1. Physically cross-linked salicylic acid-based poly(*N*-isopropylacrylamide-*co*-acrylic acid) injectable hydrogels for protein delivery 15

1.6.2. Salicylic acid-based pH-sensitive hydrogels as potential oral insulin delivery systems 16

1.6.3. Novel salicylic acid-based chemically cross-linked pH sensitive hydrogels as potential drug delivery systems 18

1.7. References 19

2. PHYSICALLY CROSS-LINKED SALICYLIC ACID-BASED POLY(N-ISOPROPYLACRYLAMIDE-*CO*-ACRYLIC ACID) HYDROGELS FOR INJECTABLE PROTEIN DELIVERY 25

2.1. Introduction 25

2.2. Experimental Section 27

2.2.1. Materials 28

2.2.2. Hydrogel formation 28

2.2.3. Swelling behavior 29

2.2.4. Hydrogel morphology 30

2.2.5. *In vitro* SA release 30

2.2.6. BSA loading and release 31

2.2.7. Cytotoxicity of the hydrogels 32

2.2.8. LCST determination 32

2.3. Results and Discussion 33

2.3.1. Hydrogel formation 33

2.3.2. Swelling behavior 36

2.3.3. Hydrogel morphology 37

2.3.4. *In vitro* SA release 39

2.3.5. BSA loading and release 40

2.3.6. Cytotoxicity of the hydrogels 42

2.3.7. LCST determination 43

2.4. Conclusion 44

2.5. References 45

3. SALICYLIC ACID-BASED pH-SENSITIVE HYDROGELS AS POTENTIAL ORAL INSULIN DELIVERY SYSTEMS 48

3.1. Introduction 48

3.2. Experimental Section 50

3.2.1. Materials 50

3.2.2. Hydrogel formation 51

3.2.3. Swelling behavior 52

3.2.4. Hydrogel morphology 53

3.2.5. Insulin loading 53

3.2.6. Insulin release 54

3.2.7. Insulin stability 54

3.2.8. *In vitro* SA release 55

3.2.9. Cytotoxicity of the hydrogels 56

3.2.10. Mucoadhesion behavior 57

3.3. Results and Discussion 57

3.3.1. Hydrogel formation 57

3.3.2. Swelling behavior 61

3.3.3. Hydrogel morphology 63

3.3.4. Insulin loading 65

3.3.5. Insulin release 66

3.3.6. Insulin stability 68

3.3.7. *In vitro* SA release 70

3.3.8. Cytotoxicity of the hydrogels 72

3.3.9. Mucoadhesion behavior 73

3.4. Conclusion 74

3.5. References 75

4. NOVEL SALICYLIC ACID-BASED CHEMICALLY CROSS-LINKED pH SENSITIVE HYDROGELS AS POTENTIAL DRUG DELIVERY SYSTEMS 79

4.1. Introduction 79

4.2. Experimental Section 80

4.2.1. Materials 80

4.2.2. Synthesis of hydrogels 81

4.2.2.1. Physicochemical characterization 81

4.2.2.2. Salicylic acid-based monomer synthesis 82

4.2.2.3. Hydrogel synthesis 82

4.2.3. Swelling behavior 85

4.2.4. Hydrogel morphology 85

4.2.5. *In vitro* SA release 86

4.2.6. Rheometry 86

4.2.7. Mucoadhesion behavior 87

4.2.8. Cytotoxicity of the hydrogels 88

4.3. Results and Discussion 88

4.3.1. Salicylic acid-based monomer and hydrogel synthesis 89

4.3.2. Swelling behavior 90

4.3.3. Hydrogel morphology 92

4.3.4. *In vitro* SA release 94

4.3.5. Rheology behavior 96

4.3.6. Mucoadhesion behavior 98

4.3.7. Cytotoxicity of hydrogels 98

4.4. Conclusion 99

4.5. References 100

5. FUTURE WORK 105

5.1. References 110

6. APPENDIX 1: CYTOCOMPATIBILITY STUDIES OF KOJIC ACID-BASED POLY(ANHYDRIDE-ESTERS) 112

6.1. Introduction 112

6.2. Cytotoxicity: Method 113

6.3. Cytotoxicity: Results 113

6.4. References 114

7. APPENDIX 2: PHYSICALLY CROSSLINKED SALICYLIC ACID-BASED POLY(*N*-ISOPROPYLACRYLAMIDE-*CO*-ACRYLIC ACID) HYDROGELS INJECTABILITY 115

7.1. Method and Results 115

8. COPYRIGHT PERMISSION 116

LIST OF FIGURES

Figure 1.1: Diagram of various drug administration routes 2

Figure 1.2: Drug concentration in (A) immediate release formulation and (B) extended release formulation.....4

Figure 1.3: Illustration of a (A) physically cross-linked and (B) chemically cross-linked hydrogel structure 7

Figure 1.4: pH-dependent ionization, poly(acrylic acid) and poly(*N,N*'-diethylaminoethyl methacrylate) 8

Figure 1.5: The most commonly used temperature-sensitive polymers: Poly(*N*-isopropylacrylamide), poly(*N,N'*-diethylacrylamide and poly(*N*-isopropylacrylamide-*co*-butyl methacrylate) 10

Figure 1.6: Synthesis of SAPAE with alternate linkers 13

Figure 1.7: PNIPAM-*co*-AA:SAPAE hydrogel systems (A) at room temperature (RT) (hydrogels are solubilized throughout the water) and (B) at 37 °C in D.I. water (hydrogels are separated from the water).....16

Figure 1.8: PAA: SAPAE hydrogel systems: (A) dry PAA:SAPAE hydrogel (B) in 0.1N HCl (pH 1.2) over 24-hour at 37°C (C) in phosphate buffer (pH 6.8) over 24-hour at 37°C..... 18

Figure 2.1: Chemical structures of (A) SAPAEs and its degradation products (salicylic acid and adipic acid), and (B) poly(*N*-isopropylacrylamide-*co*-acrylic acid).....27

Figure 2.2: Experimental values of PN:SAPAEs blends glass transition temperatures as compared to Fox equation (Equation 2.1) values as a function of PNIPAM-*co*-AA weight fraction..... 35

Figure 2.3: FT-IR spectrum of blends comparing the carbonyl and amine group region of SAPAE (green line), PNIPAM-*co*-AA (blue line) and PN:SAPAE hydrogel (red line). The peak shifting of the carbonyl (~1700 cm^{-1}) and amine groups (~1520 cm^{-1}) in FT-IR spectroscopy suggests interaction between PNIPAM-*co*-AA and SAPAE. The hydrogel spectrum at the top is the 7:3 ratio, which is also representative of the 6:4 hydrogel system..... 35

Figure 2.4: Swelling values (Q) in pH 7.4 buffer at room temperature (RT) (25 °C) and 37 °C at 2 and 24 hours for two ratios of PN:SAPAE hydrogels according to Equation 2.2. Data are presented as mean ± standard deviation (n=3 in each group). 37

Figure 2.5: SEM images of freeze-dried PN:SAPAE hydrogels at two different blending ratios (7:3 ratio at top, 6:4 ratio at bottom) at the 24-hour swelling time point. Films are shown at 150x (left) and 500x (right) magnification. 38

Figure 2.6: *In vitro* release of salicylic acid from the PN:SAPAE hydrogels represented as normalized cumulative SA release as a percentage (A) and cumulative SA amount in mg (B) in pH 7.4, as quantified by UV-Vis spectrophotometry (λ= 303 nm). Data are presented as mean ± standard deviation (n=3 in each group). 40

Figure 2.7: BSA loading of the PN:SAPAE hydrogels via swelling-diffusion technique, as determined by BCA assay. Data are presented as mean ± standard deviation (n=3 in each group) 41

Figure 2.8: *In vitro* release of BSA from the PN:SAPAE hydrogels represented as normalized cumulative BSA release as a percentage, in pH 7.4 phosphate buffer at 37 °C as determined by BCA assay. Data are presented as mean ± standard deviation (n=3 in each group). 42

Figure 2.9: Cytotoxicity profile of the different concentrations of the hydrogels after 24-, 48-, and 72-hour incubation. All groups contained 1% DMSO in cell media and the control group has no polymer. Absorbance at 490 nm after MTS treatment is proportional to cell viability. Data are presented as mean ± standard deviation (n=6 in each group). The cell viability of each of the hydrogels was not statistically different from the media with DMSO control. 43

Figure 3.1: Chemical structures of (A) SAPAEs and its degradation products (salicylic acid and adipic acid), and (B) poly(acrylic acid), (PAA) 50

Figure 3.2: (A) FT-IR spectrum of blends comparing the carbonyl region of SAPAE (blue line), PAA (green line), and PAA:SAPAE hydrogel (red line). The peak shifting of the carbonyl groups (~1700 cm-1) in FT-IR spectroscopy suggests the interaction between PAA and SAPAE. (B) FT-IR spectrum of the -OH region of the PAA:SAPAE hydrogel. The labeled peak suggests the H-bonding 59

Figure 3.3: Experimental values of PAA and SAPAEs blends glass transition temperatures as compared to the Fox equation (Equation 3.1) values as a function of PAA weight fraction. 61

Figure 3.4: Swelling values (Q values) as a function of pH: (A) pH 1.2 and (B) pH 6.8 for three ratios of PAA:SAPAE hydrogels according to Equation 3.2. Data are presented as mean ± standard deviation (n=3 in each group). 62

Figure 3.5: SEM images of freeze-dried PAA:SAPAE hydrogels at three different blending ratios (7:3, 6:4, 5:5) at the 24 hour swelling time point in deionized water. Films are shown at 150x (left) and 500x (right) magnification. 64

Figure 3.6: Insulin loading of the PAA:SAPAE hydrogels via swelling-diffusion technique for 5 hours as determined by BCA assay. Data are presented as mean ± standard deviation (n=3 in each group). 66

Figure 3.7: *In vitro* release of insulin from the PAA:SAPAE hydrogels as a function of pH: (A) pH 1.2 and (B) pH 6.8, represented as normalized cumulative insulin release as a percentage as determined by UV spectrophotometry. Data are presented as mean ± standard deviation (n=3 in each group). 67

Figure 3.8: 24-hour release samples analysis to evaluate (A) physical stability using SEC chromatography to calculate aggregation (HMW species) and (B) chemical stability using iCIEF to calculate deamidated species. 69

Figure 3.9: *In vitro* release of SA from the PAA:SAPAE hydrogels as a function of pH: (A) pH 1.2 and (B) pH 6.8, represented as normalized cumulative SA release as a percentage as determined by BCA assay. Data are presented as mean ± standard deviation (n=3 in each group). 71

Figure 3.10: Cytotoxicity profile of the different concentrations of the hydrogels after 24-, 48-, and 72-hour incubation. All groups contained 1% DMSO in cell media and the control group has no polymer. Absorbance at 490 nm after MTS treatment is proportional to cell viability. The cell viability of each of these hydrogels was not statistically different from the media with DMSO control. 72

Figure 4.1: FT-IR spectrum of (A) SAm (blue line) and (B) hydrogel system (red line) represented as examples. Key IR bands are labeled on each spectrum. The spectrum at the top is hydrogel 2 (high cross-linked) and is representative of both hydrogel systems. 90

Figure 4.2: Swelling values (Q) values in pH 1.2 and pH 7.4 at 1h and 24h time points according to Equation 4.1 for hydrogel 1 (low cross-linked) and hydrogel 2 (high cross-linked). Data are presented as mean ± standard deviation (n=3 in each group). 91

Figure 4.3: SEM images of hydrogel 1 (low cross-linked) and hydrogel 2 (high cross-linked). Hydrogels were swollen in pH 7.4 phosphate buffer for 24 hours at room temperature, and then freeze-dried for 12 hours prior to SEM imaging. Films are shown at 500x magnification. 93

Figure 4.4: *In vitro* release of salicylic acid (SA) from hydrogel 1 (low cross-linked) and hydrogel 2 (high cross-linked) in (A) pH 1.2 and (B) pH 7.4. (C) shows hydrogel degradation into salicylic acid. The inset graph is SA HPLC chromatogram after the hydrolysis. Data are presented as mean ± standard deviation (n=3 in each group).....94

Figure 4.5: Rheological behavior of hydrogel 1 (low cross-linked) and hydrogel 2 (high cross-linked), comparing hydrogels storage modulus, G', in (A) as a function of time at 1 Hz frequency and 1 Pa stress in (B) as a function of frequency at 1 Pa stress. 97

Figure 4.6: Cytotoxicity profile of the different concentrations of the hydrogels after a 24-hour incubation period. Absorbance at 490 nm after MTS treatment is proportional to cell viability. Data are presented as mean ± standard deviation (n=6 in each group). The cell viability of the hydrogels were not statistically different from the media controls. ...99

Figure 6.1: Kojic acid-based poly(anhydride-esters) 112

Figure 6.2: Cytotoxicity profile of the different concentrations of the hydrogels after 24 h, 48 h and 72 h incubation. Absorbance at 490 nm after MTS treatment is proportional to cell viability. Data presented as mean ± standard deviation, n=6 in each group.....114

LIST OF SCHEMES

Scheme 4.1: Synthesis of salicylic acid-based monomer (SAm) and hydrogel. Hydrogels were cross-linked with varying amounts of crosslinker (PEGDA). 84

Scheme 5.1: Suggested synthesis scheme of chemically cross-linked extended SA release hydrogel system. 107

Scheme 5.2: Suggested synthesis scheme of chemically cross-linked temperature-sensitive hydrogel system. 108

LIST OF TABLES

Table 2.1: Summary of the relevant FT-IR peaks of the SAPAE, PNIPAM-*co*-AA, and PN:SAPAE hydrogel systems.....36

Table 3.1: Mucoadhesion performance of PAA:SAPAE films 74

ABBREVIATIONS

% percent
° degrees
°C degrees Celcius
± plus or minus
~ approximately
λ wavelength
μg microgram
μL microliter
^{1}H NMR proton nuclear magnetic resonance
ACN acetonitrile
C=O carbonyl
$CHCl_3$ chloroform
cm^{-1} wavenumber
DMF dimethylformamide
DI deionized
DMSO dimethyl sulfoxide
DSC differential scanning calorimetry
FDA US Food and Drug Administration
FT-IR fourier transform infrared
g gram
GI gastrointestinal
HCl hydrochloric acid
H_2O water
HPLC high performance liquid chromatography
iCIEF imaged capillary isoelectric focusing
LCST lower critical solution temperature
MeOH methanol
mg milligram
mL milliliter
mM millimolar
MTS 3-(4,5-dimethylthiazol-2-yl)-5-(3-carboxymethoxyphenyl)-2-(4-sulfophenyl)-2H-tetrazolium
Mw weight-averaged molecular weight
MW molar mass
N normal
N_2 nitrogen
NaOH sodium hydroxide
NMT Not more than
PAA poly(acrylic acid)
PAE poly(anhydride-ester)
PBS phosphate buffered saline
PDI polydispersity index
PEGDA poly(ethylene glycol) diacrylate
PLGA poly(lactic-*co*-glycolic acid)

PN PNIPAM-*co*-AA
RT room temperature
SA salicylic acid
SAm Salicylic acid-based monomer
SAPAE Salicylic acid-based poly(anhydride-esters)
SEC size exclusion chromatography
SEM scanning electron microscopy
TFA trifluoroacetic acid
T_g glass transition temperature
THF tetrahydrofuran
USP United States pharmacopeia

1. INTRODUCTION

The pharmaceutical industry has been developing and using drug delivery systems to increase drug bioactivity and improve patient comfort. Drug delivery systems based on polymers have shown improved active compound solubility, bioavailability, and extended delivery to reduce the number of doses required. Many polymer-based drug delivery products have been approved by FDA, are commercially available, and can administer drugs to various *in vivo* sites.[1, 2]

1.1. Drug Administration Routes

Drugs can be introduced into the body by several routes. **Figure 1.1** displays the possible administration routes: Drugs can be taken by mouth, given by injection, sprayed through the nasal cavity, inserted into the rectum or vagina, applied to the skin, or dispersed into the eye. The administration route is chosen depending on the diseased area, active compound stability, dose requirement, and bioavailability. Each route has its own advantages and disadvantages, with oral and injection administration as the most common routes.

Oral administration is the most common drug route as it is the cheapest, safest, and most patient-friendly. Orally administrated drugs migrate through the gastrointestinal (GI) tract, such that absorption may begin in the mouth, followed by the stomach, and then in the intestine, where most of the absorption occurs. Overall, the drug passes through the

mouth, stomach, and intestine before transferring to the liver via the portal vein, having been absorbed and transported to the target site through the bloodstream.[3] Other administration routes are used when a drug has poor absorption in GI tract and a high concentration of the drug must be administrated rapidly.

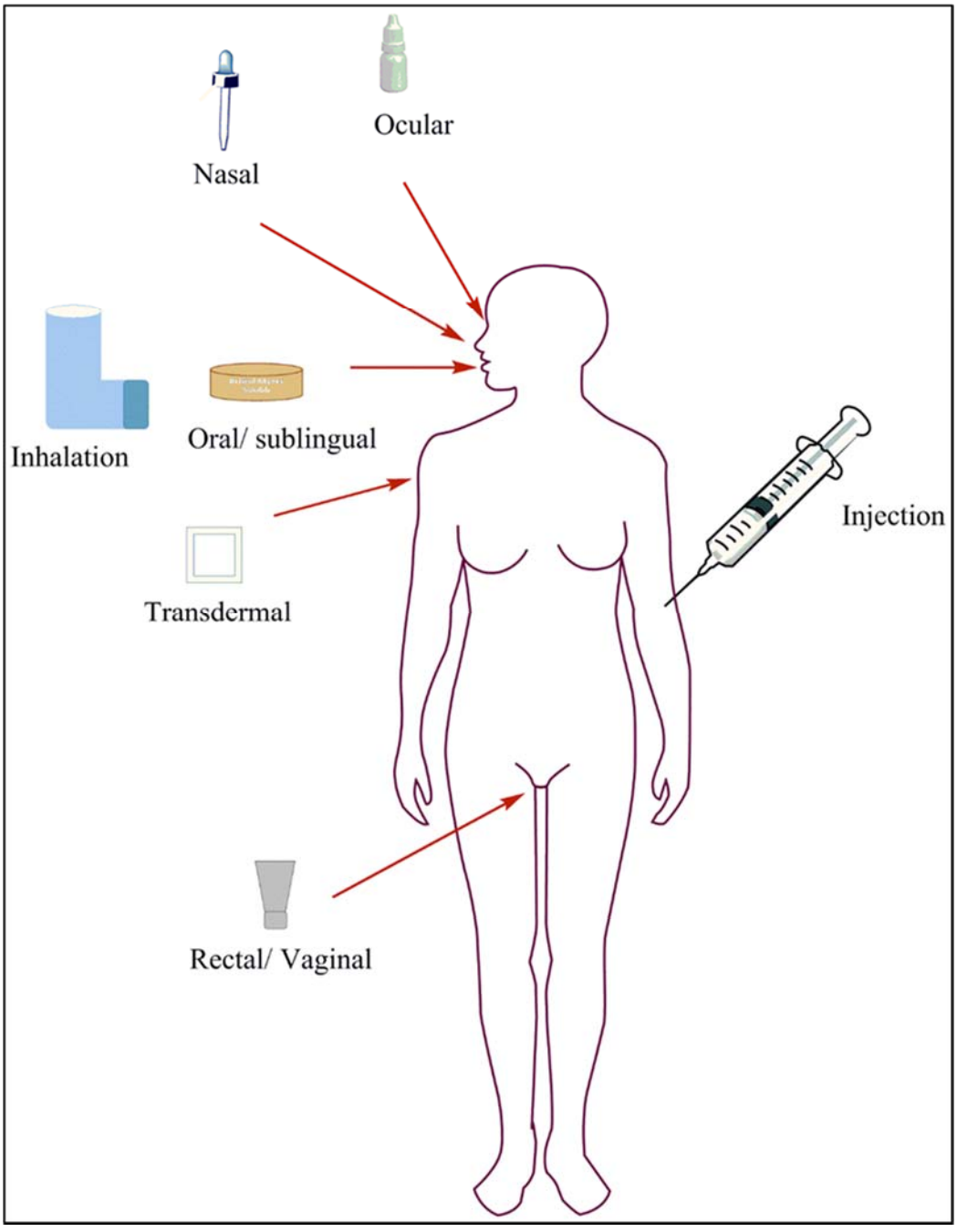

Figure 1.1: Diagram of various drug administration routes

Injection is the second most common route and is used if the drug cannot be delivered orally or if a high and rapid dose of the drug needs to be administered. There are several different types of injections: subcutaneous, intramuscular, intravenous, transdermal, and implantation. The injection route is chosen depending on the required dose and disease area. Although the injection route must be used for high concentration and rapid dosages, it is less preferred by patients as it is more painful.

1.2. Drug and Protein Delivery Systems

Drug and protein delivery systems are being developed as extended controlled release systems to increase the therapeutic level of the active compounds and overcome the poor solubility of the active compound. In immediate release systems, the active compound blood concentration spikes and falls with each administration, requiring multiple administrations (**Figure 1.2A)**. In extended release systems, drug concentration can be maintained within the therapeutic window (**Fig 1.2B**). Typically, three types of extended delivery systems for proteins have been studied: liposomes, microspheres and hydrogels.[4-6]

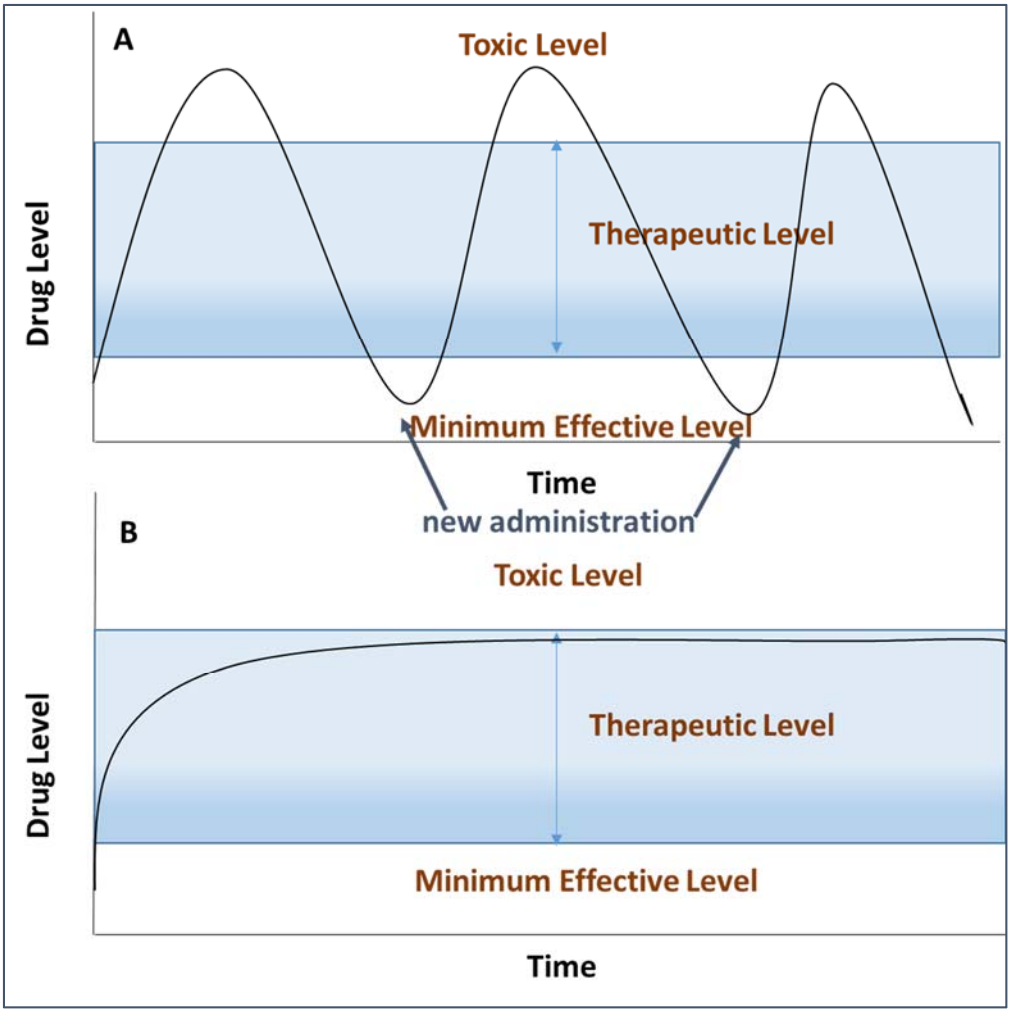

Figure 1.2: Drug concentration in (A) immediate release formulation and (B) extended release formulation

Liposomes, lipid-based delivery systems, have been heavily investigated and have proved successful in clinical studies for site-specific drug delivery applications.[1] Many liposome-based drug delivery systems are approved by the FDA[7, 8] for small molecules and have been researched for protein delivery. These systems protect proteins from denaturation and enable their extended release via diffusion and liposome disintegration.[9, 10] However, these systems need further development as the controlled protein release has

not been effectively achieved and an opsonization, liposomes clearance, needs improvement.[11]

Microspheres are small spherical particles prepared from synthetic or natural polymers. They have been studied for drug/protein delivery applications because of their ability to produce extended release profiles via diffusion.[12] Natural and synthetic polymeric systems have been evaluated as the matrix material, with poly(lactic-*co*-glycolic acid) (PLGA) being the most common, and have already received FDA approval for small molecule delivery.[13,14] However, PLGA still need improvement for protein delivery applications, it denaturates during polymer hydrolysis, which causes an acidic microenvironment.[15-17] In addition, PLGA microspheres have shown burst and incomplete release profiles.[16, 18]

The last category for drug/protein delivery are hydrogels that are used because of they can protect drug and protein structures during the encapsulation process and because protein encapsulation can be performed at low temperatures and in aqueous environments.[6] They will be discussed in more detail in **Section 1.3.** below. Diffusion is the main drug release mechanism in hydrogel systems. When the hydrogel is in aqueous media, water penetrates into the cross-linked system, which causes the network to swell and leads to drug solubilization and diffusion from hydrogel pores. The drug release rate of the hydrogel systems can easily be adjusted via cross-linked ratio.[6] Furthermore, stimuli-responsive hydrogel systems, which have been developed to deliver active compounds to different sites of the body, see **Section 1.3.2.**, have shown promising *in vivo* results compared to other stimuli-responsive systems.[4, 6]

1.3. Hydrogels

Hydrogels are cross-linked networks of hydrophilic polymers capable of retaining water and/or biological fluids. These networks were discovered in the early 1950s for soft contact lenses.[19] Since then, many hydrogels have been developed for a variety of biomedical applications including drug/protein delivery, tissue engineering, contact lenses, and stent coatings.[6,20] In this dissertation, hydrogels from biocompatible and/or biodegradable polymers are the focus of drug/protein delivery.

The cross-linked networks are achieved either through temporary physical cross-linking or through permanent chemical cross-linking methods, as shown in **Figure 1.3**. Physically cross-linked gels can be developed via non-covalent interactions, ionic interactions, hydrogen-bonding, and/or hydrophobic interactions. Chemically cross-linked systems are permanent covalent bonds between polymer chains. For example, these networks can be synthesized by radical polymerization, click chemistry, or Michael addition. Chemically cross-linked hydrogels systems are, in general, mechanically stronger than the physically cross-linked hydrogel systems, as they form permanent and irreversible covalent bonds.[21,22] Physical and chemical properties of the hydrogel systems can be changed by altering the polymer type, crosslink density (i.e., concentration of polymer to cross-linking agent), and solvent amount.

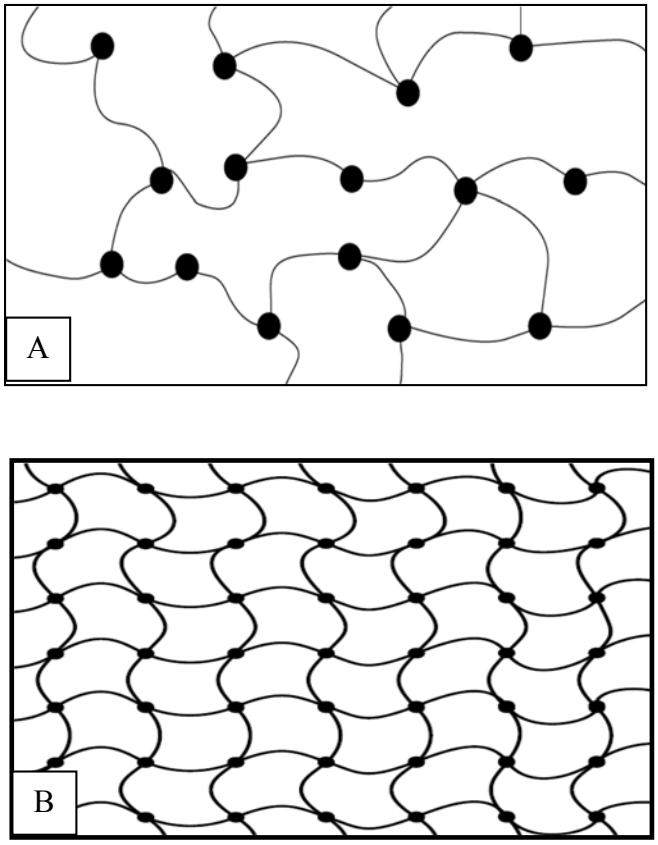

Figure 1.3: Illustration of a (A) physically cross-linked and (B) chemically cross-linked hydrogel structure

1.3.1. Smart hydrogels

Hydrogels can respond to environmental changes, such as temperature, pH, and light. Environmentally sensitive hydrogels, which are also referred to as smart hydrogels, are ideal candidates for site-specific drug delivery applications, as the active compound release can be controlled easily by changing the chemical structure of hydrogels as detailed in the following section.

1.3.1.1. pH-sensitive hydrogels

pH-sensitive hydrogels contain pendant acidic or basic group, which swell or deswell depending on the solution pH. **Figure 1.4** shows examples of acidic (top) and basic (bottom) polymers that respond to solution pH changes. Poly(acrylic acid), an anionic polymer, releases protons at high pH and leads to higher swelling when ionized (**Figure 1.4**, top). In contrast, poly*(N,N*'-diethylaminoethyl methacrylate) (PDEAEM) is a cationic polymer (**Figure 1.4**, bottom) that ionizes at low pH and swells more at lower pH values.

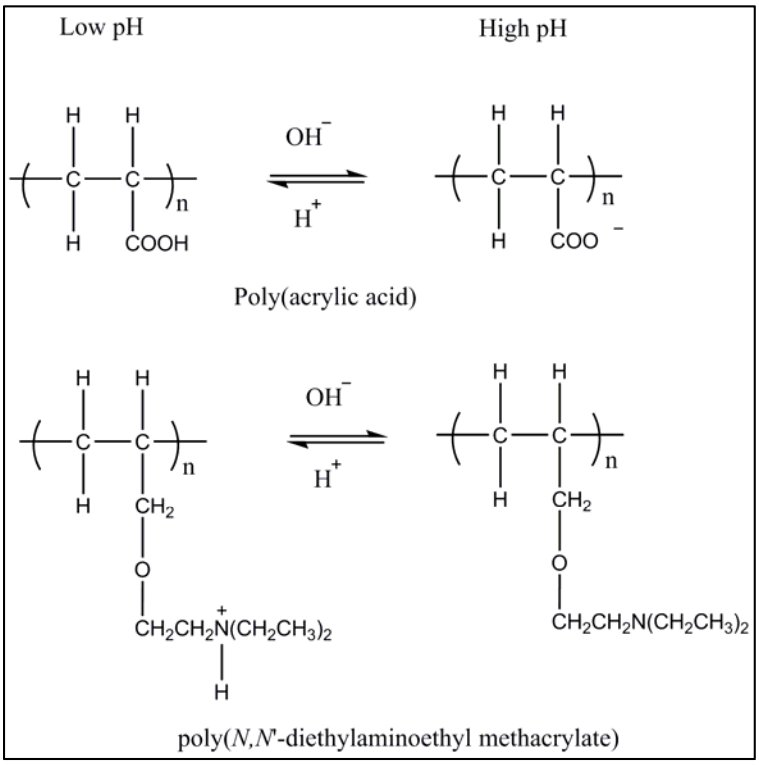

Figure 1.4: pH-dependent ionization, poly(acrylic acid) and poly(*N,N*'-diethylaminoethyl methacrylate)[23]

1.3.1.2. Temperature-sensitive hydrogels

Temperature-sensitive hydrogels respond to the local temperature of the environment. They typically contain hydrophilic and hydrophobic groups such as methyl, ethyl, and propyl. Several commonly used temperature-sensitive polymers developed for hydrogel systems are shown in **Figure 1.5** and under transitions through a lower critical temperature (LCST). Below their critical solution temperature, the hydrophilic part of the polymer dominates and forms H-bonding between water molecules. With increased temperatures, H-bonding networks between water and hydrogels are broken and the hydrophobic group dominates, leading to enhanced hydrophobic interactions. Below their LCST, these systems are swollen.

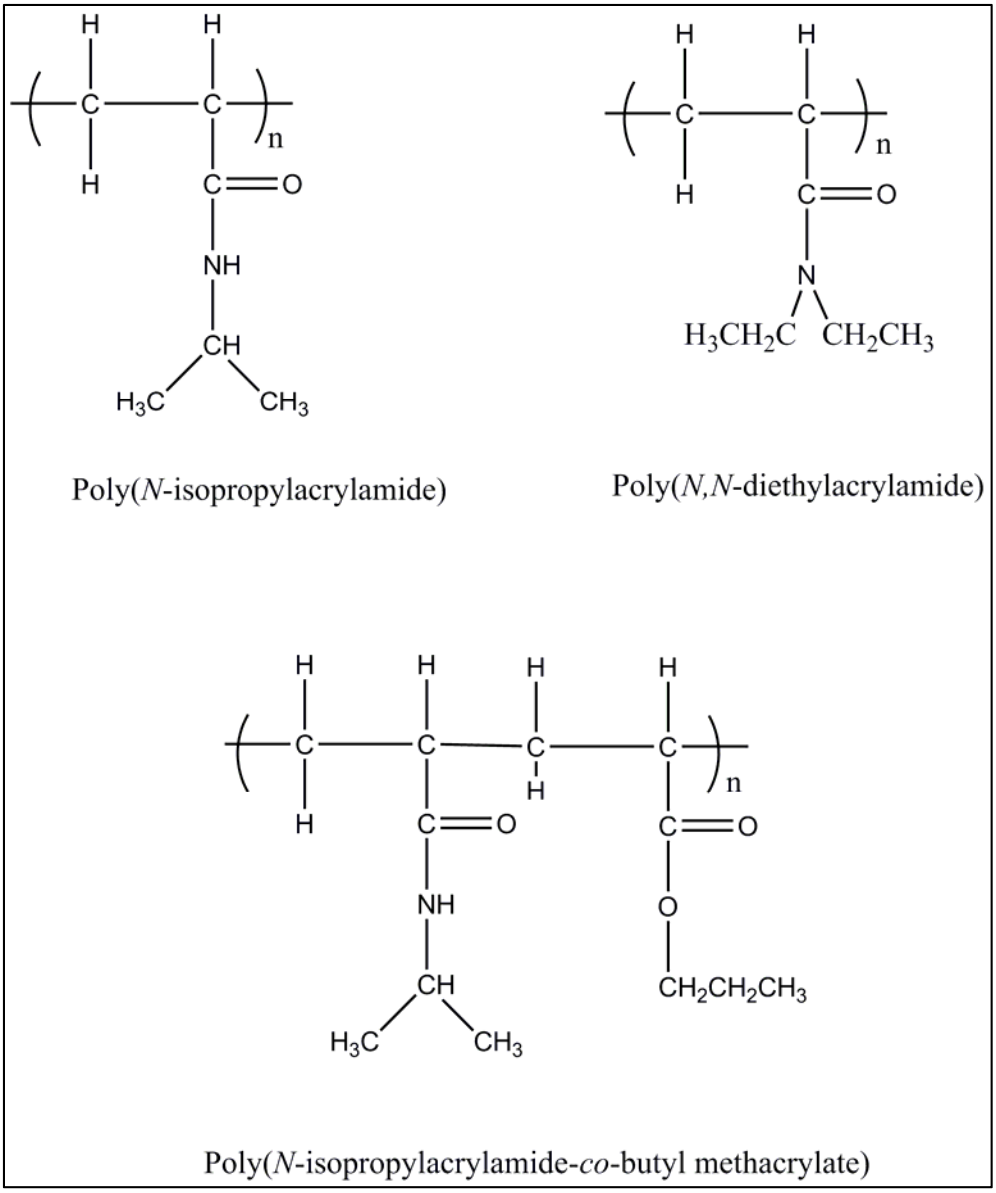

Figure 1.5: The most commonly used temperature-sensitive polymers: Poly(*N*-isopropylacrylamide), poly(*N,N'*-diethylacrylamide and poly(*N*-isopropylacrylamide-*co*-butyl methacrylate)[23]

1.3.2. Hydrogels for drug/protein delivery

Hydrogel systems are excellent candidates for a range of drug delivery devices, such as bioadhesives, targetable devices, and controlled release devices. These platforms can be used for oral, rectal, ocular, epidermal and subcutaneous injections.[24]

As described previously (**Section 1.1**), oral delivery is the preferred administration route. Hydrogel systems can deliver active compounds to the mouth, stomach, and intestine by controlled swelling and adhesion behaviors. For example, *in vivo* studies on diabetic rats show promise that, by using anionic hydrogels (described in **Section 1.3.1.1**), insulin can be orally administered to increase insulin bioavailability.[25, 26] As another example, cationic hydrogel systems can be used for stomach-specific delivery, such as delivery of antibiotics to treat Helicobacter pylori.[27] Bioadhesive hydrogel systems can treat oral cavity cancers, made with mucoadhesive polymers, hydroxypropyl cellulose, and poly(acrylic acid), is commercially available.[28]

Another drug delivery site that has received attention is subcutaneous delivery. Poly(2-hydroxyethyl methacrylate) and poly(acrylamide-*co*-monomethyl or monopropyl itaconate) have been used as biocompatible hydrogel systems designed to deliver anti-cancer drugs.[29,30] In addition, temperature-sensitive hydrogels with sol-gel phase transitions, which are soluble at room temperature and form gels at body temperature, have been designed for drug and protein delivery. [31, 32]

1.4. Polyanhydrides

Polyanhydrides are being investigated as controlled drug delivery systems due to their surface erosion behavior, hydrolytic sensitivity, and tunable degradation rate.[33, 34] The

only example of an FDA-approved device that is comprised of polyanhydrides is the biodegradable Gliadel® wafer, which delivers carmustine, a chemotherapeutic treatment for malignant glioma.[35,36] Yet, the physical encapsulation of active compounds often causes low-drug loading and a burst drug release. To overcome these limitations, the active compound can be chemically conjugated within the polymer backbone or as a pendant group to achieve higher drug loading and controlled drug release via hydrolytic cleavage.[37]

1.4.1. Salicylic acid-based poly(anhydride-esters)

Salicylic acid-based poly(anhydride-esters) (SAPAE) are unique, bioactive-based delivery systems. Salicylic acid (SA), a non-steroidal anti-inflammatory drug, was chemically incorporated to the polymer backbone via biodegradable linker, and more than 85% drug loading was achieved.[38, 39] Labile ester and anhydride bonds within the polymer are hydrolytically cleaved in a zero-order release rate. The degradation rate and thermal properties (glass transition temperature) of the delivery systems should be suited to specific applications (e.g., injection or oral). The degradation rate of SAPAE can be altered via the linker.[40, 41] As shown in **Figure 1.6**, several linkers, including aliphatic, branched, and aromatic groups, were evaluated.[40, 42] Glass transition (T_g) temperatures were also altered with the linker molecules, with longer aliphatic chains lowering T_g values and aromatic linkers achieving the highest values. Moreover, *in vitro* salicylic acid release was faster with polymers containing linear aliphatic linkers, whereas slower degradation rates were observed in aromatic and branched linkers.[40] Overall, SA release can be altered from days

to months by changing the chemical structure of the linker for desired applications and drug administration routes.

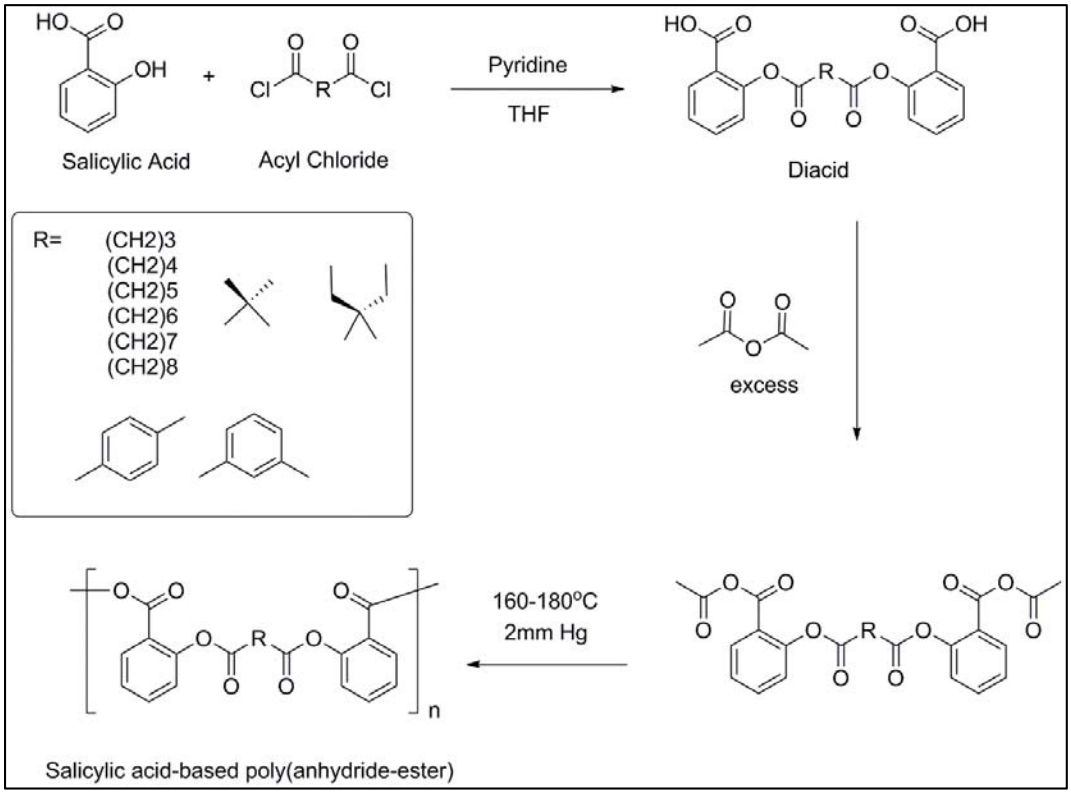

Figure 1.6: Synthesis of SAPAE with alternate linkers

1.4.1.1. Salicylic acid

SA is the active compound of the low cost anti-inflammatory drug aspirin, which hydrolyzes *in vivo* to yield SA. SA has been used as anti-inflammatory drug for decades and recent studies indicate that salicylic acid can be used to treat cancer,[43] arthritis,[44] and fungal infections.[45] Furthermore, other studies have shown that inflammation exacerbates

type 2 diabetes and that salicylates, in general can reduce insulin resistance,[46-51] suggesting that SA may affect oxidative stress, insulin resistance, and vascular inflammation.[47]

1.5. Diabetes

Diabetes is a metabolic disease in which the patient's body does not produce enough insulin or its cells do not respond to insulin. In either case, the outcome is high blood glucose (sugar) levels. About 382 million people in worldwide currently suffer from diabetes and the number may increase to 592 million by 2035.[52]

Diabetes is categorized into two types. In general, type 1 diabetes develops in early adulthood. Because their bodies do not produce enough insulin, type 1 diabetes patients are insulin-dependent.[53] In type 2 diabetes, the body does not respond to insulin properly and this is referred to as insulin resistance.[53] Obesity and unhealthy diet can cause type 2 diabetes, which may be controlled by weight loss and a healthy diet. However, patients generally need to take medication and insulin in later stages of the disease.[54]

1.6. Research Projects

Salicylic acid-based poly(anhydride esters) (SAPAEs) have been researched for nearly two decades and formulated into microspheres, films, discs, coatings, electrospun fibers, and hydrogels. In this dissertation, unique, environmentally-sensitive SAPAE-based hydrogels were developed for injectable and/or oral delivery of salicylic acid and proteins. Uniquely for biodegradable polymers, salicylic acid was chemically incorporated

into hydrogel systems to develop more robust protein delivery systems. Each chapter addresses a specific issue and is separately published or the manuscripts are under preparation.

1.6.1. Physically cross-linked salicylic acid-based poly(*N*-isopropylacrylamide-*co*-acrylic acid) injectable hydrogels for protein delivery

In this chapter, physically cross-linked injectable hydrogels were developed from SAPAEs and poly(*N*-isopropylacrylamide-*co*-acrylic acid) for protein delivery applications. These systems are developed to deliver SA and protein simultaneously to achieve synergistic effects. The physical interactions between these polymer systems were confirmed using Fourier transform infrared spectroscopy (FT-IR) and Differential scanning calorimetry (DSC). Furthermore, the pore structures of these systems were evaluated using scanning electron microscopy. A model protein, bovine serum albumin (BSA), was physically incorporated within the hydrogels systems, with sustained slow release achieved over several days. Concurrently, salicylic acid was released from the hydrogels in a sustained manner for up to 120 hours. Hydrogel systems were cytocompatible at relevant therapeutic concentrations. **Figure 1.7** shows the hydrogels behavior at room temperature and 37°C in D.I. water. Poly(*N*-isopropylacrylamide-*co*-acrylic acid) has a unique temperature-sensitive behavior, which becomes hydrophobic at temperatures above their LCST. On the left-hand side (**Fig 1.7A**), hydrogels are solubilized throughout the water. In contrast, on the right-hand side (**Fig 1.7B**), the hydrogel systems

are separated from the water. In addition to the unique combination delivery of SA and protein, these systems achieved higher BSA loading compared to commercially available PNIPAM-based hydrogels and sustained BSA release.[55]

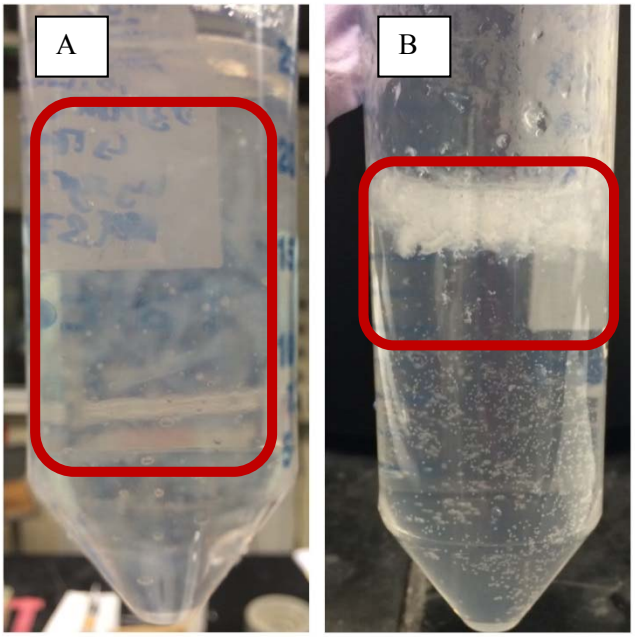

Figure 1.7: PNIPAM-*co*-AA:SAPAE hydrogel systems (A) at room temperature (RT) (hydrogels are solubilized throughout the water) and (B) at 37 °C in D.I. water (hydrogels are separated from the water)

1.6.2. Salicylic acid-based pH-sensitive hydrogels as potential oral insulin delivery systems

In this chapter, SA-based poly(anhydride-esters) were physically cross-linked with poly(acrylic acid) (PAA) in various ratios to develop pH-sensitive cross-linked hydrogel systems for intestine-specific insulin delivery. These hydrogels were characterized by FT-

IR and DSC to understand the physical interactions between these compounds. Furthermore, the pore size and swelling behavior of these hydrogels were evaluated by scanning electron microscopy (SEM). Pore size and swelling behavior were dependent on relative PAA concentrations, such that increasing PAA content increased pore size and swelling value. Moreover, when insulin was physically incorporated into hydrogels, ~50 wt% insulin was incorporated into the networks. Insulin and SA release were evaluated at pH values of 1.2 and 6.8 to simulate stomach and intestine conditions, respectively. Insulin release was minimum (~4-8 wt%) in acidic conditions (pH 1.2) over 2 hours and SA release was also minimum (~20 wt%). In more neutral conditions (pH 6.8), ~ 90% of the insulin and ~ 70% of SA were released within 24 hours. Insulin physical stability was confirmed by size exclusion chromatography and results were less than United States Pharmacopeia specification (NMT 1%). These results suggest that hydrogels can protect insulin in acidic conditions and possibly be used for oral insulin and salicylic acid delivery to benefit diabetes patients. **Figure 1.8** represents the pH-dependent behavior of the hydrogels. **Fig 1.8A** shows a dry hydrogel; **Fig 1.8B** shows a gel after incubation in 0.1 N HCl; and **Fig 1.8C** shows the gel after incubation in pH 6.8 buffer. Notably, in neutral conditions, the hydrogel volume swelled 20 times relative to dry gel. In 0.1N HCl hydrogel volume is almost the same as dry gel. The insulin loading, release profile, and mucoadhesion profile of these hydrogel systems were comparable to the published literature.[26, 56] These results suggest that these systems may have a similar *in vivo* profile. In addition, SA and insulin combination therapy may be useful for diabetes patients, as SA reduces insulin resistance.

Future work includes *in vivo* studies in diabetic rats to evaluate blood glucose levels following oral delivery.

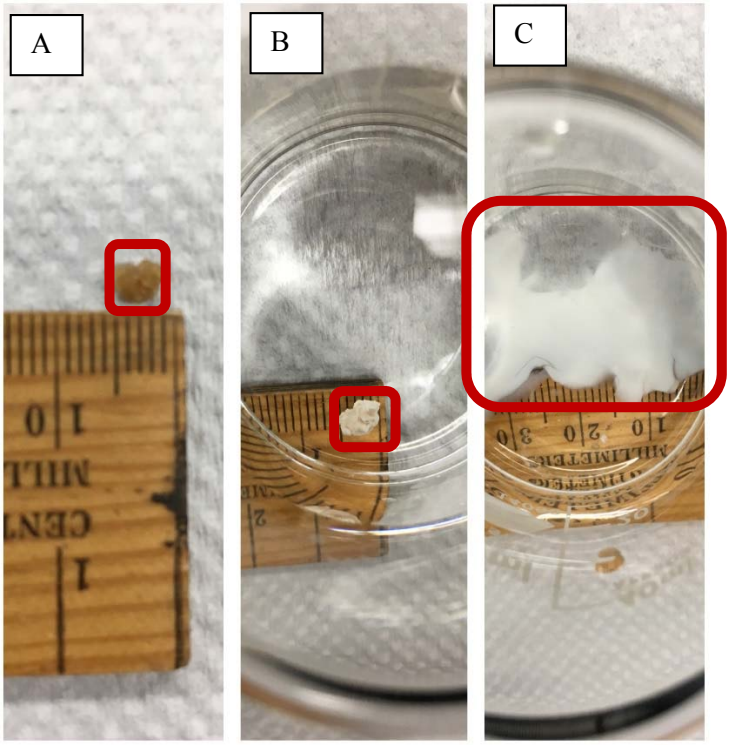

Figure 1.8: PAA: SAPAE hydrogel systems: (A) dry PAA:SAPAE hydrogel (B) in 0.1N HCl (pH 1.2) over 24-hour at 37°C (C) in phosphate buffer (pH 6.8) over 24-hour at 37°C

1.6.3. Novel salicylic acid-based chemically cross-linked pH-sensitive hydrogels as potential drug delivery systems

In this chapter, SA was chemically incorporated into hydrogel systems via covalent attachment to an itaconate moiety followed by UV-initiated cross-linking using acrylic acid

and poly(ethylene glycol) diacrylate. The structure of the hydrogel system was confirmed using FT-IR spectroscopy. These SA-based hydrogels showed pH-responsive behavior, collapsing at acidic pH (1.2) and swelling at higher pH (7.4) values. The pore structure was studied using SEM. These networks exhibit promising pore sizes (15 to 60 μm) for physically encapsulating proteins. Furthermore, the SA release was analyzed using high-pressure liquid chromatography (HPLC). The hydrogel systems exhibited a pH-dependent SA release profile: SA release was much slower in pH 1.2 as compared to pH 7.4. Under acidic pH conditions, 30 wt % SA was released after 24 hours, whereas 100 wt% SA was released in a sustained manner within 24 hour in pH 7.4 PBS buffer. In addition, rheological studies of the hydrogels proved that these systems are mechanically strong and robust. Mucoadhesive behaviors were also confirmed using a Texture Analyzer. These systems' mucoadhesion behavior and detachment force values are much higher than previously published hydrogel systems developed for oral protein delivery.[26] Furthermore, these systems are unique as they are the first chemically-conjugated SA-based hydrogel systems. These results suggest that SA-based hydrogels can be potentially used for oral delivery of bioactives in combination with SA to treat cancer and diabetes. Future work includes protein encapsulation to hydrogel systems and evaluating release behavior for dual delivery.

1.7. References

1. Y. Zhang, H. F. Chan, K. W. Leong. Advanced materials and processing for drug delivery: The past and the future. Advanced drug delivery reviews 65, 104-120 (2013).

2. R. Duncan, M. J. Vicent. Polymer therapeutics-prospects for 21st century: the end of the beginning. Advanced drug delivery reviews 65, 60-70 (2013).

3. E. Henin, M. Bergstrand, J. Standing, M. O. Karlsson. A mechanism-based approach for absorption modeling: The gastro-intestinal transit time (GITT) model. The AAPS journal 14, 150-163 (2012).

4. T. Vermonden, R. Censi, W. Hennink. Hydrogels for protein delivery. Chemical reviews 112, 2853-2888 (2012).

5. J. Shaji, V.Patole. Protein and peptide drug delivery: Oral approaches. Indian journal of pharmaceuticals sciences 70, 269-277 (2008).

6. N. A. Peppas, P.Bures, W. Leobandung, H. Ichikawa. Hydrogels in pharmaceutical formulations. European journal of pharmaceutics and biopharmaceutics 50, 27-46 (2000).

7. J. Khandare, T.Minko. Polymer-drug conjugates: Progress in polymeric prodrugs. Progress in polymer science 31, 359-397 (2006).

8. T. M. Allen, P.Cullis. Drug delivery systems; entering the mainstream. Science 303, 1818-1822 (2004).

9. M. T. Liang, N.M.Davies, I. Toth. Encapsulation of lipopeptides within liposomes: effect of number of lipid chains, chain length and method of liposome preparation. International journal of pharmaceutics 301, 247-254 (2005).

10. S. P. Vyas, M.Rawat, A. Rawat, S. Mahor, P.N. Gupta. Pegylated protein encapsulated multivesicular liposomes: A novel approach for sustained release of interferon a. Drug development and industrial pharmacy 32, 699-707 (2006).

11. X. Yan, G.L.Scherphof, J. M. Kamps. Liposome opsonization. Journal of liposome research 15, 109-139 (2005).

12. V. R. Sinha, A.Trehan. Biodegradable microspheres for protein delivery. Journal of controlled release 90, 261-280 (2003).

13. J. M. Anderson, M.S.Shive. Biodegradation and biocompatibility of PLA and PLGA microspheres. Advanced drug delivery reviews 28, 5-24 (1997).

14. H. Okada. One and three month release injectable microspheres of the LH-RH superagonist leuprorelin acetate. Advanced drug delivery reviews 28, 43-70 (1997).

15. G. Crotts, T.G.Park. Protein delivery from poly(lactic-*co*-glycolic acid) biodegradable microspheres: Release kinetics and stability issues. Journal of microencapsulation 15, 699-713 (1998).

16. H. K. Kim, T.G.Park. Microencapsulation of human growth hormone within biodegradable polyester microspheres: Protein aggregation stability and incomplete release mechanism. Biotechnology and bioengineering 65, 659-667 (1999).

17. M. Van De Weert, W.E.Hennink, W. Jiskoot. Protein instability in poly(lactic-*co*-glycolic acid) microparticles. Pharmaceutical research 17, 1159-1167 (2000).

18. Y. Yee, K.Park. Control of encapsulation efficiency and initial burst in polymeric microparticle systems. Archives of pharmacal research 27, 1-12 (2004).

19. O. Wichterle, D.Lim. Hydrophilic gels for biological use. Nature 4706, 117-118 (1960).

20. N.A. Peppas, A.G.Mikos. Hydrogels in medicine and pharmacy. CRC Press, Boca Raton, FL 1, 1-27 (1986).

21. H. Park, K. Park. Hydrogels and biodegradable polymers for bioapplications. American chemical society 627, 2-10 (1996).

22. A. Hoffman. Hydrogels for biomedical applications. Advanced drug delivery reviews 64, 18-23 (2012).

23. Y. Qiu, K.Park. Enviromental-sensitive hydrogels for drug delivery. Advanced drug delivery reviews 64, 49-60 (2012).

24. N.A. Peppas, P.Buresa., W. Leobandunga, H. Ichikawa. Hydrogels in pharmaceutical formulations. European journal of pharmaceutics and biopharmaceutics 50, 27-46 (2000).

25. M. Morishita, T.Goto, K. Nakamura, A. Lowman, K. Takayama, N. Peppas. Novel oral insulin delivery systems based on complexation polymer hydrogels: single and multiple administration studies in type 1 and 2 diabetic rats. Journal of controlled release 110, 587-594 (2006).

26. N.A. Peppas, Devices based on intelligent biopolymers for oral protein delivery. International journal of pharmaceutics 277, 11-17 (2004).

27. V. R. Patel, M.M.Amiji. Preparation and characterization of freezedried chitosan-poly(ethylene oxide) hydrogels for site-specific antibiotic delivery in the stomach. Pharmaceutical research 13, 588-593 (1996).

28. T. Nagai, Y.Machida, Y. Suzuki, H. Ikura. US patent 4226848 (1980).

29. J. M. Teijon, R.M.Trigo, O. Garca, M. D. Blanco. Cytarabine trapping in poly (2-hydroxyethyl methacrylate) hydrogels: drug delivery studies. Biomaterials 18, 383-388 (1997).

30. M.D. Blanco, C.Gomez, O. Garcia, J.M. Teijon. Ara-C release from poly(acrylamide-co-monomethyl itaconate) hydrogels: *in vitro* and *in vivo* studies. Polymer gels networks 6, 57-69 (1998).

31. Y. J. Kim, S.Choi, J. J. Koh, M. Lee, K. S. Ko, S. W. Kim. Controlled release of insulin from injectable biodegradable triblock copolymer. Pharmaceutical research 18, 548-550 (2001).

32. J. Y. Fang, J.P.Chen, Y. L. Leu, J. W. Hu. Temperature-sensitive hydrogels composed of chitosan and hyaluronic acid as injectable carriers for drug delivery. European journal of pharmaceutics and biopharmaceutics 68, 626-636 (2007).

33. A. Gopferich, J.Tessmar. Polyanhydride degradation and erosion. Advanced drug delivery reviews 54, 911-931 (2002).

34. N. Kumar, R.S.Langer, A. J. Domb. Polyanhydrides: An overview. Advanced drug delivery reviews 54, 889-910 (2002).

35. A. J. Domb, M.Maniar, A.S. T. Haffer. Biodegradable polymer blends for drug delivery. US patent 5 (1999).

36. W. Dang, T.Daviau, P. Ying al. Effects of Gliadel wafer initial moleular weight on the erosion of wafer and release of BCNU. Journal of controlled release 42, 83-92 (1996).

37. T. J. Anastasiou, K.E.Uhrich. Aminosalicylate-based biodegradable polymers-syntheses and *in vitro* characterization of poly(anhydride-ester)s and poly(anhydride-amide)s. Journal of polymer science: part A: Polymer chemistry 41, 3667-3679 (2003).

38. R.C. Schmeltzer, T.J.Anastasiou, K.E. Uhrich. Optimized synthesis of salicylate-based poly(anhydride-esters). Polymer bulletin 49, 441-448 (2003).

39. R. C. Schmeltzer, K.E.Schmalenberg, K.E Uhrich. Synthesis and cytotoxicity of salicylate-based poly(anhydride esters). Biomacromolecules 6, 359-367 (2005).

40. A. Prudencio, R.C.Schmeltzer, K. E. Uhrich. Effect of linker structure on salicylic acid-derived poly(anhydride-esters). Macromolecules 38, 6895-6900 (2005).

41. R. C. Schmeltzer, M.Johnson, J. Griffin, K. Uhrich. Comparison of salicylate-based poly(anhydride-esters) formed via melt-condensation versus solution polymerization. Journal of biomaterials science, polymer edition 19, 1295-1306 (2008).

42. A. Prudencio, A.Carbone, J. Griffin, K. Uhrich. A novel approach for incorporation of mono-functional bioactive phenols into polyanhydrides. Macromolecular rapid communication 30, 1101-1108 (2009).

43. E. Bastiannet, K.Sampieri, O. Dekkers, A. de Craen. et al. Use of aspiring postdiagnosis improves survival for colon cancer patients. British journal of cancer 106, 1564-1570 (2012).

44. R. Yamazaki, N.Kusunoki, T. Matsuzaki, et al. Aspirin and sodium salicylate inhibit proliferation and induce apoptosis in rheumatois synovial cells. Journal of pharmacy and pharmacology 54, 24-32 (2002).

45. B. F. Amborabe, P.F.-Lessard., J. F. Chollet, G. Roblin. Antifungal effects of salicylic acid and other benzoic acid derivatives towards Eutypa lata; structure-activity relationship. Plant physiology biochemistry 40, 1051-1060 (2002).

46. M. Nixon, D.J.Wake, D. E. Livingstone, R. H. Stimson, C. L. Esteves, J. R. Seckl, K. E. Chapman, R. Andrew, B. R. Walker. Salicylate downregulates 11B-HSD1 expression in adipose tissue in obese mice and in humans, mediating insulin sensitization. Diabetes 61, 790-796 (2012).

47. R.P. Raghavan, D.W.Laight, M. H. Cummings. Aspirin in type 2 diabetes, a randomised controlled study: effect of different doses on inflamation, oxidative stress, insulin resistance and endothelial function. International journal of clinical practice 68, 271-277 (2014).

48. A. B. Goldfine, V.Fonseca, S. Shoelson. Therapeutic approaches to target inflammation in type 2 diabetes. Clinical chemistry 57, 162-167 (2011).

49. R. S. Hundal, K.F.Peterson, A. B. Mayerson, P. S. Randhawa, S. Inzucchi, S. E. Shoelson, G. I. Shulman. Mechanism by which high-dose aspirin improves glucose metabolism in type 2 diabetes. Journal of clinical investigation 109, 1321-1326 (2002).

50. S. E. Shoelson, J.Lee, A. B. Goldfine Inflammation and insulin resistance. Journal of clinical investigation 116, 1793-1801 (2006).

51. J. Reid, T.D.Lightbody. The insulin equivalence of salicylate. British medical journal, 897-900 (1959).

52. L. Guariguata, D.R.Whiting, I. Hambleron, J. Beagley, U. Linnenkamp, J. E. Shaw. Global estimates of diabetes prevalence for 2013 and projections for 2035. Diabetes research and clinical practice 103, 137-149 (2014).

53. A.D.Association. Diagnosis and classification of diabetes mellitus. Diabetes care 27 (2004).

54. A.D. Association. Insulin administration. Diabetes care 25, 1 (2002).

55. R. Zhuo, W.Li. Preparation and characterization of macroporous poly(N-isopropylacrylamide) hydrogels for the controlled release of proteins. Journal of polymer science part A: polymer chemistry 41, 152-159 (2003).

56. A. Kumar, S.Lahiri, H. Singh. Development of PEGDMA: MAA based hydrogel microparticles for oral insulin delivery. International journal of pharmaceutics 323, 117-124 (2006).

2. PHYSICALLY CROSS-LINKED SALICYLIC ACID-BASED POLY(N-ISOPROPYLACRYLAMIDE-*CO*-ACRYLIC ACID) HYDROGELS FOR INJECTABLE PROTEIN DELIVERY

2.1. Introduction

Extended release bioactive-delivery systems are actively being studied to maintain therapeutic drug level while eliminating the need for multiple dosages, which sometimes cause patient discomfort and possible infections. Several delivery systems that have received commercial success, including microspheres, liposomes, and hydrogels, have also achieved extended release. Among these systems, hydrogels have become significant for protein and drug delivery applications, owing to their tunability, similarity to natural living tissue, and ability to locally deliver bioactives.[1]

Hydrogels are three-dimensional cross-linked networks of water-soluble polymers capable of imbibing large quantities of water or biological fluids.[2-4] Such polymeric networks are formed by chemical crosslinks (covalent bonds) or physical crosslinks (intermolecular interactions)[5-8] which can be used to control pore size and pore volume. Temperature-sensitive hydrogels have been studied for protein delivery, because proteins can be encapsulated at low temperatures, which reduces the risk of protein denaturation. Hydrogels contain segments of hydrophobic and hydrophilic groups, enabling unique hydrophilic-hydrophobic transitions at their lower critical solution temperature (LCST). Below the LCST, the hydrophilic component hydrogen-bonds with water molecules, leading to swelling and expansion in water. As the temperature increases, the hydrogen

bonding between water molecules and the hydrophilic part of the hydrogel weakens, whereas the hydrophobic interactions between the hydrophobic components becomes stronger, prompting hydrogel shrinking. Poly(*N*-isopropylacrylamide) (PNIPAM) systems are commonly utilized temperature-sensitive systems due to their LCST around physiological temperatures (32°C). Research has demonstrated that by copolymerizing PNIPAM with acrylic acid, the LCST value can be increased, because resulting in enhanced hydrophilic interactions.[9]

To develop combination delivery of two active compounds, such as a small molecule and a protein to achieve synergistic effect, temperature-sensitive polymer, poly(*N*-isopropylacrylamide-*co*-acrylic acid) (PNIPAM-*co*-AA) (**Figure 2.1.B**) and salicylic acid-based poly(anhydride esters) (SAPAEs) were used. Salicylic acid (SA) was chosen for this study as it has shown promising results in many diseases, such as colorectal cancer,[10] diabetes,[11, 12] and arthritis.[13] In addition, it has anti-inflammatory, analgesic, and anti-pyretic effects.[14] SAPAEs have been well researched over the past decade.[15, 16] In these systems, salicylic acid is chemically incorporated into a polymeric backbone, leading to high drug loading (85%) and enabling a controlled, sustained release of salicylic acid upon polymer degradation via hydrolysis (**Figure 2.1A**). Furthermore, these systems reduce inflammation[17] and enhance bone regeneration in diabetic animals.[18] As the gel component, PNIPAM-*co*-AA was chosen for its potential to form hydrogen bonds. The carboxylic groups of co-monomer acrylic acid also increase hydrophilicity, which increases the gel pore size and may increase encapsulation.

The purpose of this chapter was to develop physically cross-linked, SA-based hydrogels systems to deliver SA in combination with a model protein, bovine serum

albumin (BSA), in a sustained manner. To create the gels, PNIPAM-*co*-AA and SAPAEs were blended. The interactions, pore structure, and SA release were studied. Then, BSA was incorporated into the hydrogel system via a swelling-deswelling technique and its release profile evaluated. The cytocompatibility was studied using MTS assay.

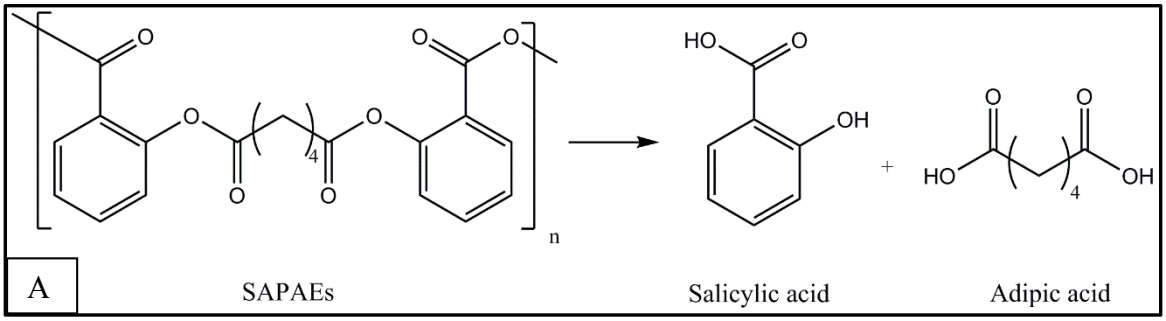

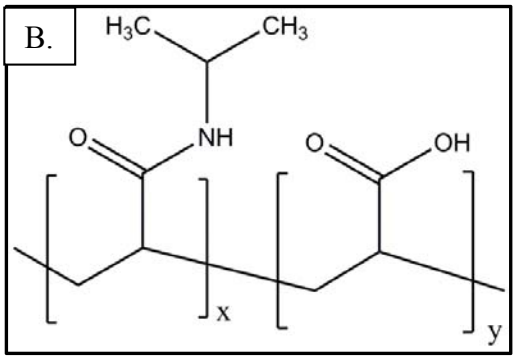

Figure 2.1: Chemical structures of (A) SAPAEs and its degradation products (salicylic acid and adipic acid), and (B) poly(*N*-isopropylacrylamide-*co*-acrylic acid).

2.2. Experimental Section

2.2.1. Materials

Fetal bovine serum was purchased from Atlanta Biologicals (Lawrenceville, GA). 3T3 mouse fibroblast cells were purchased from ATCC (Manassas, VA). Hydrochloric acid and Thermo Scientific Pierce Micro BCA (bicinchoninic acid) Protein Assay Kit were purchased from Fisher Scientific (Fair Lawn, NJ). PNIPAM-*co*-AA and all other chemicals and reagents were purchased from Sigma-Aldrich (Milwaukee, WI). All reagents were used as received from Sigma-Aldrich.

2.2.2. Hydrogel formation

SAPAEs were synthesized according to previously published methods.[15, 16] Briefly, SA (2 eq) was dissolved in 100 mL anhydrous tetrahydrofuran (THF) and pyridine (4 eq). Adipoyl chloride (1 eq), dissolved in 15 mL THF, was added drop-wise, resulting in a white suspension. The reaction mixture was quenched over water, and acidified to pH 2 using concentrated HCl. The formed precipitate was filtered, washed with water (3 × 250 mL), and dried in vacuo to yield diacid intermediate. The diacid intermediate was then suspended in 80 mL acetic anhydride and stirred overnight under argon at room temperature, producing a pale yellow solution. Excess acetic anhydride was removed *in vacuo* and the resulting acetyl-terminated monomer heated at 180°C under vacuum with mechanical stirring for 4-6 hours, yielding yellow, solid SAPAE. SAPAE was formulated into PNIPAM-*co*-AA:SAPAEs (wt:wt) (7:3 and 6:4) hydrogel by modifying a previously developed protocol.[19] PNIPAM-*co*-AA (105 mg or 90 mg) (**Figure 2.1B**) was weighed separately into scintillation vials (20 mL) and dissolved in anhydrous dimethylformamide (DMF) at room temperature and stirred for 48 hours. After 48 hours, 45 or 60 mg of SAPAE

was separately added to the PNIPAM-*co*-AA solutions and stirred for an additional 24 hours. The resulting viscous solutions (1 mL, 3% w/v) were cast into teflon beakers (28 mm diameter) via syringe and dried in a vacuum oven at 80°C overnight to acquire films.

FT-IR absorbance spectra, 64 scans per cycle were measured using Thermo Nicolet FT-IR spectrometer with diamond attenuated total reflectance (ATR) (Thermo Scientific, Somerset, NJ). Polymer blend miscibility was analyzed via DSC, using TA Instruments Q200 DSC (New Castle, DE). PNIPAM-*co*-AA:SAPAE (PN:SAPAE) films, PNIPAM-*co*-AA, and SAPAE alone (~5 mg) were analyzed by heating under dry nitrogen from -10 °C to 200 °C at rate of 10 °C/min and cooling to -10 ˚C at 10 ˚C/min with a three-cycle minimum. The data was analyzed using TA instruments Universal Analysis 2000 software. The predicted glass transition (T_g) values for blends were calculated using the Fox equation (Equation 2.1):[20]

$$\frac{1}{T_{g,blend}} = \frac{W_{PNIPAM\text{-}co\text{-}AA}}{T_{PNIPAM\text{-}co\text{-}AA}} + \frac{W_{SAPAE}}{T_{g,SAPAE}} \qquad \textbf{Equation 2.1}$$

where $T_{g,blend}$ represents the miscible blend, $T_{g,i}$ the noted pure component i (PNIPAM-*co*-AA and SAPAE), and w_i the weight fraction of noted component i.

2.2.3. Swelling behavior

Hydrogel swelling values were measured in phosphate buffer saline (PBS) pH 7.4 for 2 and 24 hours at room temperature, 23 °C and 37 °C. The dried films were immersed in PBS (50 ml), removed at 2 and 24 hours, and blotted with filter paper to remove residual

water at the hydrogel surface. The swelling values, Q, were calculated according to following equation:[21-23]

$$Q = \frac{Ws - Wd}{Wd} \qquad \textbf{Equation 2.2}$$

where W_s and W_d are the weight of the swollen and dried films, respectively. All experiments were carried out triplicate and the average values are reported.

2.2.4. Hydrogel morphology

Hydrogel morphology was investigated using SEM. The films were swollen in deionized (DI) water (50 ml) for 24 hours at room temperature, and then lyophilized for 12 hours prior to SEM imaging. The samples were coated with Au/Pd using a sputter coated (SCD 004, Balzer Union Limited) and the images obtained using an AMRAY-1830I microscope (Amray Inc.).

2.2.5. *In vitro* SA release

Polymer films (60 ± 10 mg) were placed in 50 mL centrifuge tubes containing 10 mL PBS (pH 7.4) and incubated (37 ˚C, 60 rpm). At set time points, 5 mL aliquots of media were removed and replaced with 5 mL fresh PBS. The amount of released SA was quantified by ultraviolet-visible (UV-Vis) spectrophotometry using a Perkin-Elmer Lambda XLS spectrophotometer to monitor SA release. The measurements were collected at λ = 303 nm, where the maximum SA absorbance did not overlap with PNIPAM-*co*-AA

or other degradation products. An SA calibration curve was prepared and data calculated against a standard calibration curve. The release experiments were carried out until SA release was no longer detected, and data normalized to 100%. All sets of experiments were performed in triplicate.

2.2.6. BSA loading and release

The swelling-diffusion method[24] was used to incorporate BSA into the hydrogels. BSA solution (20 mg/mL) was prepared in PBS (pH 7.4). Then, dried polymer films (20 ±5 mg) were placed in 2 mL of BSA solution for 6 hours at 4 °C. The films were removed and rinsed and collapsed with 0.1 N HCl to remove any free BSA. The remaining solution and the rinse solution were collected for further analysis. The amount of loaded protein was determined using the Micro BCA assay according to the manufacturer's protocol. Non-loaded gels were subjected to the same protocol as a negative control. Experiments were performed in triplicate and drug loading (%) calculated according to the following equation:

$$\text{Drug loading \%} = \frac{Wpl}{Wps} \times 100 \qquad \textbf{Equation 2.3}$$

$$Wpl = Wps - Wpls$$

where W_{pl}, W_{ps}, and W_{pls} are the weight of the protein loaded into gels, the protein in the solution before loading, and the protein in the solution after loading, respectively.

For the *in vitro* BSA release studies, the BSA-loaded hydrogels or non-loaded hydrogels were immersed in 50 mL centrifuge tubes containing 25 mL PBS (pH 7.4) at 37 ˚C. At set time points, 10 mL of media was removed and replaced with 10 mL fresh media.

The experiments were carried out until BSA release was no longer detected in PBS media. The BSA amount was determined using Micro BCA protein assay and normalized against the non-loaded hydrogels to eliminate possible absorbance from salicylic acid. Experiments were performed in triplicate.

2.2.7. Cytotoxicity of the hydrogels

Hydrogel cytocompatibility was performed by culturing 3T3 fibroblast cells in polymer blend-containing media. The polymer blends were dissolved in DMSO as a stock solution (10 mg/mL) and serially diluted with cell culture media. Cell culture media consisted of Dulbecco's Modified Eagle's Medium (DMEM), 10% v/v fetal bovine serum, 1% L-glutamate, and 1% penicillin/streptomycin. The cells were seeded in 96-well plate at 2,000 cells per well in 100 μL media. After incubation for 1 hour, the polymer-containing media at 0.1 mg/mL and 0.01 mg/mL were added to wells. The media with dissolved polymer was compared to DMSO-containing media (1% v/v). For the fibroblasts, cell viability was determined by using MTS (3-(4,5-dimethylthiazol-2-yl)-5-(3-carboxymethoxyphenyl)-2-(4-sulfophenyl)-2H-tetrazolium) assay. After 24-, 48-, and 72-hour incubation, MTS reagent was added to each well and further incubated for 3 hours at 37 °C, the absorbance was recorded with a microplate reader (Coulter, Boulevard Brea, CA) at λ = 490 nm.

2.2.8. LCST determination

To determine hydrogel LCST values, DSC measurements were performed using TA Instruments Q200 DSC (New Castle, DE) using a previously published procedure.[25] The films were immersed in deionized water for 24 hours at room temperature. The swollen gels (~5 mg) were heated from 20 to 50 °C at 3 °C/min under a nitrogen atmosphere. The data was analyzed using TA instruments Universal Analysis 2000 software.

2.3. Results and Discussion

2.3.1. Hydrogel formation

Different ratios of SAPAE were blended with PNIPAM-*co*-AA (8:2 to 5:5) to investigate the influence of SAPAE on hydrogel properties. Only two ratios of PNIPAM-*co*-AA:SAPAE (PN:SAPAE), 7:3 and 6:4, were selected, as the 8:2 ratio was not sufficiently stable and the pore size of the 5:5 ratio was not sufficiently large to encapsulate BSA. DSC was utilized to determine hydrogel miscibility by measuring T_g. The PN:SAPAE films showed single T_g values indicating a uniform, homogenous gel **(Figure 2.2**). "Experimental" T_g values were compared with T_g values predicted by the Fox analytical equations (**Equation 2.1**) for a binary system. The relationship between blends and individual homopolymers' T_g values correlated to the Fox Equation.[20] The predicted T_g values were very close to the measured T_g value, indicating a miscible blend. Furthermore, T_g values decreased with increasing SAPAE content, as the T_g values of SAPAE were initially much lower (56 ˚C) than PNIPAM-*co*-AA (127 ˚C).

FT-IR spectroscopy was used to investigate intermolecular molecular interactions between SAPAE and PNIPAM-*co*-AA (**Figure 2.3**). A summary of FT-IR peaks is presented in **Table 2.1**. SAPAE synthesis was confirmed by the presence of the anhydride C=O stretches at 1790 cm^{-1} and the preservation of the ester C=O stretch at 1742 cm^{-1} (**Figure 2.3**). For PNIPAM-*co*-AA, the C=O stretches of carboxylic acid were observed at 1716 cm^{-1} and 1635 cm^{-1}, whereas the amide N-H vibration occurred at 1520 cm^{-1}. In the PN:SAPAE hydrogels, PNIPAM-*co*-AA carboxylic acid groups and amide groups can interact with the carbonyl group of SAPAEs, resulting in hydrogen-bond formation. The peak shifting of the hydrogen-bonded functional groups in FT-IR spectroscopy suggests hydrogen-bond formation.[26, 27] Notably, in the spectrum of PN:SAPAE hydrogels, the C=O stretch shifted to 1746 cm^{-1}, 1709 cm^{-1}, and 1637 cm^{-1}. Additionally, the amide N-H vibration shifted to 1534 cm^{-1}. These results correlate with previously published H-bonding interactions of PNIPAM with poly(methacrylic acid).[28] The data suggest interactions between the N-H group of PNIPAM-*co*-AA and the carbonyl group of the SAPAE and PNIPAM-*co*-AA.

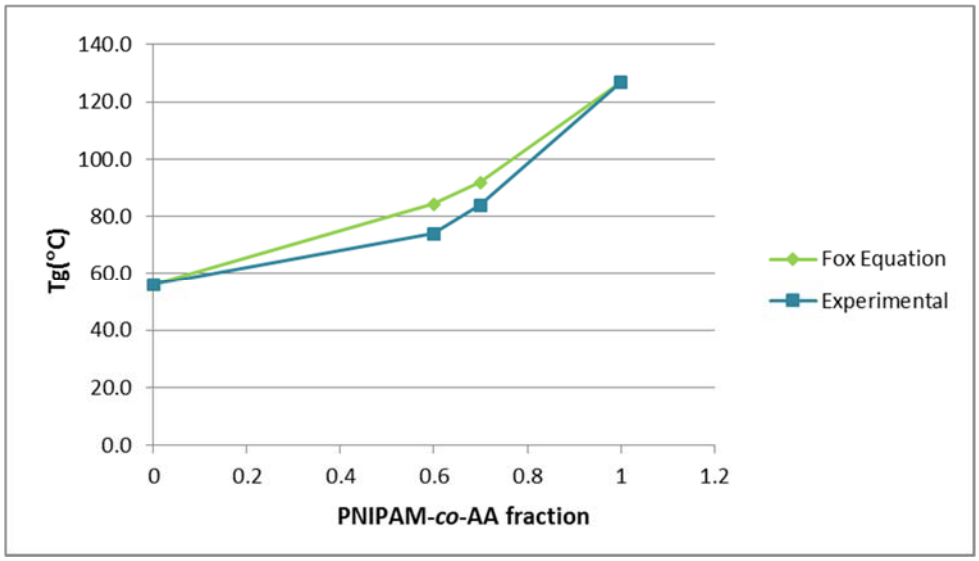

Figure 2.2: Experimental values of PN:SAPAEs blends glass transition temperatures as compared to Fox equation (Equation 2.1) values as a function of PNIPAM-*co*-AA weight fraction.

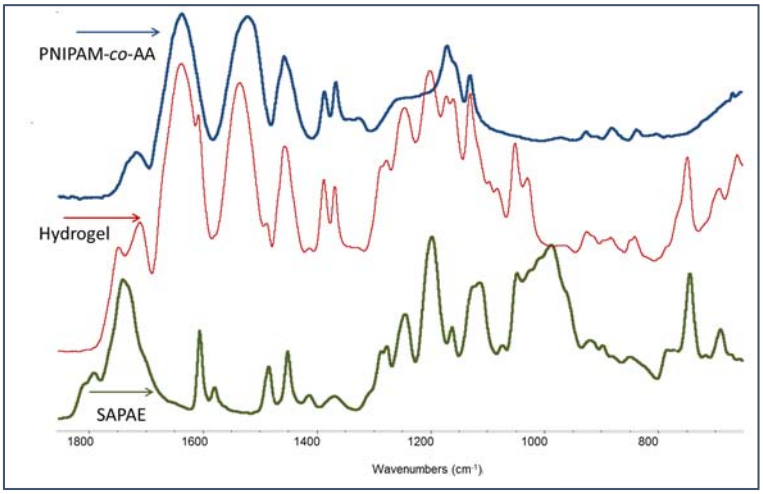

Figure 2.3: FT-IR spectrum of blends comparing the carbonyl and amine group region of SAPAE (green line), PNIPAM-*co*-AA (blue line) and PN:SAPAE hydrogel (red line). The peak shifting of the carbonyl (~1700 cm^{-1}) and amine groups (~1520 cm^{-1}) in FT-IR

spectroscopy suggests interaction between PNIPAM-*co*-AA and SAPAE. The hydrogel spectrum at the top is the 7:3 ratio, which is also representative of the 6:4 hydrogel system.

Table 2.1: Summary of the relevant FT-IR peaks of the SAPAE, PNIPAM-*co*-AA, and PN:SAPAE hydrogel systems.

Compound Name	Functional Vibrations	Wavenumbers (cm^{-1})
SAPAE	C=O stretch, anhydride	1790
	C=O stretch, ester	1742
PNIPAM-*co*-AA	C=O stretch, carboxylic acid	1716
	C=O stretch, amide	1635
	N-H deformation, amide	1520
PN:SAPAE hydrogel	C=O stretch	1746, 1709, 1637
	N-H stretch	1534

2.3.2. Swelling behavior

The swelling behaviors of PN:SAPAE hydrogels were measured in phosphate buffer (pH 7.4) at RT and 37 °C. As shown in **Figure 2.4**, increasing acrylic acid content (i.e., the hydrophilic segments of the polymer) resulted in higher swelling Q value, which is consistent with other acrylic-based hydrogels.[29] At pH 7.4, carboxylic groups are ionized, which increases intermolecular repulsion and ionic swelling forces. Similar to

previously published PNIPAM-*co*-AA based hydrogels, pH changes are the major contributors to swelling behavior.[22, 30] In previous work, swelling studies were performed at pH values lower and higher than the acrylic acid *pKa* (4.2) at different temperatures. At low pH values, temperature is the predominant influence on swelling, whereas at higher pH values, pH is the major influence.[22, 30] A similar trend was observed for PN:SAPAE hydrogel systems: The swelling values were slightly different between the two temperatures, whereas pH is the main contributor to swelling behavior.

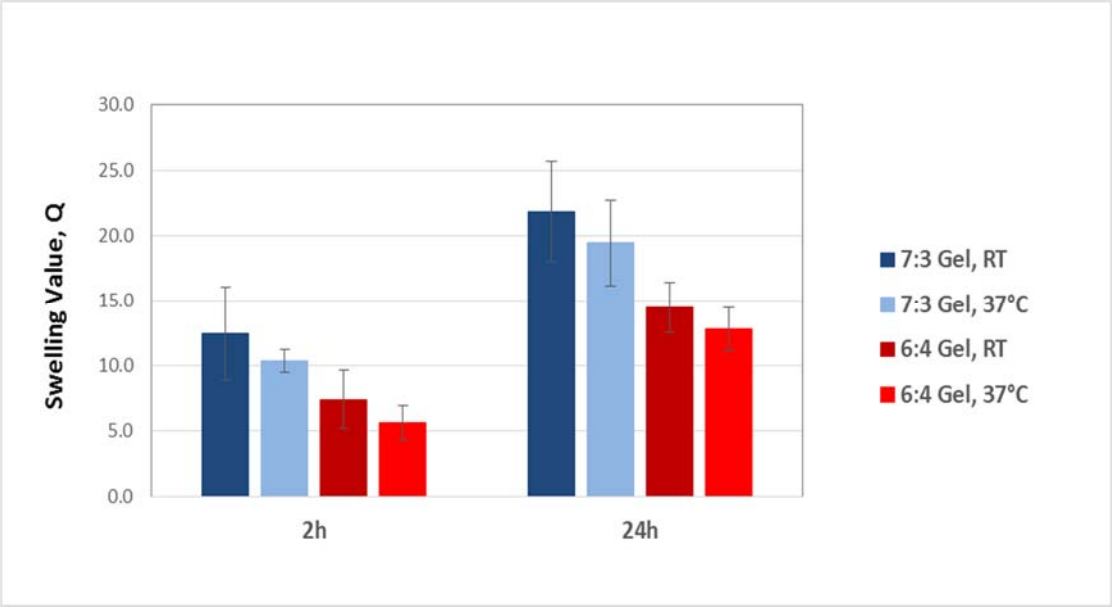

Figure 2.4: Swelling values (Q) in pH 7.4 buffer at room temperature (RT) (25 °C) and 37 °C at 2 and 24 hours for two ratios of PN:SAPAE hydrogels according to Equation 2.2. Data are presented as mean ± standard deviation (n=3 in each group).

2.3.3. Hydrogel morphology

All of the hydrogels exhibit porous structures (**Figure 2.5**), with pore sizes increasing with increasing PNIPAM-*co*-AA content. Generally, pore sizes are between 21.3–12.8 μm and 4.3–10.6 μm for the 7:3 and 6:4 ratios, respectively. Notably, these pore sizes are similar to BSA-incorporated, poly(ethylene glycol)-modified PNIPAM hydrogels,[31] which suggests that PN:SAPAE-based hydrogels exhibit sufficient pore size to incorporate BSA.

Hydrogel pore size is influenced by AA density: Increasing the AA content (i.e., the hydrophilic co-monomer) resulted in gels with the highest amount of swelling, which led to larger pore sizes. In addition, increasing the concentration of SAPAE increases the hydrophobic percentage of the hydrogels and the hydrophobic interactions between polymers. Consequently, the swelling and pore sizes of the hydrogel systems decrease. Thus, the 7:3 gel with the higher AA concentration and lower SAPAE concentration has the larger pore size.

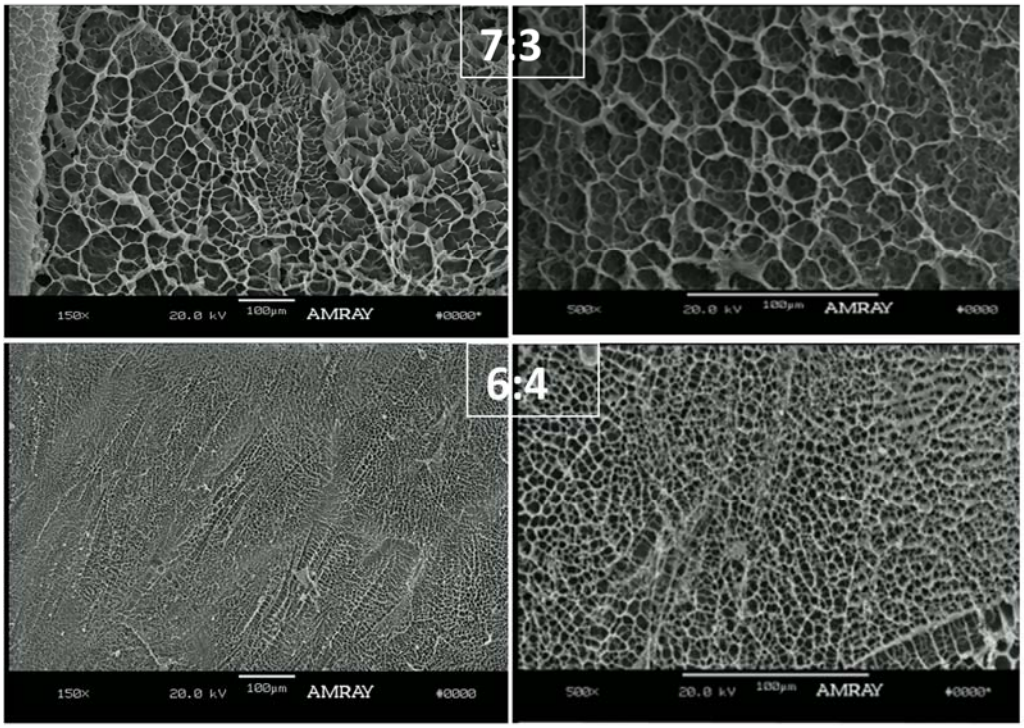

Figure 2.5: SEM images of freeze-dried PN:SAPAE hydrogels at two different blending ratios (7:3 ratio at top, 6:4 ratio at bottom) at the 24-hour swelling time point. Films are shown at 150x (left) and 500x (right) magnification.

2.3.4. *In vitro* SA release

PN:SAPAE hydrogels were designed to release SA and physically incorporated proteins (i.e., BSA) in a controlled manner. A correlation between pore size and SA release rate was observed, with larger pore sizes releasing SA faster. This effect is presumably due to greater water penetration into the films. The faster water penetration promotes quicker SA release, as the anhydride and ester bonds are more readily hydrolyzed. Thus, the gel with higher pore size (i.e., 7:3 gel) exhibits a slightly faster SA release rate. As shown in **Figure 2.6**, 93.3% (12 mg) and 79.9% (10 mg) salicylic acid was released from the 7:3 and 6:4 gels, respectively, within 72 hours. The 7:3 gel released 100% SA within 4 days, while the 6:4 gel achieved 100% SA release in 5 days. In previous publications, similar trends were observed, with increasing pore size correlating to increased release profile.[29]

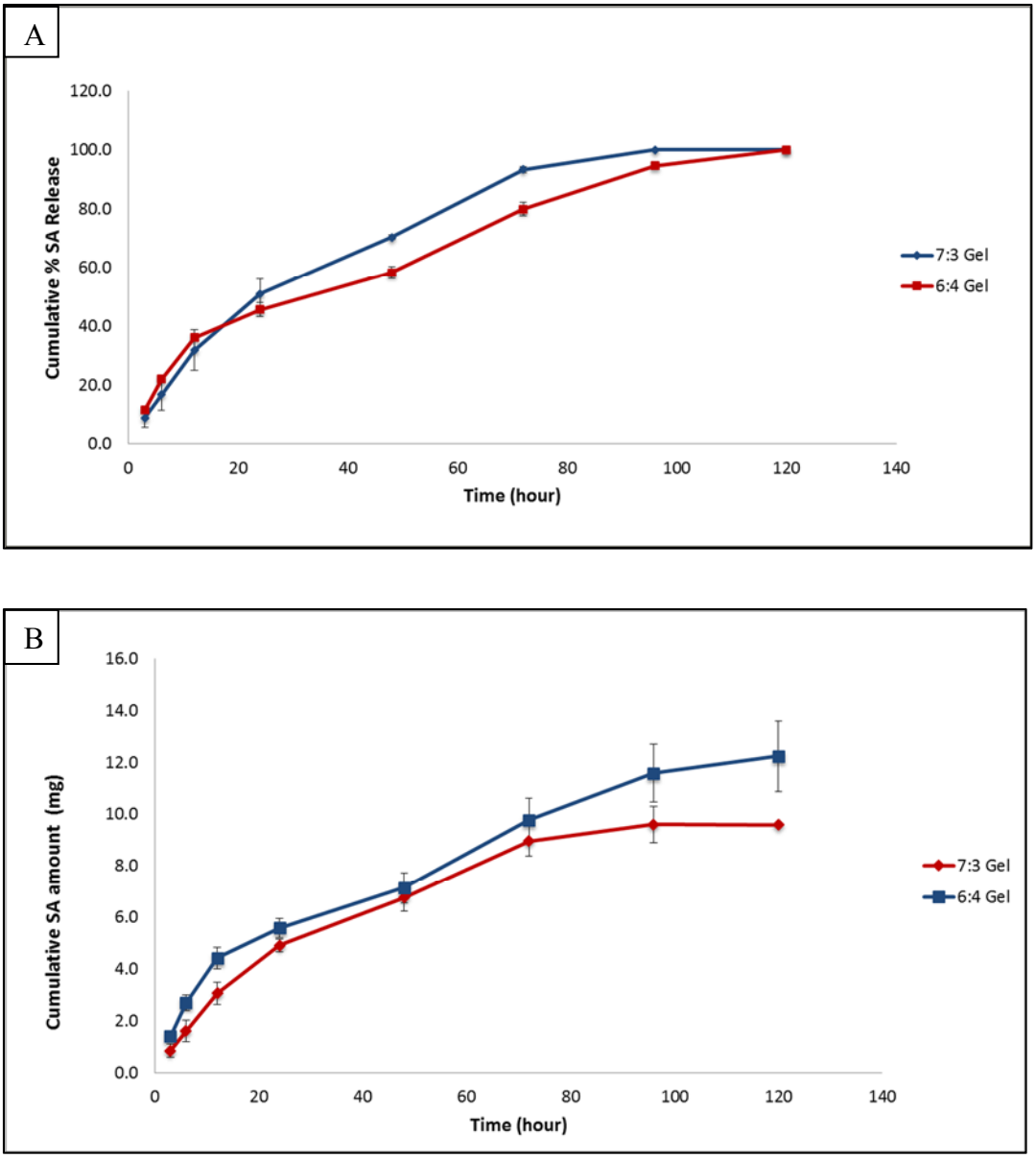

Figure 2.6: *In vitro* release of salicylic acid from the PN:SAPAE hydrogels represented as normalized cumulative SA release as a percentage (A) and cumulative SA amount in mg (B) in pH 7.4, as quantified by UV-Vis spectrophotometry (λ= 303 nm). Data are presented as mean ± standard deviation (n=3 in each group).

2.3.5. BSA loading and release

BSA loading was achieved via a swelling-diffusion technique[24] in PBS buffer (pH 7.4). Overall, hydrogels had sufficient pore size to incorporate BSA into the swollen networks. As shown in **Figure 2.7**, 23% and 17% BSA was encapsulated into the 7:3 and 6:4 gels, respectively. Similar to SA release, the correlation between pore size and loading percentage was observed: The 7:3 gel has the larger pore size and higher percent BSA loading. Moreover, the BSA loading of the 7:3 and 6:4 gels are higher than conventional PNIPAM hydrogels loading (~10%), as conventional hydrogels pore sizes are significantly smaller.[31]

Conventional PNIPAM hydrogels did not exhibit extended release behavior, as these hydrogels do not exhibit pore structures capable of encapsulating BSA.[31] Compared to conventional hydrogels, PN:SAPAE hydrogels exhibit controlled BSA release, as the BSA molecules enter into PN:SAPAE hydrogels, which results in slower BSA release. As shown in **Figure 2.8**, BSA released slightly faster in 7:3 gel, correlating well with pore size. After 72 hours, 87% and 78% of BSA was released from the 7:3 and 6:4 gels, respectively. Moreover, 100% BSA release was achieved in 4 days, similar to SA release.

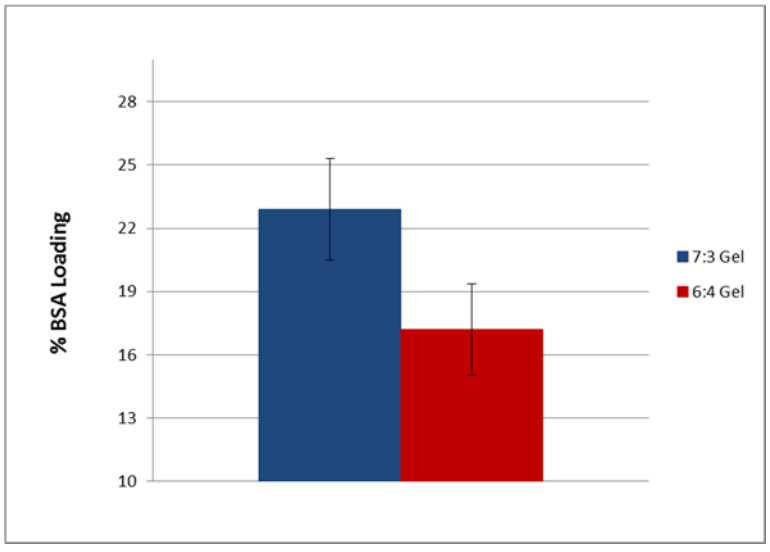

Figure 2.7: BSA loading of the PN:SAPAE hydrogels via swelling-diffusion technique as determined by BCA assay. Data are presented as mean ± standard deviation (n=3 in each group).

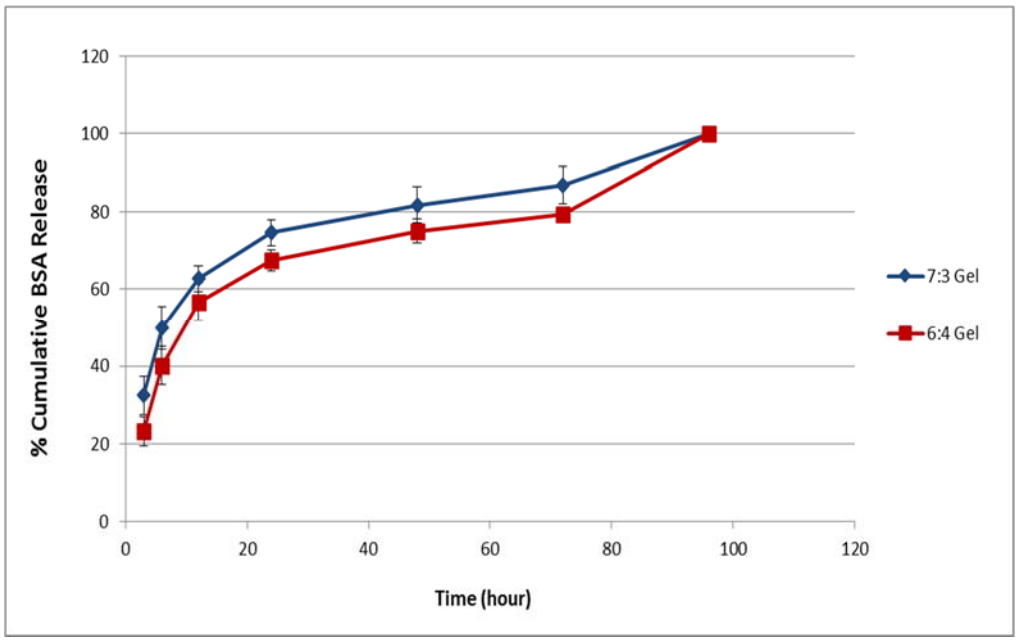

Figure 2.8: *In vitro* release of BSA from the PN:SAPAE hydrogels represented as normalized cumulative BSA release as a percentage, in pH 7.4 phosphate buffer at 37 °C as determined by BCA assay. Data are presented as mean ± standard deviation (n=3 in each group).

2.3.6. Cytotoxicity of the hydrogels

Cytotoxicity against 3T3 cells was determined at two different concentrations of the polymer solution in which the anti-inflammatory effect of the SA is observed, 0.1

mg/mL and 0.01 mg/mL, with DMSO (1%) used as control. As shown in **Figure 2.9**, the results indicated that cell viabilities in the presence of the gels were not statistically different from the DMSO controls.

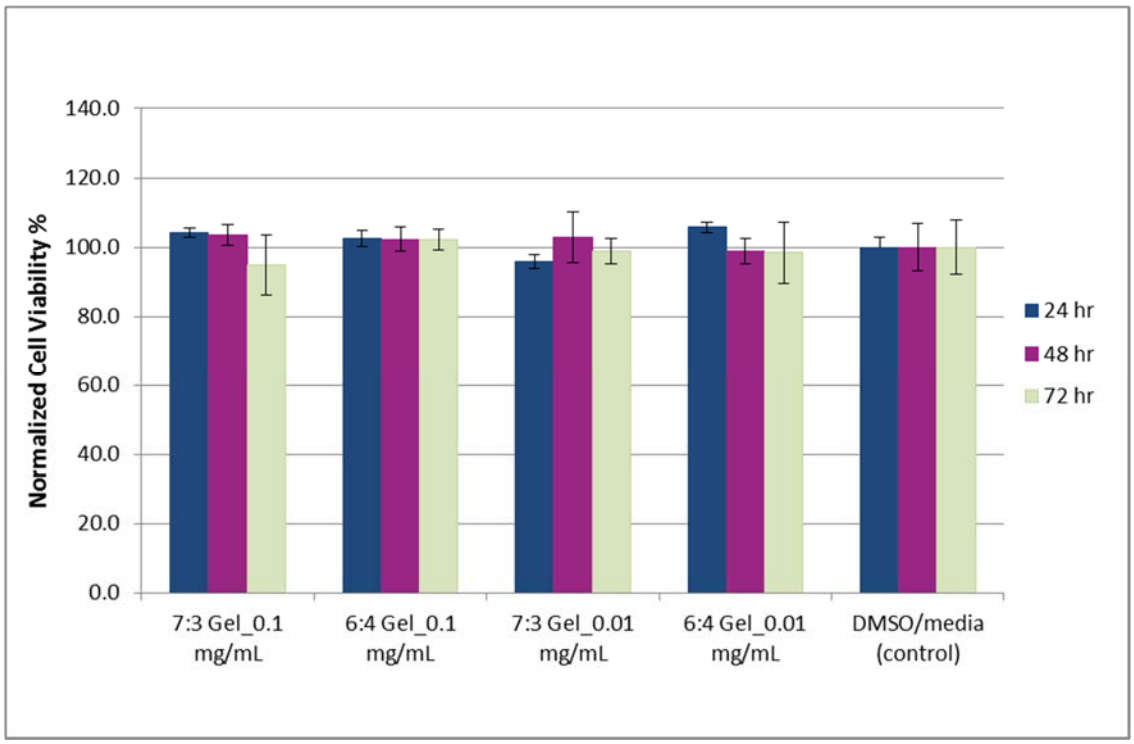

Figure 2.9: Cytotoxicity profile of the different concentrations of the hydrogels after 24-, 48-, and 72-hour incubation. All groups contained 1% DMSO in cell media and the control group has no polymer. Absorbance at 490 nm after MTS treatment is proportional to cell viability. Data are presented as mean ± standard deviation (n=6 in each group). The cell viability of each of the hydrogels was not statistically different from the media with DMSO control.

2.3.7. LCST determination

As these hydrogels contain a temperature-sensitive polymer and LCST measurements were performed to evaluate temperature-responsive behavior. At lower temperatures, PNIPAM-*co*-AA forms hydrogen bonds with water molecules and the hydrophilic component is more dominant: As the temperature increases, the hydrophobic interactions become stronger.[9,32] At the LCST, the transition between hydrophilic to hydrophobic interactions is observed.[32] In general, polymers that contain the larger hydrophobic domains have a lower LCST. Previously, LCST differences between PNIPAM and PNIPAM-*co*-AA have been investigated.[33] As the hydrophobic density of PNIPAM is much higher compared to PNIPAM-*co*-AA, the LCST was lower than PNIPAM-*co*-AA.[34] In PN:SAPAE hydrogels, the introduced hydrophobic SAPAE affects the LCST values: 31.0 °C ± 0.5 and 28.1 °C ± 1.1 for the 7:3 and 6:4 gels, respectively. The hydrogel blends have lower LCST compared to the polymer alone, PNIPAM-*co*-AA at 33.0 °C. Moreover, the LCST of the 6:4 gel is lower than that of the 7:3 gel, as its SAPAE content (hydrophobic segment of the hydrogel) is higher.

2.4. Conclusion

Physically cross-linked PN:SAPAE hydrogels were developed at different ratios via a solvent-casting method to form films. These hydrogel systems showed porous structures that enable incorporation of the protein, BSA, which is then released in a sustained manner. In addition to BSA, these hydrogel systems released SA over 4 days in a sustained manner. These systems are unique as they can deliver SA in conjugation with

a model protein, BSA, which can potentially increase the bioactivity of each component through synergistic effects.

2.5. References

1. C.S. Satish, K.P.Satish, H.G. Shivakumar. Hydrogels as controlled drug delivery systems: Synthesis, crosslinking, water and drug transport mechanism. Indian journal of pharmaceutical sciences 68, 133-140 (2006).

2. L.Brannon-Peppas, R.S.Harland. Absorbent polymer technology. Elsevier, 45-66 (1990).

3. M.S. Bindu, V.Ashok, A. Chatterjee. As a review on hydrogels as drug delivery in the pharmaceutical field. International Journal of pharmaceutical and chemical sciences 1 (2), 642-661 (2012).

4. N.A. Peppas, A.G.Mikos. Hydrogels in medicine and pharmacy. CRC press, Boca Raton, FL 1, 1-27 (1986).

5. N.A. Peppas, Y.Huang, M. Torres-Lugo, J.H. Ward, J. Zhang. Physicochemical foundations and structural design of hydrogels in medicine and biology. Annual review of biomedical engineering 2, 9-29 (2000).

6. L. C. Lopérgolo, A. B. Lugão, L. H. Catalani. Direct UV photocrosslinking of poly(N-vinyl-2-pyrrolidone) (PVP) to produce hydrogels. Polymer 44, 6217-6222 (2003).

7. T.R. Hoare, D.S.Kohane. Hydrogels in controlled release formulation: Network design and mathematical modeling. Advanced drug delivery reviews 58, 1379-1408 (2008).

8. H. Park, K. Park. Hydrogels and biodegradable polymers for bioapplications. American chemical society 627, 2-10 (1996).

9. Y. Qiu, K.Park. Environment-sensitive hydrogels for drug delivery. Advanced drug delivery reviews 64, 49-60 (2012).

10. E. Bastiannet, K.Sampieri, O. Dekkers, A. de Craen. et al. Use of aspiring postdiagnosis improves survival for colon cancer patients. British journal of cancer 106, 1564-1570 (2012).

11. R. S. Hundal, et al. Mechanism by which high-dose aspirin improves glucose metabolism in type 2 diabetes. Journal of clinical investigation 109, 1321-1326 (2002).

12. M. Nixon, D.J.Wake, D. E. Livingstone, R. H. Stimson, C. L. Esteves, J. R. Seckl, K. E. Chapman, R. Andrew, B. R. Walker. Salicylate downregulates 11B-HSD1 expression in adipose tissue in obese mice and in humans, mediating insulin sensitization. Diabetes 61, 790-796 (2012).

13. R. Yamazaki, N.Kusunoki, T. Matsuzaki, et al. Aspirin and sodium salicylate inhibit proliferation and induce apoptosis in rheumatois synovial cells. Journal of pharmacy and pharmacology 54, 24-32 (2002).

14. K. Wu. Aspirin and salicylate: and old remedy with a new twist. Circulation 102, 2022-2023 (200).

15. A. Prudencio, R.C.Schmeltzer, K. E. Uhrich. Effect of Linker Structure on Salicylic Acid-Derived Poly(anhydride-esters). Macromolecules 38, 6895-6901 (2005).

16. R. C. Schmeltzer, T.J.Anastasiou, K. E. Uhrich. Optimized synthesis of salicylate-based poly(anhydride-esters). Polymer bulletin 49, 441-448 (2003).

17. M. A. Reynolds, A.Prundencio, M.E. Aichelmann-Reidy, et al. Non-steroidal anti-inflammatory drug (NSAID)-derived poly(anhydride-esters) in bone and periodontal regeneration. Current drug delivery 4, 233-239 (2007).

18. K. Wada, W.Yu, M. Elazizi, S. Barakat, M. Ouimet, R. Rosario-Melendez, J. Fiorellini, D. Graves, K. Uhrich. Locally delivered salicylic acid from a poly(anhydride-ester): impact on diabetic bone regeneration. Journal of controlled release 171, 33-7 (2013).

19. M. A. Ouimet. Design, synthesis, and fabrication of biodegradable, bioactive-based polymers for controlled release applications. Thesis, Rutgers, The State University of New Jersey (2013).

20. W. Brostow, R.Chiu, I. M. Kalogeras, A. Vassilikou-Dova. Prediction of glass transition temperatures: Binary blends and copolymers. Materials letters 62, 3152-3155 (2008).

21. K. Nakamura, R.Murray, J. Joseph, N. Peppas, M. Morishita, A. Lowman. Oral Insulin delivery using P(MAA-g-EG) hydrogels: Effect of network morphology on insulin delivery characteristics. Journal of controlled release, 589-599 (2004).

22. X. Gao, Y.Cao, X. Song, Z. Zhang, C. Xiao, C. He, X. Chen. pH and thermo-responsive poly(N-isopropylacrylamide-*co*-acrylic acid derivative) copolymers and hydrogels with LCST dependent on pH and alkyl side groups. Journal of materials chemistry B 1, 5578-5587 (2013).

23. L. Yin, L.Fei, F. Cui, C. Tang, C. Yin. Superporous hydrogels containing poly(acrylic acid-*co*-acrylamide)/ O-carboxymethyl chitosan interpenetrating polymer networks. Biomaterials 28, 1258-1266 (2007).

24. M. Morishita, A.M.Lowman, K. Takayama, T. Nagai, N.A. Peppas. Elucidation of the mechanism of incorporation of insulin in controlled release systems based on complexation polymers. Journal of controlled release 81, 25-32 (2002).

25. J. Shi, N.Alves, J. Mano. Drug release of pH/temperature-responsive calcium alginate/poly(N-isopropylacrylamide) semi-IPN beads. Macromolecular bioscience 6, 358-363 (2006).

26. J. Koening. Chemical microstructure of polymer. Wiley (1980).

27. T. Aoki, M.Kawashima, H. Katono, K. Sanui, N. Ogata, T. Okano. Temperature-responsive interpenetrating polymer networks constructed with poly(acrylic acid) and poly(N,N-dimethylacrylamide). Macromolecules 27, 947-952 (1994).

28. J. Zhang, N.Peppas. Molecular interactions in poly(methacrylic acid)/poly(N-isopropyl acrylamide) interpenetrating polymer networks. Journal of applied polymer science 82, 1077-1082 (2001).

29. B. Demirdirek, K.U. Salicylic acid-based pH-sensitive hydrogels as potential oral insulin delivery systems. Journal of drug targeting (2015).

30. C. Zhao, X.Zhuang, P.He, C. Xiao, C. He, J. Sun, X. Chen, X. Jing. Synthesis of biodegradable thermo- and pH-responsive hydrogels for controlled drug release. Polymer 50, 4308-4316 (2009).

31. R. Zhuo, W.Li. Preparation and characterization of macroporous poly(Nisopropylacrylamide) hydrogels for the controlled release of proteins. Journal of polymer science part A: polymer chemistry 41, 152-159 (2003).

32. G. Grassi, R.Farra, P. Caliceti, G. Guarnieri, S. Salmaso, M. Carenza, M. Grassi. Temperature-sensitive Hydrogels. American journal of drug delivery 3, 239-251 (2005).

33. X. Lin, D.Tang, Z. Yu, Q. Feng. Stimuli-responsive electrospun nanofibers from poly(N-isopropylacrylamide)-*co*-poly(acrylic acid) copolymer and polyurethane. Journal of materials chemistry 2, 651-658 (2013).

34. R. Stile, W.Burghardt, K. Healy. Synthesis and characterization of injectable poly(N-isopropylacrylamide)-based hydrogels that support tissue formation in vitro. Macromolecules 32, 7370-7379 (1999).

3. SALICYLIC ACID-BASED pH-SENSITIVE HYDROGELS AS POTENTIAL ORAL INSULIN DELIVERY SYSTEMS

Reprinted with edits with permission from Demirdirek B., Uhrich KE, Journal of Drug Targeting 2015, 23:7-8, 716-724 ©2015 Taylor & Francis

3.1. Introduction

Hydrogel systems are important for protein delivery owing to their biocompatibility, tunable drug release by pore size control, and ability to protect proteins from denaturation in low pH.[1] Hydrogels are cross-linked networks of water-soluble polymers, capable of imbibing water or biological fluids [2-4] in which the networks are formed by chemical crosslinks (covalent bonding) or physical crosslinks (intermolecular interactions).[4-8] Acidic pH-sensitive hydrogels that contain pendant carboxylic acid moieties, such as acrylic acid, have attracted considerable interest for oral protein delivery due to their responsiveness to the pH shift in the gastro-intestinal (GI) tract.[9-12] Hydrogels comprised of polyanions minimally swell in the stomach (pH 1-2.5),[13] which makes protein release minimal. In the intestine, hydrogel swelling increases due to the rise in pH (6.0-7.5),[13] leading to faster protein release. In addition, carboxylic acid-based polymers, such as poly(acrylic acid) (PAA), exhibit mucoadhesive behavior,[14, 15] which enables adhesion to mucosal membranes and improves the bioavailability of oral protein therapeutics

through decreasing the drug clearance rate.[15-17] Furthermore, PAA-based hydrogel systems can be used to mitigate degradation in acidic environments and poor membrane permeability of orally-administrated insulin.[15, 16, 18]

Currently, individuals suffering from diabetes must administer insulin via injection.[19, 20] However, injection is not the most favorable route of administration due to pain, discomfort, and potential infections.[16] Oral insulin delivery can thus benefit many diabetic patients and has been pursued by many research teams.

Recent studies have shown that inflammation exacerbates type 2 diabetes and that salicylates, a family of anti-inflammatory compounds, can reduce insulin resistance.[21-25] These studies suggest that salicylic acid may affect oxidative stress, insulin resistance and vascular inflammation and is not dose-dependent.[26] In light of this work, an oral delivery system was investigated that could deliver both insulin and salicylic acid. Salicylic acid-based poly(anhydride esters) (SAPAEs) have been researched over the past decade.[27, 28] Within these systems, salicylic acid is chemically incorporated into the polymer backbone, leading to high drug loading (85%) and enabling a controlled, sustained release of salicylic acid upon polymer degradation (**Figure 3.1**). Furthermore, SAPAEs can mitigate inflammation when implanted *in vivo*.[29] In this research, (SAPAEs) with an adipic linker molecule were blended with poly(acrylic acid), (PAA) to generate pH-sensitive, physically cross-linked hydrogels, which can be used to overcome oral insulin delivery challenges and benefit diabetes patients by releasing salicylic acid (SA) and insulin in a controlled manner.

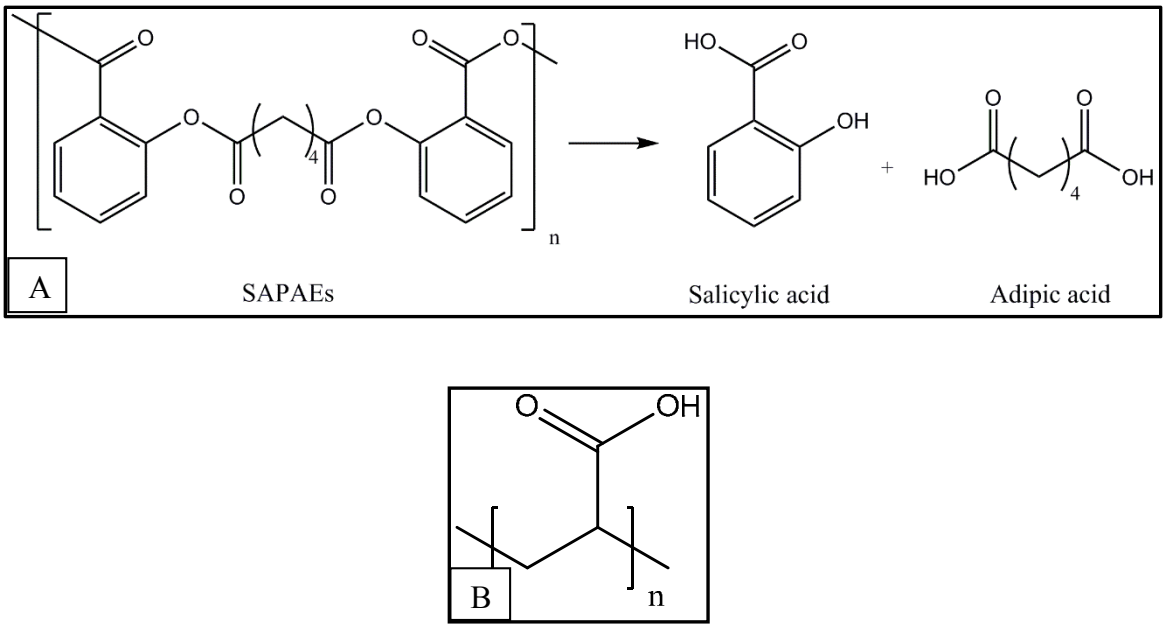

Figure 3.1: Chemical structures of (A) SAPAEs and its degradation products (salicylic acid and adipic acid), and (B) poly(acrylic acid), (PAA).

3.2. Experimental Section

3.2.1. Materials

Fetal bovine serum (FBS) was purchased from Atlanta Biologicals (Lawrenceville, GA). Fibroblast cells were purchased from ATCC (Manassas, VA). Hydrochloric acid and Thermo Scientific Pierce Micro bicinchoninic acid (BCA) Protein Assay Kit were purchased from Fisher Scientific (Fair Lawn, NJ). Poly(acrylic acid), Mw =1,250,000 and

all other chemicals and reagents were purchased from Sigma-Aldrich (Milwaukee, WI). All reagents were used without further purification.

3.2.2. Hydrogel formation

SAPAEs were synthesized according to a previously published method.[27,28] Briefly, salicylic acid was dissolved in tetrahydrofuran (THF) and pyridine. Adipoyl chloride (1 eq) was dissolved in THF and added drop-wise, forming a white suspension. The reaction mixture was quenched over water, and acidified to pH 2 using concentrated HCl. The formed precipitate was filtered, washed with water (3 × 250 mL), and dried in vacuo to yield diacid intermediate. The diacid intermediate was added to an excess of acetic anhydride, then stirred overnight under argon at room temperature. The excess acetic anhydride was removed *in vacuo*. The resulting acetyl-terminated monomer was heated at 180 °C under vacuum for 4-6 hours to yield yellow, solid SAPAE. Following successful SAPAE synthesis, PAA:SAPAE physically cross-linked hydrogels were formulated using a slightly modified method.[30] Varying weight ratios of PAA:SAPAE (7:3, 6:4, 5:5) were prepared: PAA at 105, 90, and 75 mg (**Figure 3.1**) was separately weighed into scintillation vials (20 mL) and dissolved in anhydrous DMF at room temperature and stirred for 48 hours. After 48 h, SAPAE (45, 60, and 75 mg) were added separately to the PAA solutions and stirred for an additional 24 hours at room temperature. The resulting viscous solutions (1 mL, 5% w/v) were solvent-cast into Teflon beakers (28 mm diameter) via syringe and dried in a vacuum oven at 80 °C overnight to form films (n=3).

FT-IR absorbance spectra were measured on a Thermo Nicolet FT-IR spectrometer to analyze polymer blend interactions. Miscibility was analyzed using DSC using TA Instruments Q200 DSC (New Castle, DE). PAA:SAPAE films, PAA, and SAPAE alone (~5 mg) were analyzed by heating under dry nitrogen from -10 °C to 200 °C at a rate of 10 °C/min and cooling to -10 ˚C at 10 ˚C/min with a three-cycle minimum. The data was analyzed using TA instruments Universal Analysis 2000 software.

The predicted glass transition (T_g) values for blends were calculated using the Fox equation (Equation 3.1).[31]

$$\frac{1}{T_{g,blend}} = \frac{W_{PAA}}{T_{PAA}} + \frac{W_{SAPAE}}{T_{g,SAPAE}} \qquad \textbf{Equation 3.1}$$

where $T_{g,blend}$ represents the miscible blend, $T_{g,i}$ the noted pure component i (PAA and SAPAE), and w_i the weight fraction of noted component i.

3.2.3. Swelling behavior

To measure the swelling values of the hydrogels, the dried films were immersed in pH 6.8 phosphate buffer and 0.1 N HCl for 2 and 24 hours at room temperature. The swelling values, Q, were calculated according to following equation:[32-34]

$$Q = \frac{Ws - Wd}{Wd} \qquad \textbf{Equation 3.2}$$

where W_s and W_d are the weights of the swollen and dried films, respectively. All experiments were carried out triplicate and the average values reported.

3.2.4. Hydrogel morphology

The hydrogel morphology was investigated using SEM. PAA:SAPAE films were swollen in deionized water (50 mL) for 24 hours and then lyophilized for 12 hours for SEM imaging. The samples were coated with Au/Pd using a sputter coater (SCD 004, Balzer Union Limited) and images were obtained using an AMRAY-1830I microscope (Amray, Inc.).

3.2.5. Insulin loading

To incorporate insulin into PAA:SAPAE hydrogels, a swelling-diffusion method was used.[35] In brief, dried PAA:SAPAE films (80 ±10 mg, 3.0 cm) were incubated in 4 mL of premade insulin solutions in phosphate-buffer saline (PBS) (1 mg/mL, pH 7.4) at 4 °C. After 5 hours, the films were removed and rinsed and collapsed with ~5 mL of 0.1 N HCl. The remaining insulin solution and rinse solutions were collected for insulin analysis. The amount of protein was determined using a Micro BCA assay according to the manufacturer's protocol. Non-loaded gels were subjected to the same protocol as a negative control. Experiments were performed in triplicate. The drug loading (%) was calculated according to the following equation:[33]

$$\text{Drug loading \%} = \frac{Wpl}{Wps} \times 100, \qquad \textbf{Equation 3.3}$$

$$Wpl = Wps - Wpls$$

where W_{pl}, W_{ps} and W_{pls} are the weights of the protein loaded into gels, the protein in the solution before loading, and the protein in the solution after loading, respectively.

3.2.6. Insulin release

To monitor insulin *in vitro* release, insulin-loaded hydrogels or non-loaded hydrogels were immersed in 50 mL centrifuge tubes containing either 10 mL PBS (pH 6.8) or 0.1 N HCl (pH 1.2) at 37 ˚C. At set time points, 5 mL of media was removed and replaced with 5 mL fresh media. The insulin amount was determined using Micro BCA protein assay and normalized against the non-loaded hydrogels to eliminate possible absorbance from salicylic acid. The experiments were carried out until insulin release was no longer detected in PBS media. Experiments were performed in triplicate.

3.2.7. Insulin stability

To analyze the insulin physical and chemical stability, insulin-loaded hydrogels were immersed in 50 mL centrifuge tubes containing 10 mL PBS (pH 6.8) at 37 ˚C for 24 hours. After 24 hours, the release solution was analyzed using size exclusion chromatography (SEC) to evaluate possible aggregates (high molecular weight species)

and imaged capillary isoelectric focusing (iCIEF) to evaluate possible deamidation via measuring the isoelectric point of the insulin.

SEC was performed using Agilent 1100 system with 7.8 mm 30 cm TSKgel G3000SWXL SEC column from Tosoh Bioscience at 276 nm. The flow rate was 0.7 mL/min and the injection volume was 100 µL. The mobile phase composition was 1 mg/mL of L-arginine, acetonitrile, and glacial acetic acid (65:20:15).

iCIEF was performed using Protein Simple iCE equipment. The sample was prepared using the following chemical compositions: 70 µL 1% methyl cellulose, 8 µL Pharmalyte 3-10, 1 µL pI Marker 4.22, 1 µL pI Marker 8.79, 50 µL 8M urea, 45 µL Milli-Q Water, and 25 µL sample. The system suitability was prepared using 5.78 pI marker. The samples were compared with insulin standard loading solution (LDS), which was stored for 24 hours at 37°C.

3.2.8. *In vitro* SA release

PAA:SAPAE films (60 ± 10 mg) were placed in 50 mL centrifuge tubes containing either 10 mL phosphate-buffer saline (PBS) (pH 6.8) or 0.1 N HCl (pH 1.2) and incubated (37 ˚C, 60 rpm). At set time points, 5 mL aliquots of media were removed and replaced with 5 mL fresh PBS. Released SA was monitored by ultraviolet (UV) spectrophotometry using a Perkin Elmer Lambda XLS spectrophotometer. The measurements were collected at λ = 303 nm, where the maximum SA absorbance did not overlap with PAA or other degradation products. A SA calibration curve was prepared and absorbance data was

calculated by using a calibration curve. The release experiment was carried out until SA release was no longer detected in pH 6.8 buffer. In 0.1 N HCl media, release experiments continued until SA release slowed significantly. 0.1 N NaOH was then added to hydrolyze any remaining SA. The experiments were normalized to 100%. All sets of experiments were performed in triplicate.

3.2.9. Cytotoxicity of the hydrogels

Hydrogel cytocompatibility was performed by culturing 3T3 fibroblast cells in media containing the dissolved polymer blends. The polymer blends were dissolved in DMSO as a stock solution and serially diluted with cell culture media. Cell culture media consisted of Dulbecco's Modified Eagle's Medium (DMEM), 10% v/v fetal bovine serum, 1% L-glutamate, and 1% penicillin/streptomycin. The cells were seeded in a 96-well plate at 2,000 cells per well in 100 μL media. After incubation for 1 hour, the polymer-containing media in 1% DMSO at various concentrations at which anti-inflammatory effects were observed (0.1 mg/mL, 0.01 mg/mL and 0.001 mg/mL) were added to the wells. The media with dissolved polymer was compared to DMSO-containing media (1% v/v) as a control. For the fibroblasts, cell viability was determined by using MTS (3-(4,5-dimethylthiazol-2-yl)-5-(3-carboxymethoxyphenyl)-2-(4-sulfophenyl)-2H-tetrazolium) assay at 24, 48, and 72 hours. After 3 hours incubation, the absorbance was recorded with a microplate reader at λ = 490 nm.

3.2.10. Mucoadhesion behavior

A previously published method was performed to analyze mucoadhesion properties of the hydrogels using Texture Analyzer, TA-XT2.[36, 37] The hydrogels were adhered to the upper holder and wetted with pH 6.8 phosphate buffer and 30% mucin gel in pH 6.8 phosphate buffer was attached to the lower, stationary part of the Texture Analyzer. The mucin layer and hydrogels were brought in contact for 100 seconds with 7.8 N applied force, then the upper part was raised at a speed of 0.1 mm/s. The mucin layer alone was used as a control. The force of detachment and distance was recorded. The mucoadhesion performance of the gels was determined by measuring the resistance to the withdrawal of the upper holder, maximum detachment force F_{max} in "g" and work of adhesion is F_{max} * distance. Experiments were performed in triplicate.

3.3. Results and Discussion

3.3.1. Hydrogel formation

To develop salicylic acid-based pH-sensitive hydrogel systems, SAPAEs were blended with PAA at three different ratios: 7:3, 6:4, and 5:5 (PAA:SAPAE). Blends were solvent-cast into films and characterized by FT-IR, DSC, and swelling studies.

FT-IR studies determined interactions between SAPAE and PAA, notably between the carbonyl groups. In the FT-IR spectrum of SAPAE, peaks at 1790 cm^{-1} represent the -C=O double-bond stretching vibrations in the anhydride groups, whereas the peak at 1742 cm^{-1} represents the -C=O double-bond stretching vibration in the ester groups of SAPAEs, as shown in **Figure 3.2**. The peak at 1700 cm^{-1} represents the C=O double-bond stretching vibration of the PAA carboxylic acid groups. In the PAA:SAPAE films, the PAA carboxylic acid groups can interact with the carbonyl group of SAPAEs, resulting in hydrogen-bond formation. The peak shifting of the hydrogen-bonded functional groups in FT-IR spectroscopy suggests hydrogen-bond formation.[38,39] Notably, in the FT-IR spectrum of the PAA:SAPAE films, the C=O double bonds shift to 1740 and 1696 cm^{-1}, as shown in **Figure 3.2**. In addition, the C-O-C bond shifted from 1112 to 1129 cm^{-1}. Lastly, the hydrogen bonded -OH, 3456 cm^{-1}, was observed in PAA:SAPAE hydrogel (as shown in **Figure 3.2)**. Furthermore, the C-H stretch at 2940 cm^{-1} shifted to 2930 cm^{-1}, and the ArH peak 3109 cm^{-1} disappeared. The FT-IR results highlight the interactions between the carboxyl groups of PAA and carbonyl groups of SAPAE and PAA, which indicate that hydrogen-bonding occurs within the hydrogels. In addition, the width of the C=O peaks is increased compared to polymers, indicating hydrogen bond formation. Furthermore, the shift changes in the alkane and aromatic groups indicates hydrophobic interactions between polymers.

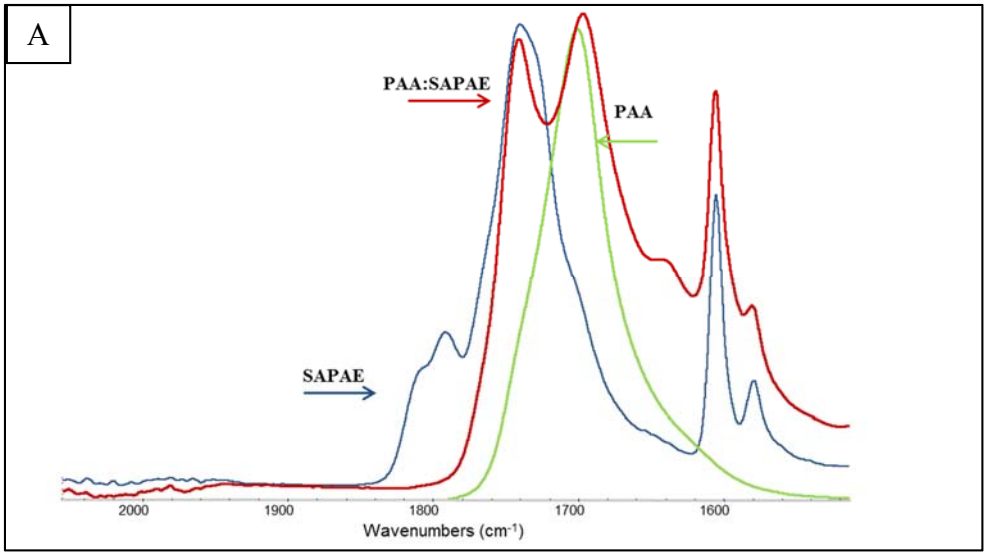

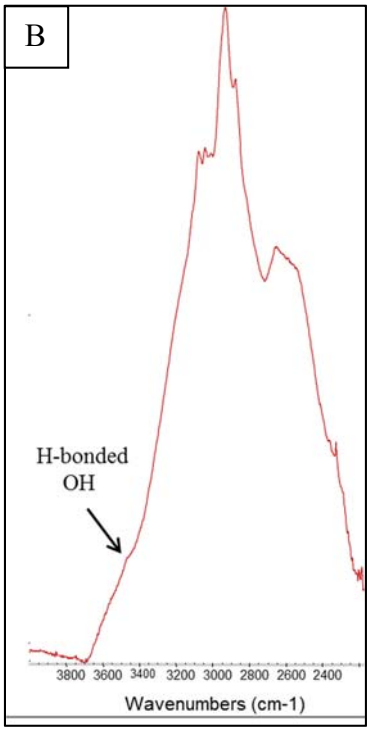

Figure 3.2: (A) FT-IR spectrum of blends comparing the carbonyl region of SAPAE (blue line), PAA (green line), and PAA:SAPAE hydrogel (red line). The peak shifting of the carbonyl groups (~1700 cm^{-1}) in FT-IR spectroscopy suggests the interaction between

PAA and SAPAE. (B) FT-IR spectrum of the -OH region of the PAA:SAPAE hydrogel. The labeled peak is consistent with H-bonding.

The T_g values of the films (PAA, SAPAE, and PAA:SAPAE) were analyzed using DSC (**Figure 3.3**) to determine if homogenous blends were formed. The T_g values of the hydrogels were 70, 75 and 81 for the 7:3 gel, 6:4 gel, and 5:5 gel ratios, respectively (**Figure 3.3**). The PAA:SAPAE films showed single T_g values, indicating uniform, homogenous gels. These experimental T_g values were compared with T_g values predicted by Fox analytical equations for a binary system.[31] The predicted T_g values were very close to the measured T_g values, which further validates that the polymer blends are miscible. Additionally, T_g values increased with increasing PAA content, as the PAA T_g values were much higher than the SAPAEs.

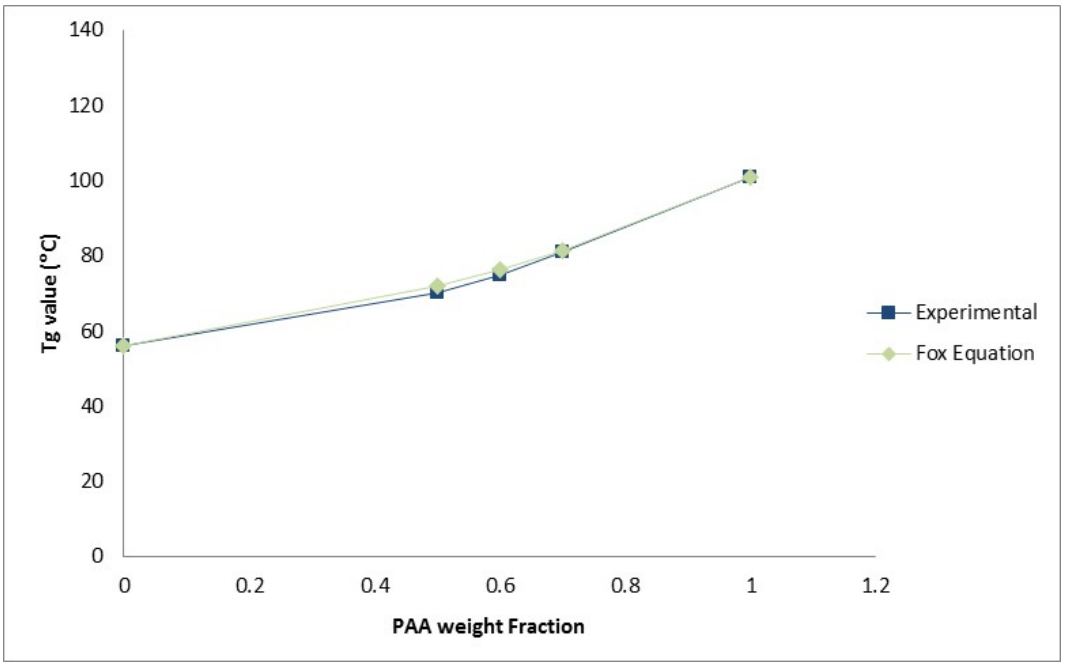

Figure 3.3: Experimental values of PAA and SAPAEs blends glass transition temperatures as compared to the Fox equation (Equation 3.1) values as a function of PAA weight fraction.

3.3.2. Swelling behavior

Swelling studies were performed to confirm whether hydrogels exhibited pH-responsive swelling behavior. The swelling behaviors of gels 7:3, 6:4, and 5:5 were measured in two different solutions: 0.1 N HCl (pH 1.2) and phosphate buffer solution (pH 6.8). As shown in **Figure 3.4.**, none of the gels swelled significantly at pH 1.2. The gels exhibited less swelling behavior at pH 1.2 as the amount of PAA increased. At pH 1.2, Q values of the gels within 2 hours were 1.80, 2.10, and 2.20 for 7:3, 6:4, and 5:5 gel ratios,

respectively. However, at higher pH values, gels swelled significantly. Increasing the PAA content resulted in gels with the highest amounts of swelling. At pH 6.8, Q values within 24 hours were 48.8, 29.6, and 19.1 for 7:3, 6:4 and 5:5 gel, respectively. These results correlated with trends previously published on acrylic acid-based polymers.[40-42] The hydrogels' pH-dependent properties come from the polyelectrolyte behavior of the PAA part of the physically cross-linked hydrogels. As the pH of the media increased, the hydrogels expand and incorporate water into the gels due to electric repulsion from the ionized carboxylic groups, which increase the ionic swelling force.[1] In addition to the PAA's pH-dependence, hydrophobic interactions between these polymeric systems are likely responsible for these physical cross-linked hydrogels. As a result, increasing hydrophobic SAPAEs concentration decreases swelling value in DI water.

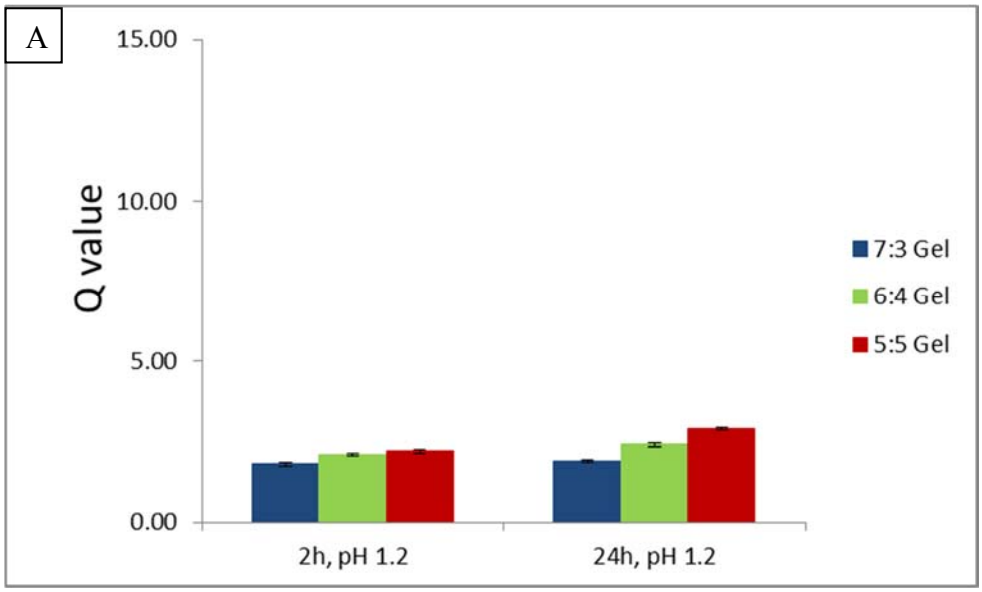

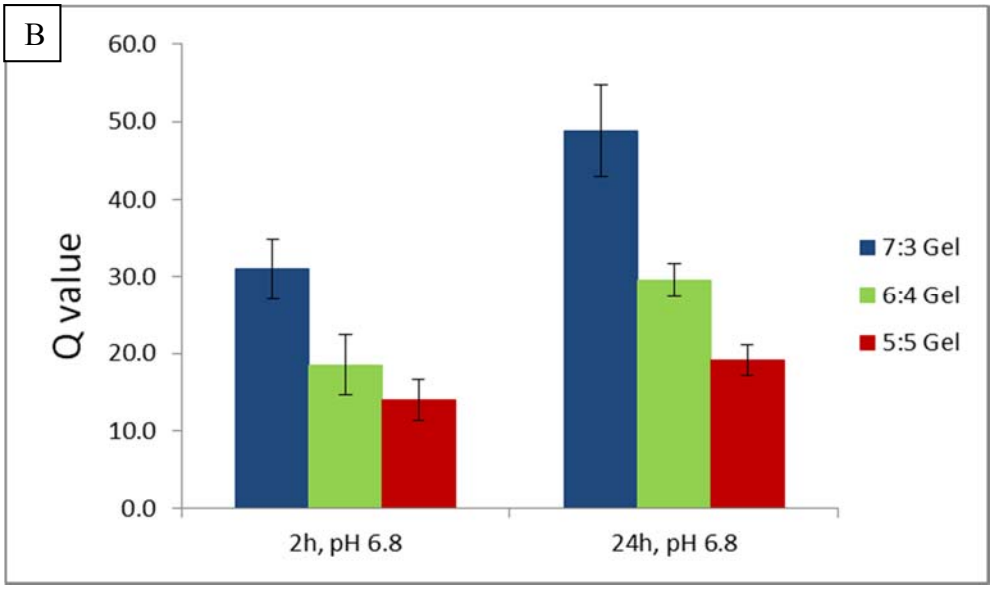

Figure 3.4: Swelling values (Q values) as a function of pH: (A) pH 1.2 and (B) pH 6.8 for three ratios of PAA:SAPAE hydrogels according to Equation 3.2. Data are presented as mean ± standard deviation (n=3 in each group).

3.3.3. Hydrogel morphology

As shown in **Figure 3.5**, all hydrogels exhibited porous structures, while the pore sizes differ with varying concentration of SAPAEs: As the SAPAE concentration decreased, pore size increased. The pore sizes of hydrogels are between 71.4–100 μm, 42.9–57.1 μm and 14.3–28.5 μm for the 7:3, 6:4, and 5:5 gel ratios, respectively.

In protein or drug delivery applications, porous hydrogels are beneficial as they allow for drug or protein diffusion and gas exchange. SEM was performed to examine the pore structure of the hydrogel in a swollen state. The pore sizes correlate to hydrophobic

interactions between the PAA and SAPAEs. Increasing the concentration of the SAPAEs appears to increase hydrophobic interactions between the two polymers such that the 5:5 gels have the smallest pore size. The pore sizes of the PAA:SAPAE hydrogels are in the range of previously published acrylic acid-based pH-dependent hydrogel systems.[34, 43]

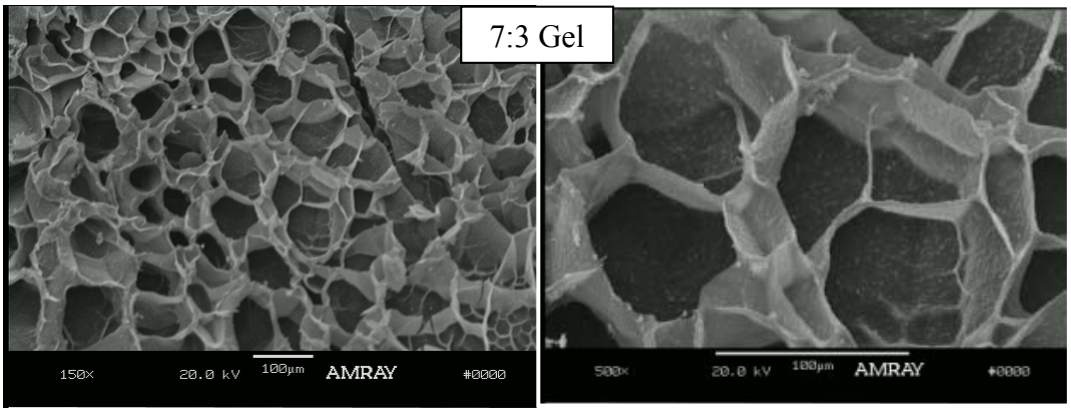

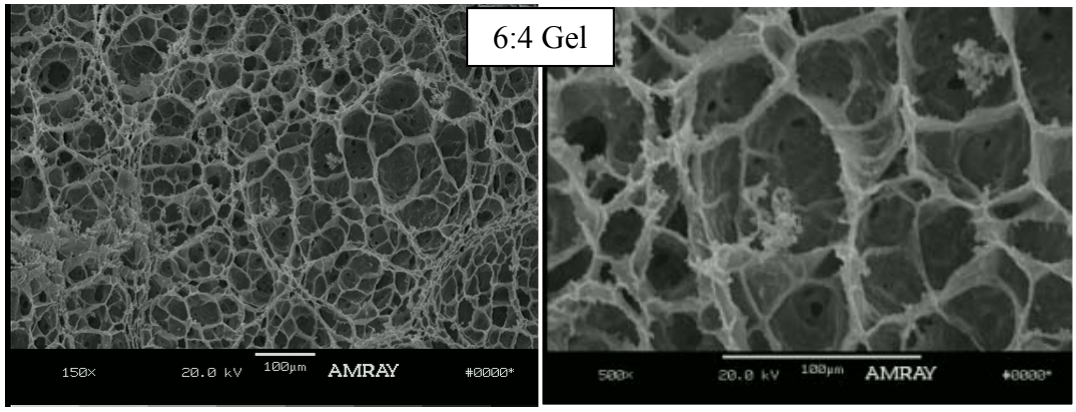

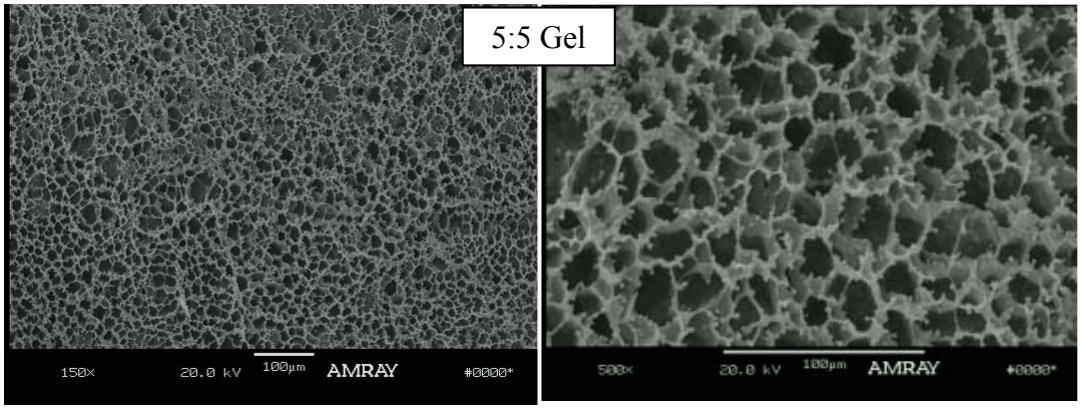

Figure 3.5: SEM images of freeze-dried PAA:SAPAE hydrogels at three different blending ratios (7:3, 6:4, 5:5) at the 24 hour swelling time point in deionized water. Films are shown at 150x (left) and 500x (right) magnification.

3.3.4. Insulin loading

Insulin loading was achieved via a swelling-diffusion technique in PBS buffer (pH 7.4). The insulin loading profile is shown in **Figure 3.6**. The insulin loading percentage of the 7:3, 6:4, and 5:5 gel ratios were 57.4%, 53.6%, 51.8%, respectively.

Higher pore size is anticipated to have higher insulin loading. However, significant differences between the three hydrogel systems were not observed. All hydrogel systems had sufficient pore size to incorporate insulin into the swollen networks; insulin is a relatively low molecular weight protein. The PAA:SAPAE hydrogels loading capacity is comparable to previously reported insulin delivery systems.[34, 43]

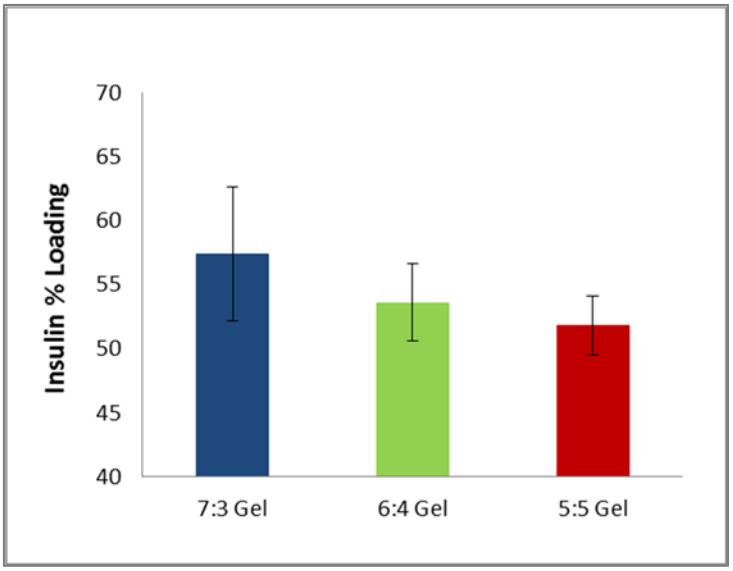

Figure 3.6: Insulin loading of the PAA:SAPAE hydrogels via swelling-diffusion technique for 5 hours as determined by BCA assay. Data are presented as mean ± standard deviation (n=3 in each group).

3.3.5. Insulin release

To monitor *in vitro* release of insulin, dried insulin-loaded PAA:SAPAE gels were dispersed into 0.1 N HCl (pH 1.2) or in PBS buffer (pH 6.8) at 37 °C. After 24 hours, 97.9%, 85.1%, and 74.4% of insulin was released from the 7:3, 6:4, and 5:5 gel ratios in pH 6.8, respectively (**Figure 3.7B**). In 2 hours, only 4.8%, 7.4%, and 8.8% of insulin was released from the 7:3, 6:4, and 5:5 gels in pH 1.2, respectively (**Figure 3.7A**).

As shown in **Figure 3.7**, insulin is released faster in the 7:3 ratio gel, followed by the 6:4 and 5:5 ratio gels in PBS. This trend correlates well with the swelling behavior and

pore sizes. Overall, the highest PAA ratio (7:3) gel at pH 6.8 has the fastest release rate, the highest swelling value, and the largest pore size. Increasing the pore size increases the diffusion rate of the hydrogel system, resulting in faster insulin release.

In contrast, the release of insulin under acidic conditions was much lower than pH 6.8 media. The 7:3 ratio has the slowest release rate in 0.1 N HCl. The PAA:SAPAE hydrogels have an insulin release profile similar to previously published acrylic acid-based insulin delivery systems.[43, 44]

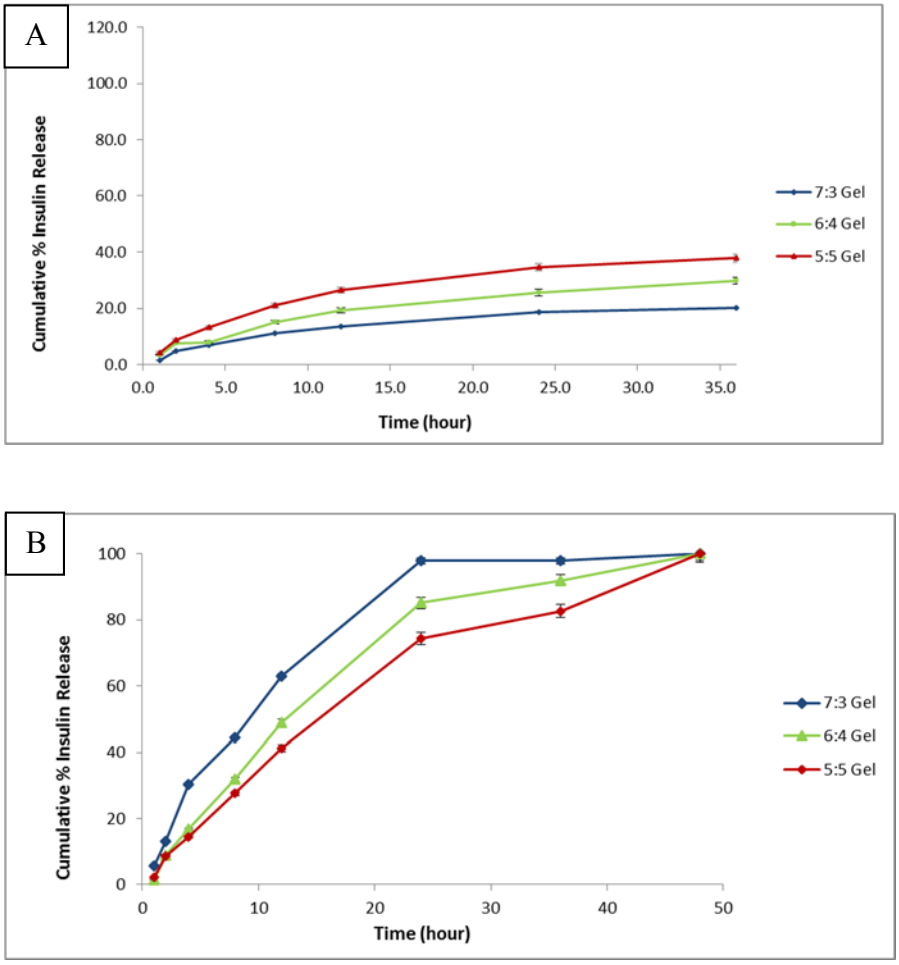

Figure 3.7: *In vitro* release of insulin from the PAA:SAPAE hydrogels as a function of pH: (A) pH 1.2 and (B) pH 6.8, represented as normalized cumulative insulin release as a

percentage as determined by BCA assay. Data are presented as mean ± standard deviation (n=3 in each group).

3.3.6. Insulin stability

Insulin stability is an important factor, as the loss of stability will cause loss of bioactivity: Insulin can form aggregates and undergo chemical changes. SEC is the approved method by the FDA to measure soluble aggregation, higher molecular weight (HMW) species. The USP specification for HMW of insulin is 1.0%.[45] In this study, the samples were compared against insulin standard loading solution (LDS). As shown in **Figure 3.8**, the samples' HMW percentage was close to LDS and lower than USP specification; around 0.1% HMW was observed.

iCIEF is one of the recommended techniques by the FDA and used by the pharmaceutical industry to measure the chemical degradation of the proteins.[46] iCIEF results aligned with SEC results: The main insulin chemical degradation mechanism, deamidation, was observed at the low level, similar to LDS. Both measurements confirmed that insulin was physically and chemically stable once released from the hydrogel systems.

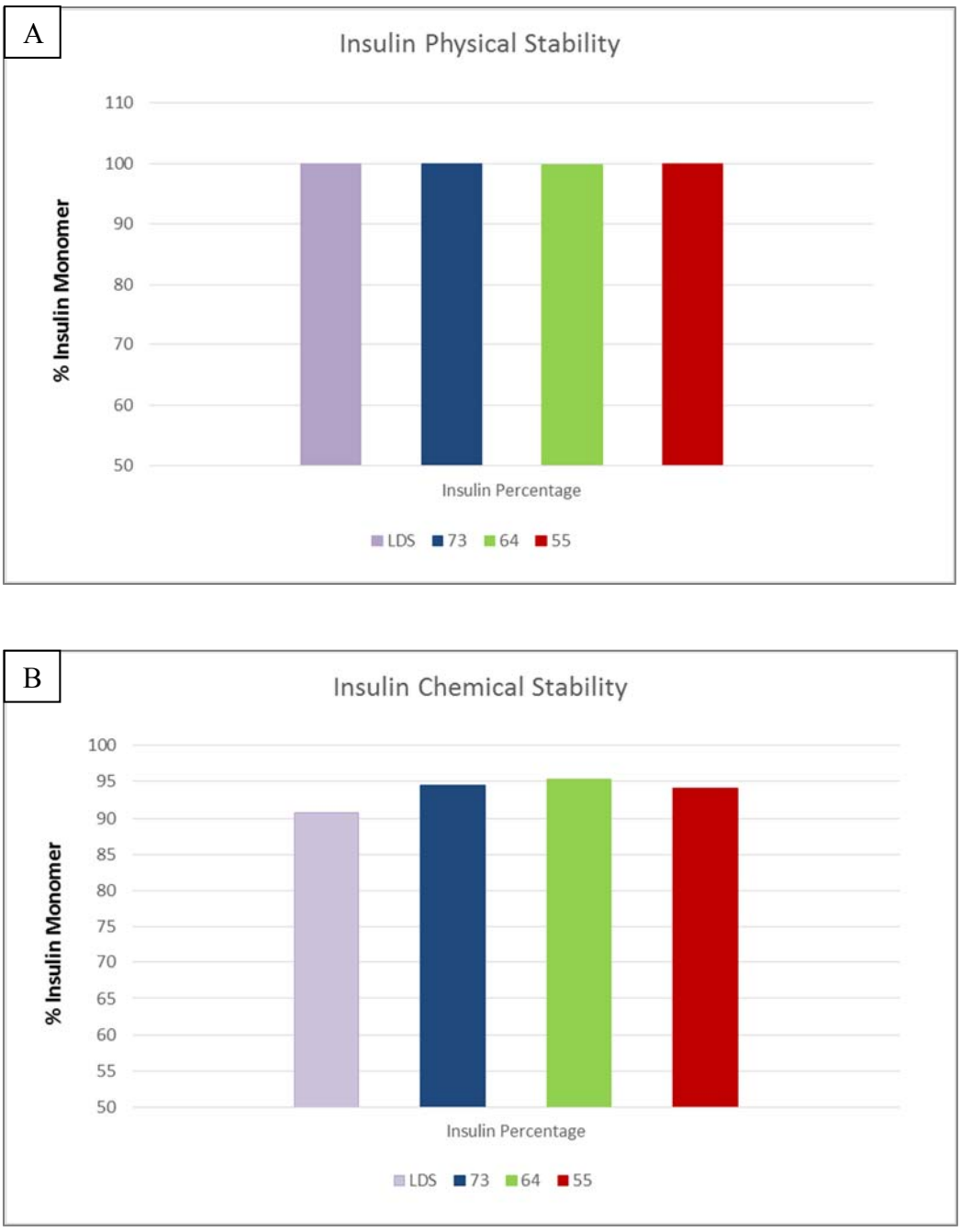

Figure 3.8: 24-hour release samples analysis to evaluate (A) physical stability using SEC chromatography to calculate aggregation (HMW species) and (B) chemical stability using iCIEF to calculate deamidated species.

3.3.7. *In vitro* SA release

Given the intended application of using PAA:SAPAE hydrogels to release both insulin and salicylic acid, the *in vitro* SA release profiles of the hydrogels were monitored. To monitor *in vitro* release of salicylic acid, dried PAA:SAPAE gels were dispersed into PBS buffer (pH 6.8) or 0.1 N HCl (pH 1.2) at 37 °C. Within 24 hours, 70.1 %, 67.6%, and 66.4% salicylic acid was released from the 7:3, 6:4, and 5:5 gel ratios in pH 6.8, respectively (**Figure 3.9B**). Within 24 hours, 27.6%, 28.2%, and 30% salicylic acid was released from the 7:3, 6:4, and 5:5 gel ratios in 0.1N HCl (pH 1.2), respectively (**Figure 3.9A**).

As for the SA release, a strong correlation between swelling values was observed. The higher the swelling value, the higher the SA release rate at the early time points. In this study, the 7:3 ratio swelled the most and released the most SA in pH 6.8. A similar trend was observed in previously published work using polyvinylpyrolidone (PVP) as the gelling polymers. In the PVP:SAPAE hydrogel systems, the SA release rate was higher in the higher swelling polymer blends.[30] Notably, the SA release rate was much faster in this PAA:SAPAE system compare to PVP:SAPAE, likely because the swelling value of poly(acrylic acid) is much higher.

In contrast, the release of SA was much lower under acidic conditions. In pH 6.8, carboxyl groups of PAA are ionized and increase SAPAE hydrolysis. On the other hand, in acidic conditions, carboxyl groups are protonated which results in gel shrinkage and minimize the insulin and SA release. The release was correlated to swelling trend in 0.1 N

HCl (pH 1.2). 5:5 gel had the highest swelling ratio and higher SA release rates compared to the 7:3 and 6:4 gel ratios.

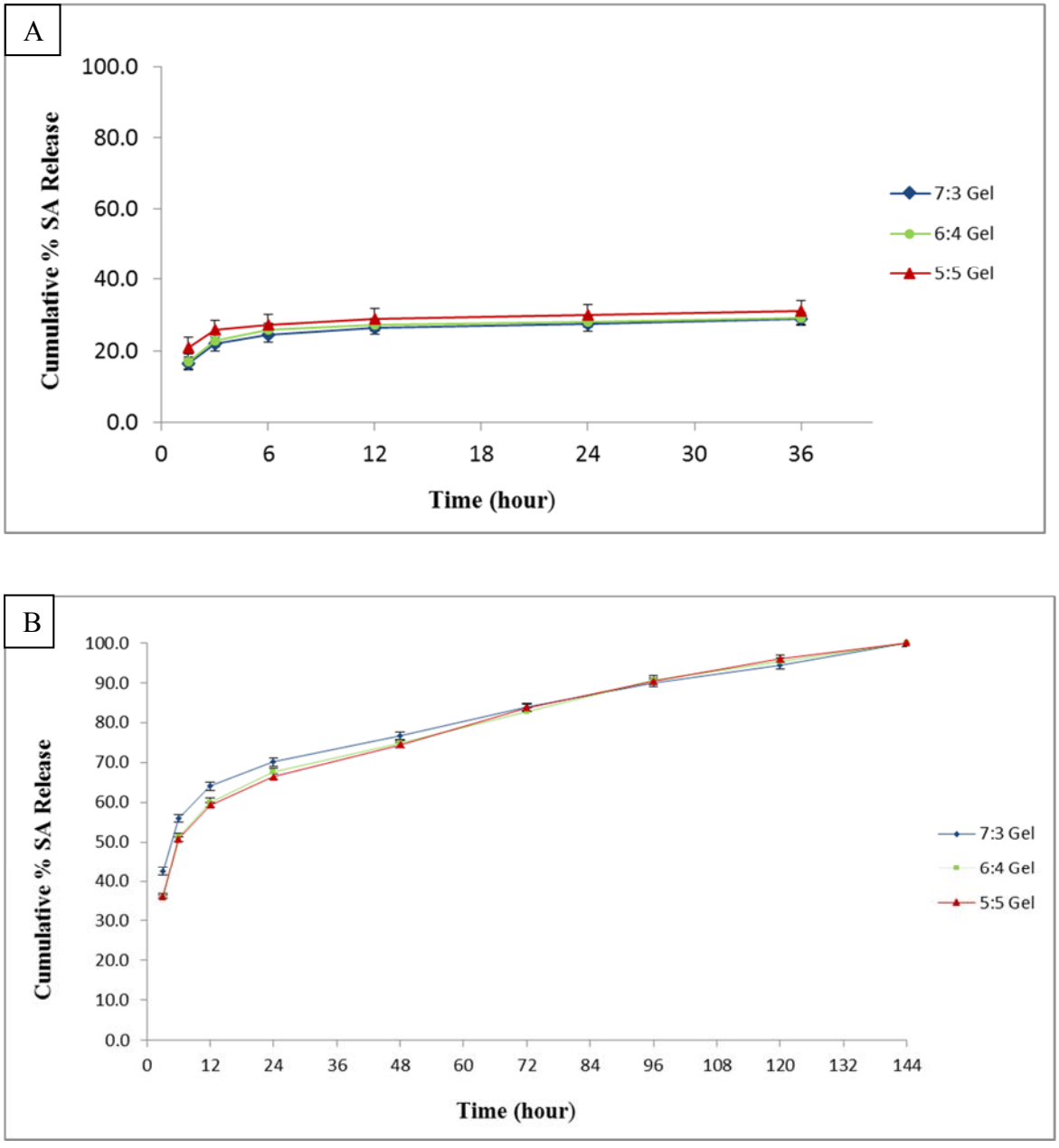

Figure 3.9: *In vitro* release of SA from the PAA:SAPAE hydrogels as a function of pH: (A) pH 1.2 and (B) pH 6.8, represented as normalized cumulative SA release as a

percentage as determined by UV spectrophotometry. Data are presented as mean ± standard deviation (n=3 in each group).

3.3.8. Cytotoxicity of the hydrogels

Cytotoxicity against 3T3 cells was determined as a function of three different polymers solution, in which the anti-inflammatory effect of the SA is observed: 0.1 mg/mL, 0.01 mg/mL, and 0.001 mg/mL, with DMSO (1%) used as control. The results (**Figure 3.10**) indicated that the viability of each of these hydrogels cell was not statistically different from the DMSO controls.

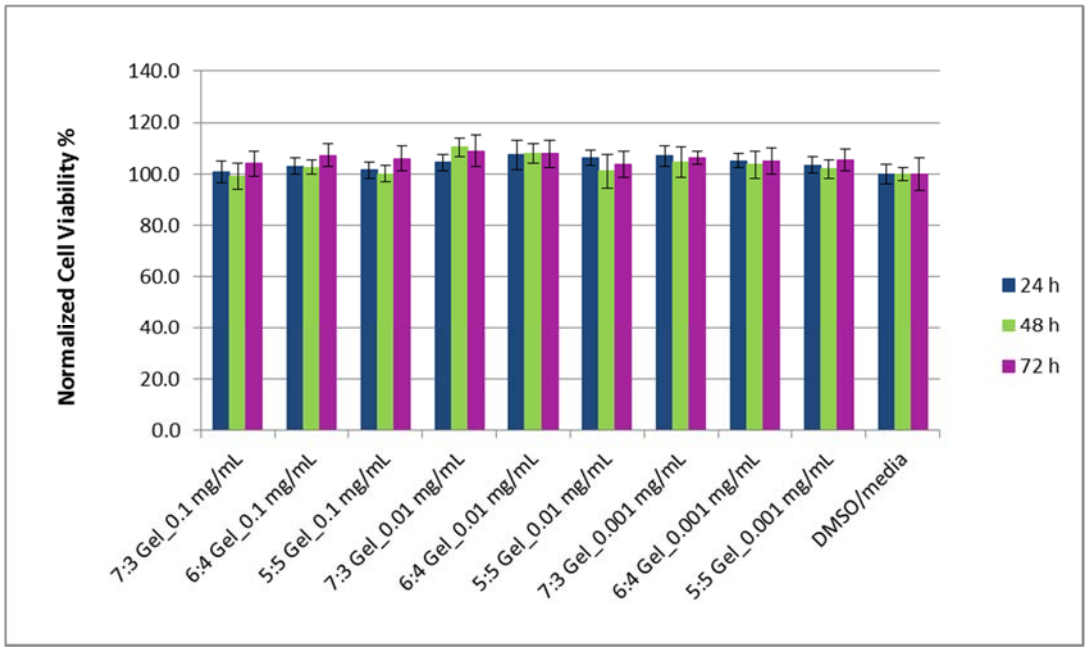

Figure 3.10: Cytotoxicity profile of the different concentrations of the hydrogels after 24-, 48-, and 72-hour incubation. All groups contained 1% DMSO in cell media and the

control group has no polymer. Absorbance at 490 nm after MTS treatment is proportional to cell viability. The cell viability of each of these hydrogels was not statistically different from the media with DMSO control.

3.3.9. Mucoadhesion behavior

The mucoadhesion behavior of the PAA:SAPAE hydrogels were evaluated using Texture Analyzer. The maximum detachment force of the 7:3, 6:4, and 5:5 gel ratios were 37.1, 21.4, and 16.3, respectively, whereas adhesion values were 222.6, 124.0, and 104.0, respectively.

Protein permeability is one of the biggest challenges for oral protein delivery.[16] One of most promising approaches to increase permeability are mucoadhesive systems as it decrease the drug clearance rate and increase the time availability for absorption, which are often based upon PAA and cellulose.[16] The mucoadhesion behavior of PAA:SAPAE hydrogels were evaluated using Texture Analyzer and the maximum detachment force and adhesion work of the PAA:SAPAE- hydrogels are summarized in Table 1. The PAA:SAPAE 7:3 gel mucoadhesion detachment force was higher than acrylic acid-based gels, which were developed for insulin oral delivery, at 0.6 g.[47] Overall, increasing PAA percent increased the detachment force of the hydrogels.

Table 3.1: Mucoadhesion performance of PAA:SAPAE films

	Detachment force (g)	**Work of adhesion (g x mm)**
7:3 Gel	37.1 ± 10.6	222.6 ± 63.8
6:4 Gel	21.4 ± 2.8	124.0 ± 22.6
5:5 Gel	16.3 ± 6.3	104.0 ± 37.5

3.4. Conclusion

Different ratios of physically cross-linked PAA:SAPAEs hydrogel systems were formulated by solvent-casting. The resulting miscible blends displayed a porous structure able to incorporate insulin. These hydrogel systems exhibited different swelling values depending on the media pH. The swelling values and insulin release at 0.1N HCl (pH 1.2) decreased with the increasing PAA ratio, which is beneficial for oral insulin delivery to protect the insulin from degradation in the stomach. Concurrently, hydrogel systems released SA in a manner that follows the insulin release curve. The ability to deliver an anti-inflammatory compound that reduces insulin resistance in conjunction with insulin delivery is unique. Moreover, these hydrogel systems also show mucoadhesive behaviors, which may ultimately increase protein permeability. In summary, these polymer gels are uniquely able to deliver insulin and salicylic acid in combination. Such an approach may

be useful as an oral insulin delivery vehicle for diabetes patients. Future work includes *in vivo* studies in diabetic rats to evaluate the blood glucose levels following oral delivery.

3.5. References

1. Y. Qiu, K.Park. Enviromental-sensitive hydrogels for drug delivery. Advanced drug delivery reviews 64, 49-60 (2012).

2. L.Brannon-Peppas, R.S.Harland. Absorbent polymer technology. Elsevier, 45-66 (1990).

3. N.A. Peppas, A.G.Mikos. Hydrogels in medicine and pharmacy. CRC press, Boca Raton, FL 1, 1-27 (1986).

4. M. S. Bindu, V.Ashok, A. Chatterjee. As a review on hydrogels as drug delivery in the pharmaceutical field. International Journal of pharmaceutical and chemical sciences 1 (2), 642-661 (2012).

5. L. C. Lopérgolo, A. B. Lugão, L. H. Catalani. Direct UV photocrosslinking of poly(N-vinyl-2-pyrrolidone) (PVP) to produce hydrogels. Polymer 44, 6217-6222 (2003).

6. T.R. Hoare, D.S.Kohane. Hydrogels in controlled release formulation: Network design and mathematical modeling. Advanced drug delivery reviews 58, 1379-1408 (2008).

7. H. Park, K. Park. Hydrogels and biodegradable polymers for bioapplications. American chemical society 627, 2-10 (1996).

8. N.A. Peppas, Y. Huang, M. Torres-Lugo, J.H. Ward, J. Zhang. Physicochemical foundations and structural design of hydrogels in medicine and biology. Annual review of biomedical engineering 2, 9-29 (2000).

9. D.Q. Wu, Y.X.Sun, X.D. Xu, S.X. Cheng, X.Z. Zhang, R.X. Zhuo. Biodegradable and pH-Sensitive Hydrogels for cell encapsulation and controlled drug release. Biomacromolecules 9, 1155-1162 (2008).

10. P.B. Sutar, R.K.Mishra, K. Pal, A.K. Banthia. Development of pH-sensitive polyacrylamide grafted pectin hydrogel for controlled drug delivery system. Journal of material science: Materials in medicine 19, 2247-2253 (2008).

11. X. Y. Gao, C.L.He, C. S. Xiao, X. L. Zhuang, X. S. Chen. Synthesis and characterization of biodegradable pH-sensitive poly(acrylic acid) hydrogels crosslinked by

2-hydroxyethyl methacrylate modified poly(L-glutamic acid). Materials letter 77, 74-77 (2012).

12. D. Myung, W.U.Koh, J. M. Ko, Y. Hu, M. Carrasco, J. Noolandi, C. N. Ta, C. W. Frank. Biomimetic strain hardening in interpenetrating polymer network hydrogels. Polymer 48, 5376-5387 (2007).

13. D. F. Evans, G.Pye, R. Bramley, A. G. Clark, T. J. Dyson, J. D. Hardcastle. Measurement of gastrointestinal pH profiles in normal ambulant human subjects. Gut 29, 1035-1041 (1988).

14. A. Bernkop-Schnurch. Mucoadhesive polymers: strategies, achievements and future challenges. Advanced drug delivery reviews 57, 1553-5 (2005).

15. J. Renukuntla, A.D.Vadlapudi, A. Patel, S. H. S. Boddu, A. K. Mitra. Approaches for enhancing oral bioavailability of peptides and proteins. International Journal of pharmaceutics 447, 75-93 (2013).

16. J. Shaji, V.Patole. Protein and peptide drug delivery: Oral approaches. Indian journal of pharmaceuticals sciences 70, 269-277 (2008).

17. C. M. Lehr. Bioadhesion Technologies for the delivery of peptide and protein drugs to the gastrointestinal tract. Critical reviews in therapeutic drug carrier systems 11, 119-160 (1994).

18. E. Deat-Laine, V.Hoffart, G. Garrait, J. F. Jarrige, J. M. Cardot, M. Subirade, E. Beyssac. Efficacy of mucoadhesive hydrogel microparticles of whey protein and alginate for oral insulin delivery. Pharmaceutical research 30 (2013).

19. D. P. Huynh, G.J.Im, S. Y. Chae, K. C. Lee, D. S. Lee. Controlled release of insulin from pH/temperatire-sensitive injectable pentablock copolymer hydrogel. Journal of controlled release 137, 20-24 (2009).

20. K. Zhang, X.Y.Wu. Modulated insulin permeation across a glucose-sensitive polymeric composite membrane. Journal of controlled release 80, 169-178 (2002).

21. M. Nixon, D.J.Wake, D. E. Livingstone, R. H. Stimson, C. L. Esteves, J. R. Seckl, K. E. Chapman, R. Andrew, B. R. Walker. Salicylate downregulates 11B-HSD1 expression in adipose tissue in obese mice and in humans, mediating insulin sensitization. Diabetes 61, 790-796 (2012).

22. A. B. Goldfine, V.Fonseca, S. Shoelson. Therapeutic approaches to target inflammation in type 2 diabetes. Clinical chemistry 57, 162-167 (2011).

23. R. S. Hundal, K.F.Peterson, A. B. Mayerson, P. S. Randhawa, S. Inzucchi, S. E. Shoelson, G. I. Shulman. Mechanism by which high-dose aspirin improves glucose metabolism in type 2 diabetes. Journal of clinical investigation 109, 1321-1326 (2002).

24. S. E. Shoelson, J.Lee, A. B. Goldfine. Inflammation and insulin resistance. Journal of clinical investigation 116, 1793-1801 (2006).

25. J. Reid, T.D.Lightbody The insulin equivalence of salicylate. British medical journal, 897-900 (1959).

26. R. P. Raghavan, D.W.Laight, M. H. Cummings. Aspirin in type 2 diabetes, a randomised controlled study: effect of different doses on inflamation, oxidative stress, insulin resistance and endothelial function. International journal of clinical practice 68, 271-277 (2014).

27. A. Prudencio, R.C.Schmeltzer, K. E. Uhrich. Effect of linker structure on salicylic acid-derived poly(anhydride-esters). Macromolecules 38, 6895-6901 (2005).

28. R. C. Schmeltzer, T.J.Anastasiou, K. E. Uhrich. Optimized synthesis of salicylate-based poly(anhydride-esters). Polymer bulletin 49, 441-448 (2003).

29. M.A. Reynolds, A.Prudencio, M.E. Aichelmann-Reidy, K. Woodward, K.E. Uhrich. Non-steroidal anti-inflammatory drug (NSAID)-derived poly(anhydrideesters) in bone and periodontal regeneration. Current drug delivery 4, 233-239 (2007).

30. M.Ouimet, R.Fogacam, S.Snyder, S. Sathaye, L. Catalani, D. Pochan, K.E. Uhrich. Poly(anhyride-ester) and poly(N-vinyl-2-pyrrolidone) blends: salicylic acid-releaseing blends with hydrogel-like properties that reduce inflammation. Macromolecular bioscience 10, 1002 (2014).

31. W. Brostow, R.Chiu, I. M. Kalogeras, A. Vassilikou-Dova. Prediction of glass transition temperatures: Binary blends and copolymers. Materials letters 62, 3152-3155 (2008).

32. K. Nakamura, R.Murray, J. Joseph, N. Peppas, M. Morishita, A. Lowman. Oral Insulin delivery using P(MAA-g-EG) hydrogels: Effect of network morphology on insulin delivery characteristics. Journal of controlled release, 589-599 (2004).

33. X. Gao, Y.Cao, X. Song, Z. Zhang, C. Xiao, C. He, X. Chen. pH and thermo-responsive poly(N-isopropylacrylamide-co-acrylic acid derivative) copolymers and hydrogels with LCST dependent on pH and alkyl side groups. Journal of materials chemistry B 1, 5578-5587 (2013).

34. L. Yin, L.Fei, F. Cui, C. Tang, C. Yin. Superporous hydrogels containing poly(acrylic acid-co-acrylamide)/ O-carboxymethyl chitosan interpenetrating polymer networks. Biomaterials 28, 1258-1266 (2007).

35. M. Morishita, A.M.Lowman, K. Takayama, T. Nagai, N.A. Peppas. Elucidation of the mechanism of incorporation of insulin in controlled release systems based on complexation polymers. Journal of controlled release 81, 25-32 (2002).

36. X. Xu, Y.Shen, W. Wang, C. Sun, C. Li, Y. Xiong, J. Tu. Preparation and in vitro characterization of thermosensitive and mucoadhesive hydrogels for nasal delivery of phenylephrine hydrochloride. European journal of pharmaceutics and biopharmaceutics 2014, 998-1004 (2014).

37. E. Hagesaether, S.A.Sande. In vitro measurements of mucoadhesive properties of six types of pectin. Drug development and industrial pharmacy 33, 417-425 (2007).

38. J. Koening. Chemical microstructure of polymer. Wiley (1980).

39. T. Aoki, M.Kawashima, H. Katono, K. Sanui, N. Ogata, T. Okano. Temperature-responsive interpenetrating polymer networks constructed with poly(acrylic acid) and poly(N,N-dimethylacrylamide). Macromolecules 27, 947-952 (1994).

40. A. Khare, N.Peppas. Swelling/ deswelling of anionic copolymer gels. Biomaterials 16, 559-567 (1995).

41. A. Foss, T.Goto, M. Morishita, N. Peppas. Development of acrylic-based copolymers for oral insulin delivery. European journal of pharmaceutics and biopharmaceutics 57, 163-169 (2004).

42. N. A. Peppas, P.Bures, W. Leobandung, H. Ichikawa. Hydrogels in pharmaceutical formulations. European journal of pharmaceutics and biopharmaceutics 50, 27-46 (2000).

43. A. Kumar, S.Lahiri, H. Singh. Development of PEGDMA: MAA based hydrogel microparticles for oral insulin delivery. International journal of pharmaceutics 323, 117-124 (2006).

44. B. Kim, N.Peppas. In vitro release behavior and stability of insulin in complexation hydrogels as oral drug delivery carriers. International journal of pharmaceutics 266, 29-37 (2003).

45. U.S.pharmacopeia. Insulin, revision bulletin. United states pharmacopeial convention (2013).

46. D. A. Michels, O.S.Solano., C. Felten. Imaged capillary isoelectric focusing for charge-variant analysis of biopharmaceuticals. Bioprocess technical 9, 48-52.

47. N. A. Peppas. Devices based on intelligent biopolymers for oral protein delivery. International journal of pharmaceutics 277, 11-17 (2004).

4. NOVEL SALICYLIC ACID-BASED CHEMICALLY CROSS-LINKED pH-SENSITIVE HYDROGELS AS POTENTIAL DRUG DELIVERY SYSTEMS

4.1. Introduction

Hydrogels are chemically or physically cross-linked networks of water-soluble polymers that are capable of imbibing high concentrations of water or biological fluids.[1-6] Owing to their greater mechanical integrity and tenability, chemically cross-linked hydrogels are preferred to physically cross-linked gels for drug and/or protein delivery applications.[7, 8]

When using hydrogels for drug and/or protein delivery, the release profile is modified by changing the cross-linking density as well as the functional groups. pH-sensitive hydrogels are often utilized for oral delivery systems to target the different pH ranges of the digestive tract. More specifically, acrylic acid moieties have attracted considerable interest for oral protein delivery due to their responsiveness to the pH shift in the gastro-intestinal (GI) tract.[9-12] Hydrogels comprised of polyanions swell minimally in the stomach (pH 1-2.5),[13] with increased swelling in the intestine (pH 6.4-7.5).[13] In addition, poly(acrylic acid) (PAA) exhibits mucoadhesive behavior which can adhere to mucosal membranes, and, thus, could improve bioavailability.[14-16]

In this research, pH-dependent, chemically cross-linked SA-based hydrogels were developed. Recent studies have shown that salicylic acid (SA), a nonsteroidal, anti-inflammatory analgesic and anti-pyretic agent,[17] is effective in treating colorectal cancer,[18]

diabetes,[19, 20] and arthritis.[21] For these diseases, extended release formulations are preferred to immediate release formulations to improve therapeutic levels. To meet this goal, SA has been chemically incorporated into poly(anhydride-esters)[22] and shown to deliver SA from days to months.[23] In addition, these systems have been formulated with PAA to form physically cross-linked pH-sensitive hydrogels capable of encapsulating insulin and concurrently releasing both insulin and SA.[24] However, the release is slow: Only 70% of SA was released within 24 hours.

To overcome the limited SA release, an SA-based monomer was prepared using an itaconic acid linker followed by free radical polymerization with acrylic acid and poly(ethylene glycol) diacrylate (PEGDA) as the cross-linking agent (**Scheme 4.1**). Two hydrogel systems were prepared: hydrogel 1 and hydrogel 2, which have low and high crosslinker density, respectively. In this study, the effects of crosslink density on swelling values, SA release, pore structure, and rheological and mucoadhesion behavior were studied.

4.2. Experimental Section

4.2.1. Materials

Fetal bovine serum (FBS) was purchased from Atlanta Biologicals (Lawrenceville, GA). Fibroblast cells were purchased from ATCC, (Manassas, Virginia). Hydrochloric

acid was purchased from Fisher Scientific (Fair Lawn, NJ). Irgacure 2959 (1-[4-(2-Hydroxyethoxy)-phenyl]-2-hydroxy-2-methyl-1-propane-1-one) was purchased from Ciba Specialty Chemical Corp. (Tarrytown, NY). All other chemicals and reagents were purchased from Sigma-Aldrich (Milwaukee, WI).

4.2.2. Synthesis of hydrogels

4.2.2.1. Physicochemical characterization

^{1}H NMR spectra were obtained on Varian 400 MHz using DMSO-d_6 as a solvent. FT-IR spectra were recorded using a Thermo Nicolet FT-IR spectrometer (Thermo Scientific, Somerset, NJ) with a 64-scan cycle. Waters SQD Acquity Liquid Chromatography Mass Spectrometry (LC-MS) was used to confirm molecular weight. LC-MS analysis was performed on Phenomenex C18 column with water/acetonitrile 70:30 (v/v) in 0.05% Trifluoroacetic acid (TFA) with 0.4 mL/min flow rate using MS scan ES+ ion mode. The glass transition temperature (T_g) of the hydrogels was analyzed via DSC using TA Instruments Q200 DSC (New Castle, DE). The hydrogels (~5 mg) were analyzed by heating under dry nitrogen from -10 °C to 200 °C at a rate of 10 °C/minute and cooling

to -10 ˚C at 10 ˚C/minute, with a three-cycle minimum. The data was analyzed using TA instruments Universal Analysis 2000 software.

4.2.2.2. Salicylic acid-based monomer (SAm) synthesis

SA (2 eq) was dissolved in 100 mL of THF and pyridine (4 eq). Itaconyl chloride (1 eq) was dissolved in 15 mL THF and added dropwise (over 1 hour) to yield a suspension. After stirring for 2 hours at RT, the supernatant was concentrated *in vacuo* and the resulting residue re-dissolved in ethyl acetate (50 ml). The solution was then washed with 1 N HCl (3 X 50 mL) and then the organic layer dried over $MgSO_4$. The solvent was removed *in vacuo* to yield crude product, which was then purified using Biotage SNAP ULTRA C18 column via Biotage flash chromatography. 1% Trifluoroacetic acid **(**TFA) in water and 1% TFA in acetonitrile (ACN) was used as mobile phase A (MPA) and B (MPB), respectively. The purification was started using 4:1 (MPA:MPB) and increased to 1:1 (MPA:MPB) in 5 column volumes. The samples were collected and lyophilized overnight. Yield: 40% (white solid). ^{1}H NMR showed characteristics peaks at δ 7.16-8.08 (m, 8H, Ar-H), 6.46 (m, 1H, CH_2), 6.08 (m, 1H, CH_2), 11.20 (s, 1H, OH) and 3.85 (s, 2H, CH_2). The molecular weight of the SAm, 370.3, was confirmed using LC-MS. FT-IR showed characteristics peak at 1732 cm^{-1} (C=O, ester), 1690 cm^{-1} (C=O, carboxylic acid), 1643 cm^{-1} (C=C).

4.2.2.3. Hydrogel synthesis

Hydrogels were prepared by UV-initiated free-radical polymerization. SAm (1 eq) and acrylic acid (AA) (2 eq) were dissolved in 1 mL of acetone:water (6:4 v/v). PEGDA (Mw= 250 Da) was added in 0.075 mmol (low crosslink) and 0.15 mmol (high crosslink) of PEGDA per total monomer (SAm and AA) for hydrogel 1 and hydrogel 2, respectively. The mixtures were stirred for 15 minutes at RT to dissolve all components and purged under nitrogen for 30 minutes. To initiate the reactions, Irgacure 2959 at 3% of the weight of total reagents was added to the solutions, stirred for 10 minutes at RT, and subsequently pipetted into Teflon beakers (28 mm diameter) under nitrogen. The beakers were then positioned horizontally to the direction under the UV light at 365 nm using a UVP Lamp (UVP LLC, Upland, CA) and the solution was cured for 45 minutes at RT. The hydrogels were then soaked in 50:50 acetone:water (50 ml) for 1 hour at RT and subsequently washed with acetone (3 x 100 mL) and water (3 x 100 mL) to remove residual monomers. FT-IR showed characteristics peak at 1731 cm^{-1} (C=O, ester), 1700 cm^{-1} (C=O, carboxylic acid), 1160 cm^{-1} (C-O-C). T_g= 77 °C (hydrogel 1); 85 °C (hydrogel 2).

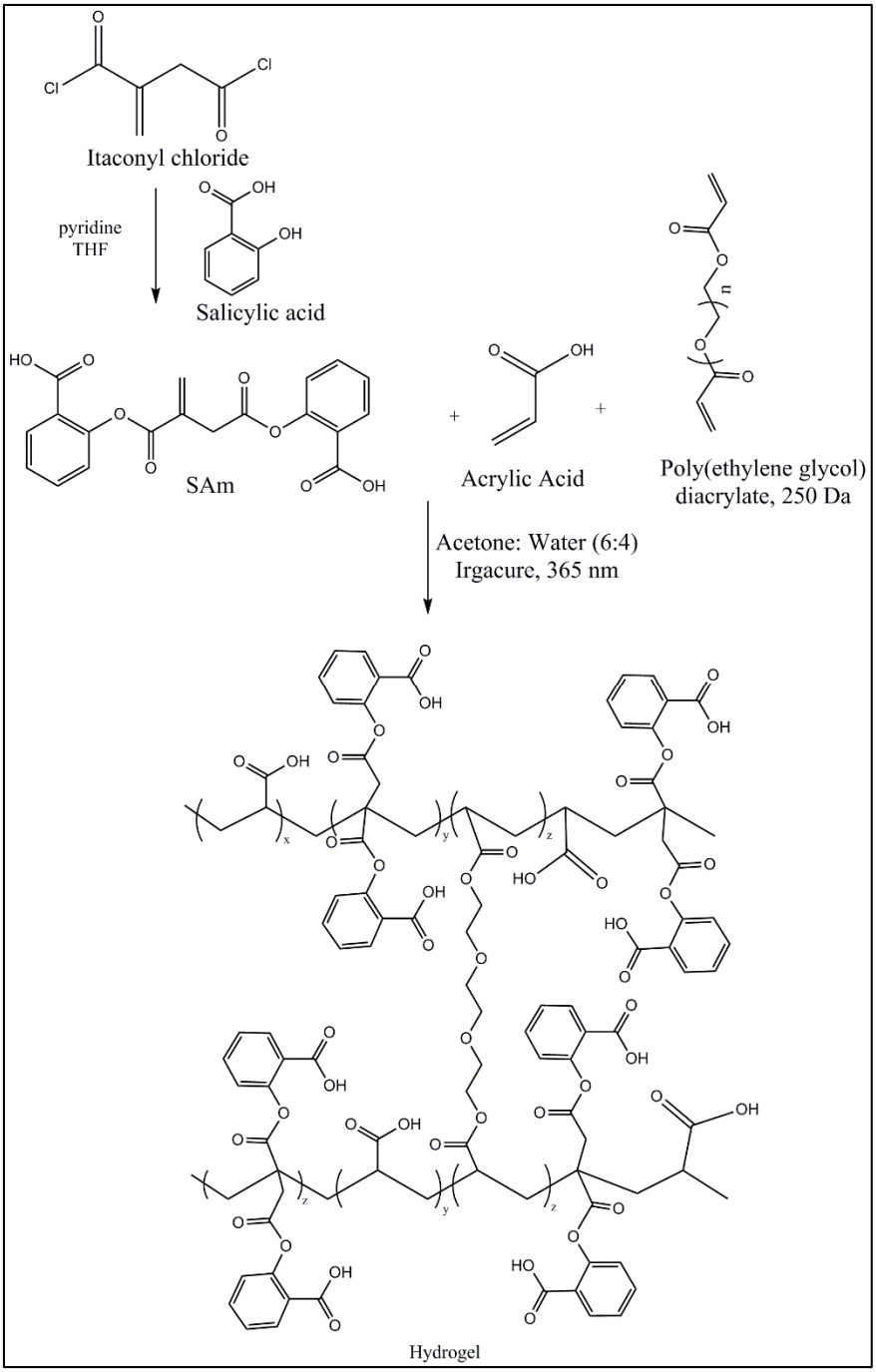

Scheme 4.1: Synthesis of salicylic acid-based monomer (SAm) and hydrogel. Hydrogels were cross-linked with varying amounts of crosslinker (PEGDA).

4.2.3. Swelling behavior

Swelling experiments were performed in phosphate buffer saline (PBS) buffer (pH 7.4) or 0.1 N HCl (pH 1.2) for 1 and 24 hours at 37 °C. Given that orally administered compounds pass through the stomach in 15-60 min and stay in the GI tract around 24 hours,[25, 26] the time points of 1 and 24 h were chosen to represent retention in the stomach and GI tract. Approximately 60 ± 10 mg of dried hydrogel was immersed in the media (15 ml) in a 20 mL scintillation vial. At 1 and 24 h time points, gels were removed from the solution, dried with kimwipes, and weighed. The swelling percentage was calculated according to following equation.[27-29]

$$Q = \frac{Ws - Wd}{Wd} \ , \qquad \textbf{Equation 4.1}$$

where W_s and W_d are the weight of the swollen and dried films, respectively. All experiments were carried out triplicate and the average values reported.

4.2.4. Hydrogel morphology

Hydrogel morphology was investigated using scanning electron microscopy (SEM). Hydrogel films were swollen in PBS buffer (20 ml) for 24 hours at room temperature and subsequently lyophilized for 12 hours prior to SEM imaging. Samples were coated with Au/Pd using a sputter coater (SCD 004, Balzer Union Limited) and images were obtained using an AMRAY-1830I microscope.

4.2.5. *In vitro* SA release

Hydrogels (60 ± 10 mg) were placed in 20 mL scintillation vials containing 10 mL PBS (pH 7.4) and 0.1 N HCl (pH 1.2) and then incubated using a controlled environment incubator-shaker (New Brunswick Scientific Co., Edison, NJ) (37 ˚C, 60 rpm). At set time points, 5 mL aliquots of media were removed and replaced with 5 mL fresh media. The amount of release SA was quantified by high performance liquid chromatography (HPLC) to monitor SA release. HPLC C18 reverse phase column was used in the Waters HPLC system. For the analysis, water/acetonitrile 70:30 (v/v) in 0.1% phosphoric acid with 0.4 mL/min flow rate was used to elute SA. The detection wavelength was 303 nm. The SA calibration curve was prepared from SA standards and the data was calculated against a calibration curve. The release experiment was carried out until SA was no longer detected in the PBS buffer. In 0.1 N HCl media, release experiments continued for 24 hours, then 0.1 N NaOH was added to hydrolyze any remaining SA. The experiments were normalized to 100%. All sets of experiments were performed in triplicate.

4.2.6. Rheometry

The rheological behaviors of the hydrogels were measured using oscillatory rheology with AR 2000, TA Instruments (New Castle, DE). The rheological behavior was measured using dynamic storage modulus (or elastic modulus), G’; loss modulus, G’’

(viscous behavior); and loss tangent as a function of time and frequency. The measurements were performed using parallel plate geometry (8 mm) at 25°C. Hydrogels were swollen for 12 hours prior to testing in PBS (pH 7.4) at RT. Storage, loss modulus, and loss tangent were measured in a frequency range 10 to 60 rad/s with a constant stress of 1 Pa and constant normal force 1 N during the frequency sweep experiment. The time sweep was performed at 1 Hz frequency and at 1 Pa stress for 900 seconds. Experiments were performed in triplicate.

4.2.7. Mucoadhesion behavior

Hydrogel mucoadhesion properties were analyzed via previously published methods using Texture Analyzer TA-XT2 (Hamilton, MA).[30, 31] Hydrogels were adhered to the upper holder and wetted with pH 7.4 phosphate buffer, whereas 30% mucin gel in pH 7.4 phosphate buffer was attached to the lower, stationary part of the texture analyzer. The mucin layer and hydrogels were brought into contact for 100 seconds with 7.8 N applied force and then the upper part raised at 1.0 mm/s. The mucin layer alone was used as a control, and the force of detachment and distance recorded. The mucoadhesion performance of the gels was determined by measuring the resistance to the withdrawal of the upper holder, maximum detachment force F_{max} in "g." The work of adhesion was calculated by area under the curve (AUC) of the force distance plot (g x mm). Experiments were performed in triplicate.

4.2.8. Cytotoxicity of the hydrogels

Hydrogels cytocompatibility was performed in a 96-well plate by MTS ((3-(4,5-dimethylthiazol-2-yl)-5-(3-carboxymethoxyphenyl)-2-(4-sulfophenyl)-2H-tetrazolium) assay. 3T3 fibroblast cells were cultured in hydrogel-containing media. Cell culture media consisted of Dulbecco's Modified Eagle's Medium (DMEM), 10% v/v fetal bovine serum, 1% L-glutamate and 1% penicillin/streptomycin. The hydrogels were first sterilized under UV at λ=254nm for 900 seconds (Spectronics Corporation, Westbury, NY), and further incubated in cell culture media for 24 hours. Supernatant was used for cell viability and compared against cell culture media alone. Cells were seeded in a 96-well plate at 2,000 cells per well in 100 μL media. After incubation for 1 hour, the hydrogel-incubated media were added to the wells at various concentrations (0.1 mg/mL, 0.01 mg/mL, and 0.001 mg/mL), in which anti-inflammatory effects were observed. After 24 hours incubation, MTS reagent was added to each well and further incubated for 3 hours at 37 °C, the absorbance was recorded with a microplate reader (Coulter, Boulevard Brea, CA) at λ = 490 nm.

4.3. Results and Discussion

4.3.1. Salicylic acid-based monomer and hydrogel synthesis

As shown in **Figure 4.1**, SAm was successfully synthesized by modifying a previously published procedure.[32] The appearance of the ester IR band at 1732 cm^{-1} and the carboxylic acid IR band at 1690 cm^{-1}, along with alkene stretching at 1643 cm^{-1}, confirmed the occurrence of a successful reaction that did not affect the alkene bond. Following the SAm synthesis, the hydrogels were prepared by UV-initiated free radical polymerization. **Figure 4.1** compares the FT-IR spectra of the SAm and hydrogel systems. In the FT-IR spectrum of the hydrogels, the C=C stretches at 1643 cm^{-1} disappeared, confirming that the itaconic acid and acrylic acid monomers reacted. In addition, the C=O of SAm was shifted in the presence of PEGDA as previously observed.[33] The peak shifting of the hydrogen-bonded functional groups in the FT-IR spectrum suggests possible hydrogen bond formation with PEG.[33] In addition, the characteristic C-O-C stretching of PEG was observed at 1160 cm^{-1}., DSC measurements were performed on hydrogels to confirm the uniformity, showed that T_g values of hydrogels 1 (low cross-linked) and 2 (high cross-linked) were 77°C and 85°C, respectively. T_g values increase with increasing crosslink content, as the hydrogel becomes more rigid.

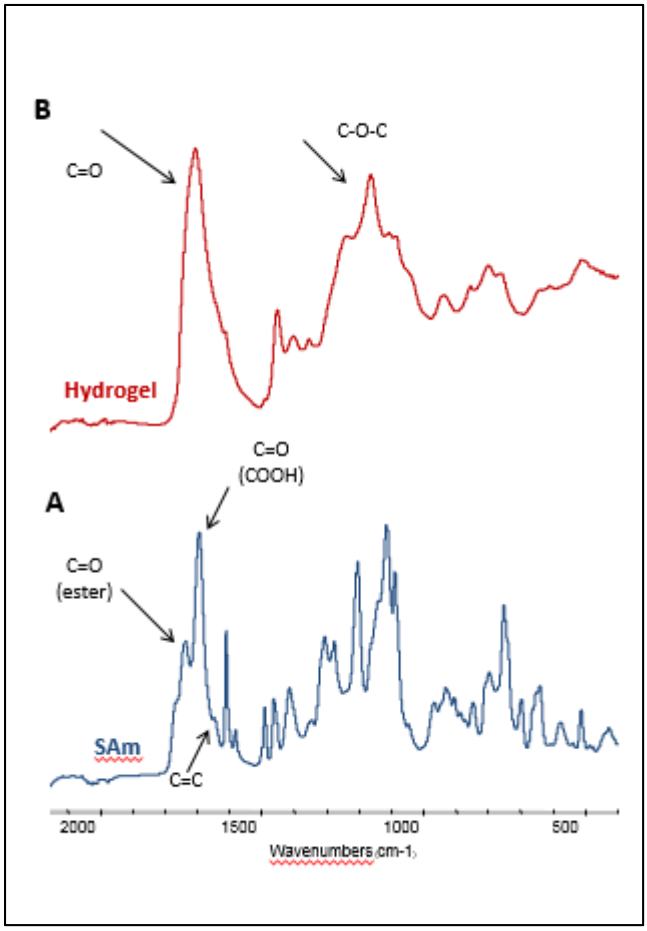

Figure 4.1: FT-IR spectrum of (A) SAm (blue line) and (B) hydrogel system (red line) represented as examples. Key IR bands are labeled on each spectrum. The spectrum at the top is hydrogel 2 (high cross-linked) and is representative of both hydrogel systems.

4.3.2. Swelling behavior

Swelling studies were performed to confirm whether the hydrogels exhibited pH-responsive swelling behavior. The swelling behaviors of hydrogel 1 (low cross-linked) and hydrogel 2 (high cross-linked) were immersed in two different solutions, 0.1 N HCl (pH 1.2) and PBS (pH 7.4), and allowed to swell for 1 and 24 hours at 37°C. None of the gels

significantly swelled in pH 1.2. As shown in **Figure 4.2**, the swelling value of the gels within 24 hours was 0.35 and 0.29 for hydrogels 1 and 2, respectively, at pH 1.2. The pH-dependent properties arise from the polyelectrolyte behavior of the carboxylic acid component: As the pH increases, the hydrogels expand and incorporate water due to the electric repulsion between the ionized carboxylic groups, which increase the ionic swelling force.[34] The swelling value within 24 hours was 9.4 and 4.3 for hydrogels 1 and 2, respectively, in pH 7.4 PBS buffer. Under both conditions, higher crosslinker density yielded lower swelling values. These results followed the same trend as observed for many systems in the literature: Increased cross-linking decreases the swelling percentage due to increasing entanglement, which limits the interchain repulsion and slows media permeation.[33]

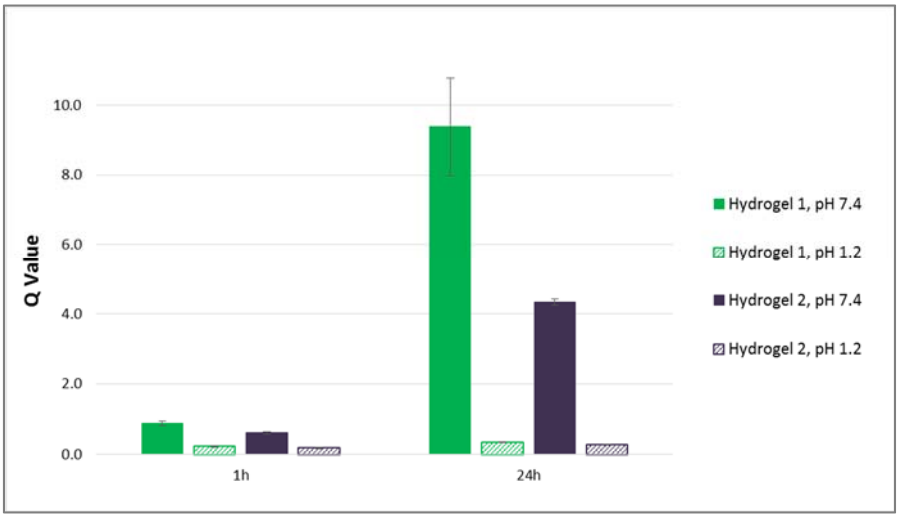

Figure 4.2: Swelling values (Q) values in pH 1.2 and pH 7.4 at 1 h and 24 h time points according to Equation 4.1 for hydrogel 1 (low cross-linked) and hydrogel 2 (high cross-linked). Data are presented as mean ± standard deviation (n=3 in each group).

4.3.3. Hydrogel morphology

Porosity is an important characteristic of hydrogels, as high porosity is beneficial for high drug loading and improved drug release via diffusion.[5,6] Pore structures of these chemically cross-linked hydrogels in the swollen state were examined using SEM. As shown in **Figure 4.3**, all the hydrogel systems exhibited porous structures. However, the pore sizes differ with varying PEGDA and crosslinker concentration: As the concentration of the PEGDA increased, the pore sizes decreased. The effect of crosslink density on pore size was previously observed: Increasing crosslink density decreased pore size.[35] The pore sizes of the hydrogels are 66.7–37.8 μm and 15.6–8.9 μm for hydrogel 1 and hydrogel 2, respectively. The porosity percentage was calculated using ImageJ software, to be 69.6% and 47.4% for hydrogel 1 and hydrogel 2, respectively. Hydrogel pore size was in the same range with previously published work (Chapter 3) on insulin-loaded SA-based physically cross-linked hydrogels.[24] Furthermore, the pore sizes are similar to cross-linked PEG hydrogels, in which avastin, a monoclonal antibody used for colon cancer treatment, was encapsulated and released in a sustained manner.[36] These results suggest that a wide range of different-sized molecules, such as insulin or avastin, can potentially be incorporated into both hydrogel systems.

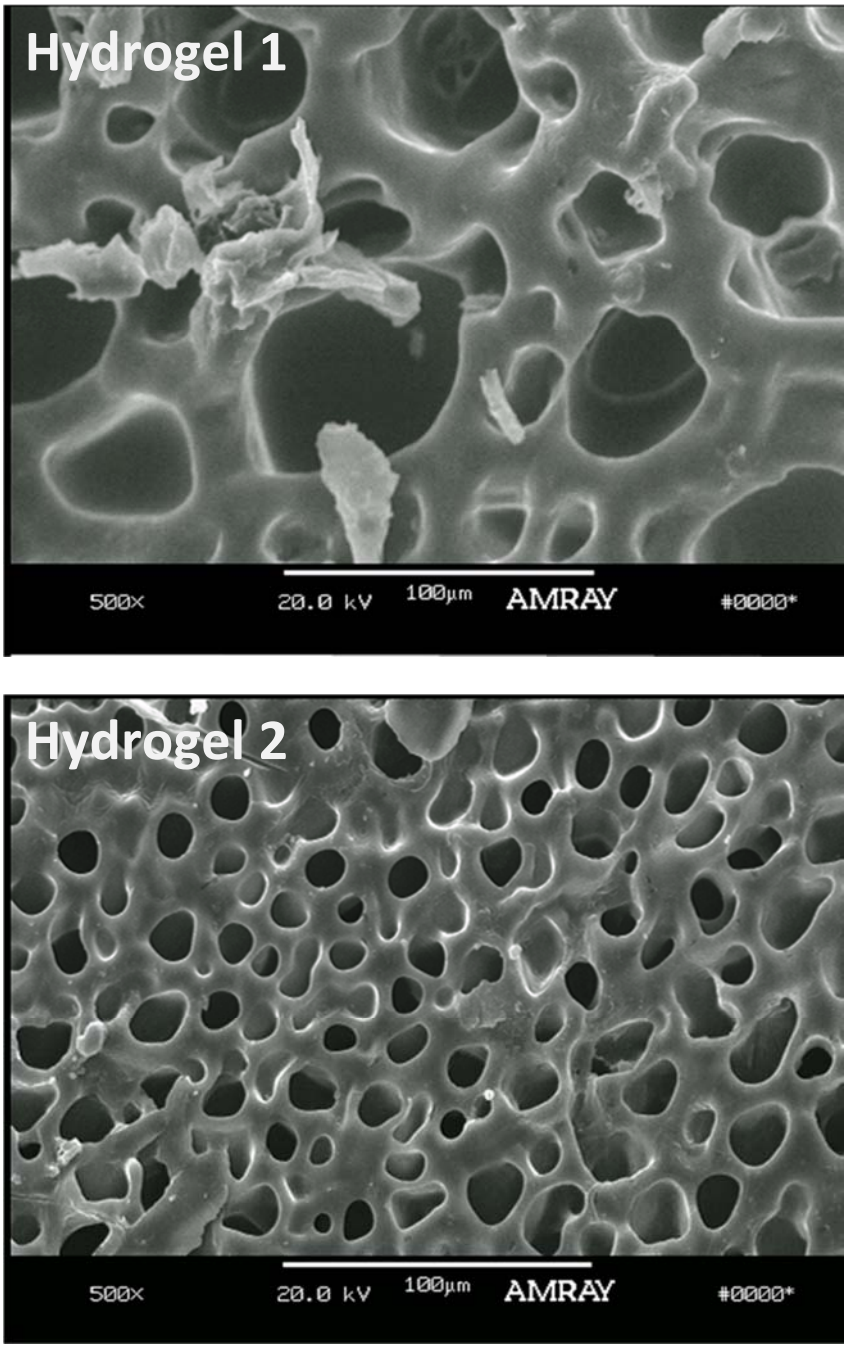

Figure 4.3: SEM images of hydrogel 1 (low cross-linked) and hydrogel 2 (high cross-linked). Hydrogels were swollen in pH 7.4 phosphate buffer for 24 hours at room temperature, and then freeze-dried for 12 hours prior to SEM imaging. Films are shown at 500x magnification.

4.3.4. *In vitro* SA release

To assess *in vitro* SA release from SA-based hydrogels, dry hydrogels were dispersed into 0.1 N HCl (pH 1.2) and pH 7.4 buffer solutions to simulate stomach and intestine and psychological pH conditions, respectively. Hydrogel swelling was observed to directly influence SA release, as higher swelling percentages enabled more water penetration and diffusion into the hydrogel network. As shown in **Figure 4.4**, 100% of the SA was released from hydrogel 1 and hydrogel 2 in pH 7.4 buffer within 24 hours. The SA release rate was slightly slower in hydrogel 2, which correlates to swelling values in the pH 7.4 buffer system. As expected, slower SA release was observed in pH 1.2, with only 30% released over the 24 hour time period and less than 2% over 2 hours. These results revealed that these systems may be beneficial for colon-specific oral delivery. As an orally administered medicine has a 15-60 minute transit time through the stomach,[25] these systems show promise with lower release and swelling values after 60 minutes.

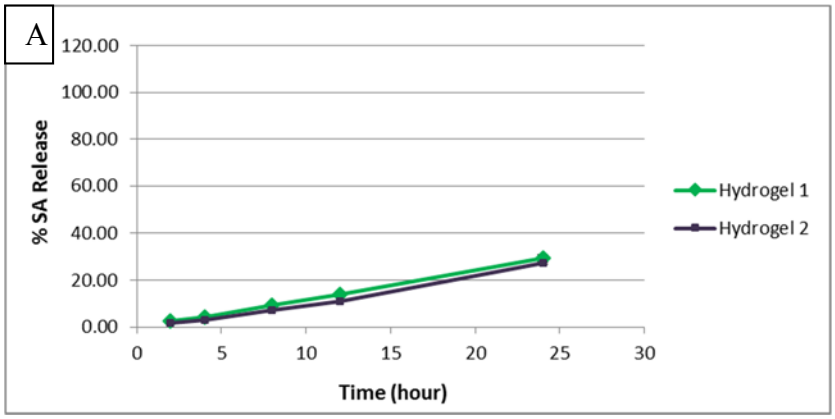

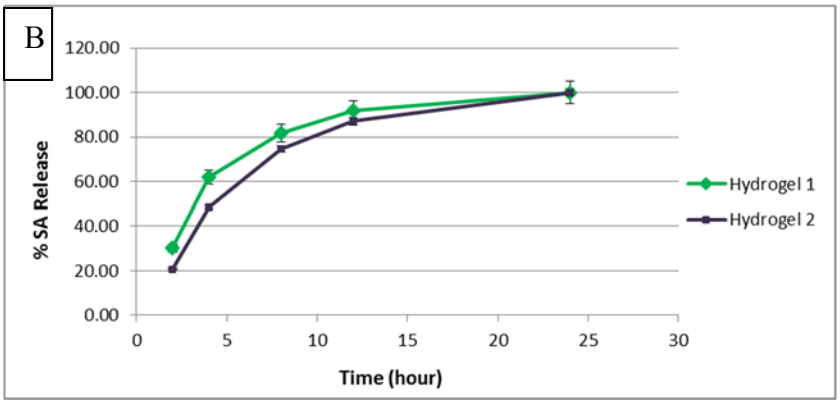

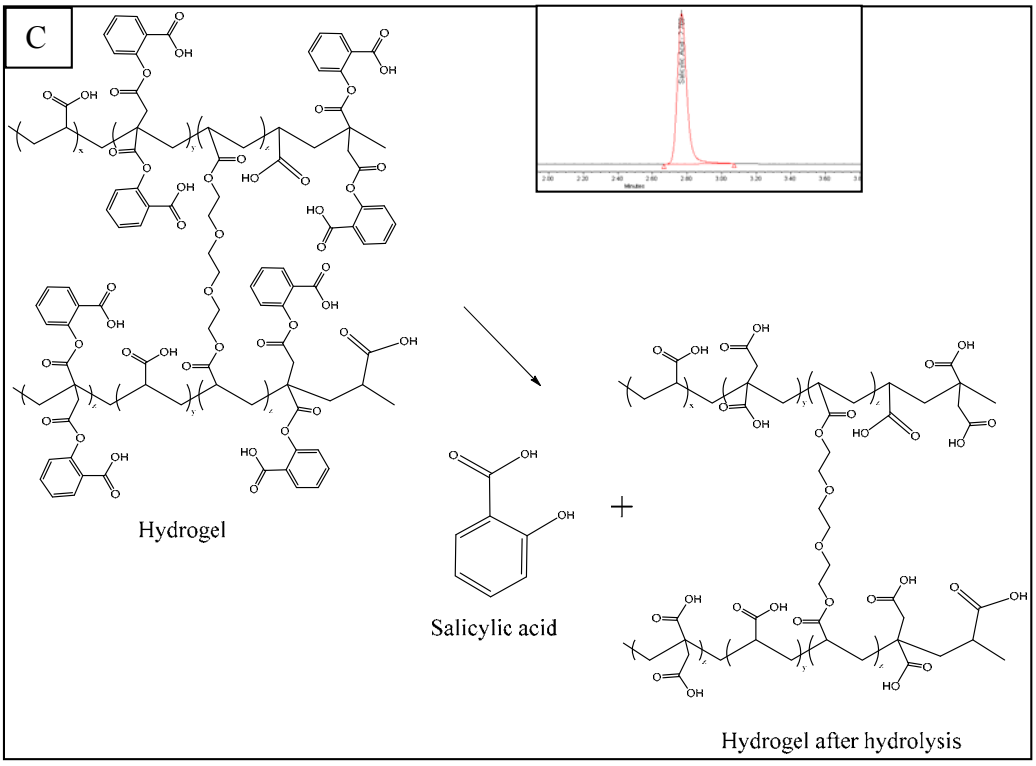

Figure 4.4: *In vitro* release of salicylic acid (SA) from hydrogel 1 (low cross-linked) and hydrogel 2 (high cross-linked) in (A) pH 1.2 and (B) pH 7.4. (C) shows hydrogel degradation into salicylic acid. The inset graph is SA HPLC chromatogram after the hydrolysis. Data in A and B are presented as mean ± standard deviation (n=3 in each group).

4.3.5. Rheology behavior

Rheology is a quick and sensitive method for characterizing the mechanical properties of a hydrogel, providing information about the rigidity, elasticity, and deformability of the sample structure.[37, 38] The energy stored and recovered per cycle of deformation is defined as the storage modulus, G', which is a measure of sample resistance to elastic deformation. Storage modulus G' is representative of the viscoelastic parameter in dynamic oscillatory measurements. The loss modulus, G", records energy loss per cycle and quantifies the viscous component, which shows the lack of structure and the liquid-like material.[39] Another useful parameter is loss tangent (tan δ), which describes the viscoelastic nature of the materials. Loss tangent is the ratio of G"/G' and tan $\delta < 1$ indicates a solid-like, elastic response. Tan δ becomes smaller as viscoelastic behavior increases and the gels become stiffer.

To confirm the gel-like behavior and cross-linked effect, different parameters were evaluated. According to the literature, G' is frequency independent and tan $\delta < 1$ for gels.[40] The SA-based gel showed frequency independent behavior and tan δ was smaller than 1 for both systems. As shown in **Figure 4.5,** the time sweep measurements display a constant storage modulus over time. In addition, the cross-linked effect was similar to literature showing that increasing the cross-link percentage increases the G' value.[41] Moreover, increasing the crosslink percentage decreased tan δ, which means that the hydrogels become stiffer. For both gels, G" was smaller than G'. G' was 16000 and 70000 Pa for hydrogel 1 and hydrogel 2, respectively, while G" was 2000 and 6000 Pa for hydrogel 1

and hydrogel 2, respectively. Compared to physically cross-linked, acrylic acid-based hydrogels (e.g., Carbopol) and chemically cross-linked acrylic acid-based hydrogels, the SA-based, chemically cross-linked hydrogels showed higher G' values, which indicate stiffer, higher viscoelastic behavior.[40, 42] Stiffer gels would be beneficial for drug and protein delivery implants, as they are less sensitive to displacement and can protect protein in the presence of biological fluids.

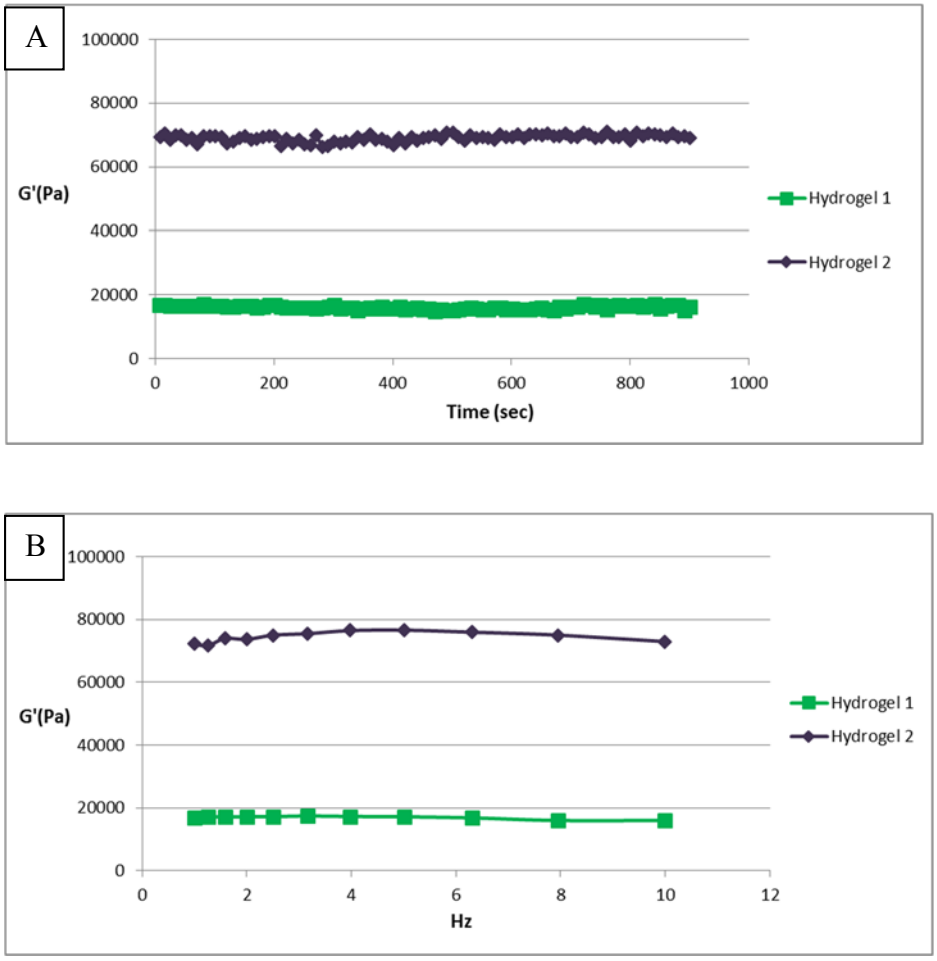

Figure 4.5: Rheological behavior of hydrogel 1 (low cross-linked) and hydrogel 2 (high cross-linked), comparing hydrogels storage modulus, G', in (A) as a function of time at 1 Hz frequency and 1 Pa stress in (B) as a function of frequency at 1 Pa stress.

4.3.6. Mucoadhesion behavior

Mucoadhesive systems such as poly(acrylic acid)-based systems have been extensively studied to increase the permeability of peptides and proteins.[14,16] The maximum detachment force of hydrogel 1 and hydrogel 2 were 133.5 ± 30.7 g and 73.2 ± 12 g, respectively. The work of adhesion of hydrogel 1 and hydrogel 2 were 290.1 ± 73.4 and 219.8 ± 45.6, respectively. The maximum detachment force of both hydrogels were higher than previously published PEG-based acrylic acid hydrogels developed for oral insulin delivery. In addition to mucoadhesion behavior, serum glucose levels in rats of previously published insulin incorporated PEG-based acrylic acid hydrogels were investigated.[43, 44] These systems controlled the blood glucose level in diabetic rats.[44] These results suggest that these SA-based systems may increase bioavailability. Furthermore, increasing crosslink density decreased mucoadhesion strength. The same trend has been reported in the literature.[45]

4.3.7. Cytotoxicity of the hydrogels

Cytotoxicity against 3T3 cells was determined by the MTS assay as a function of three different concentrations in which the anti-inflammatory effect of the SA is observed.

Media was used as control. The results (**Figure 4.6**) indicate that cell viability was not statistically different from the media controls for both gels.

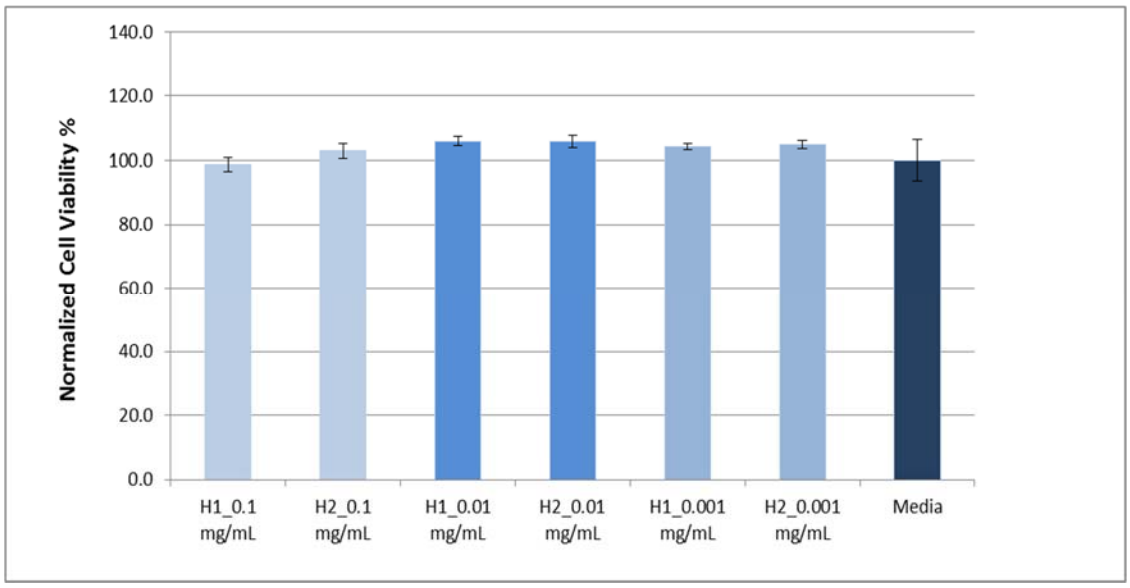

Figure 4.6: Cytotoxicity profile of the different concentrations of the hydrogels after a 24-hour incubation period. Absorbance at 490 nm after MTS treatment is proportional to cell viability. Data are presented as mean ± standard deviation (n=6 in each group). The cell viability of the hydrogels were not statistically different from the media controls.

4.4. Conclusion

Different cross-linking ratios of SA-based hydrogel systems were developed by UV-initiated free radical polymerization. These hydrogel systems exhibited different swelling values depending on the media pH. Swelling values and SA release decreased with increasing cross-linking density. The SA amount and release profile can be further

tuned by increasing salicylic acid-based monomer and by changing crosslinker density. These hydrogel systems showed porous structures, which is beneficial for protein encapsulation and controlled release. In addition, rheological studies proved that these systems are mechanically strong and robust. Moreover, these hydrogel systems also showed good mucoadhesive behaviors, which is important for drug delivery applications. In summary, these hydrogels can deliver SA in a sustained manner and can potentially be used for protein delivery.

4.5. References

1. L.Brannon-Peppas, R.S.Harland. Absorbent polymer technology. Elsevier, 45-66 (1990).

2. N.A. Peppas, A.G.Mikos. Hydrogels in medicine and pharmacy. CRC press, Boca Raton, FL 1, 1-27 (1986).

3. H. Park, K. Park. Hydrogels and biodegradable polymers for bioapplications. American chemical society 627, 2-10 (1996).

4. L. C. Lopérgolo, A. B. , Lugão, L. H. Catalani. Direct UV photocrosslinking of poly(N-vinyl-2-pyrrolidone) (PVP) to produce hydrogels. Polymer 44, 6217-6222 (2003).

5. M. S. Bindu, V.Ashok, A. Chatterjee. As a review on hydrogels as drug delivery in the pharmaceutical field. International Journal of pharmaceutical and chemical sciences 1 (2), 642-661 (2012).

6. N.A. Peppas, Y.Huang, M. Torres-Lugo, J.H. Ward, J. Zhang. Physicochemical foundations and structural design of hydrogels in medicine and biology. Annual review of biomedical engineering 2, 9-29 (2000).

7. H. Omidian, K. Park. Hydrogels. Fundamentals and applications of controlled release drug delivery 4, 75-106 (2012).

8. A. S. Hoffman. Hydrogels for biomedical applications. Advanced drug delivery reviews 64, 18-23 (2012).

9. D.Q. Wu, Y.X.Sun, X.D. Xu, S.X. Cheng, X.Z. Zhang, R.X. Zhuo. Biodegradable and pH-sensitive hydrogels for cell encapsulation and controlled drug release. Biomacromolecules 9, 1155-1162 (2008).

10. P.B. Sutar, R.K.Mishra, K. Pal, A.K. Banthia. Development of pH sensitive polyacrylamide grafted pectin hydrogel for controlled drug delivery system. Journal of materials science: Materials in medicine 19, 2247-2253 (2008).

11. X. Y. Gao, C.L.He, C. S. Xiao, X. L. Zhuang, X. S. Chen. Synthesis and characterization of biodegradable pH-sensitive poly(acrylic acid) hydrogels crosslinked by 2-hydroxyethyl methacrylate modified poly(L-glutamic acid). Materials letter 77, 74-77 (2012).

12. D. Myung, W.U.Koh, J. M. Ko, Y. Hu, M. Carrasco, J. Noolandi, C. N. Ta, C. W. Frank. Biomimetic strain hardening in interpenetrating polymer network hydrogels. Polymer 48, 5376-5387 (2007).

13. D. F. Evans, G.Pye, R. Bramley, A. G. Clark, T. J. Dyson, J. D. Hardcastle. Measurement of gastrointestinal pH profiles in normal ambulant human subjects. Gut 29, 1035-1041 (1988).

14. J. Shaji, V.Patole. Protein and peptide drug delivery: Oral approaches. Indian journal of pharmaceuticals sciences 70, 269-277 (2008).

15. C. M. Lehr. Bioadhesion technologies for the delivery of peptide and protein drugs to the gastrointestinal tract. Critical reviews in therapeutic drug carrier systems 11, 119-160 (1994).

16. J. Renukuntla, A.D.Vadlapudi, A. Patel, S. H. S. Boddu, A. K. Mitra. Approaches for enhancing oral bioavailability of peptides and proteins. International Journal of pharmaceutics 447, 75-93 (2013).

17. K. K. Wu. Aspirin and salicylate: and old remedy with a new twist. Circulation 102, 2022-2023 (200).

18. E. Bastiannet, K.Sampieri, O. Dekkers, A. de Craen. et al. Use of aspiring postdiagnosis improves survival for colon cancer patients. British journal of cancer 106, 1564-1570 (2012).

19. R. S. Hundal, K.F.Peterson, A. B. Mayerson, P. S. Randhawa, S. Inzucchi, S. E. Shoelson, G. Shulman. Mechanism by which high-dose aspirin improves glucose metabolism in type 2 diabetes. Journal of clinical investigation 109, 1321-1326 (2002).

20. M. Nixon, D.J.Wake, D. E. Livingstone, R. H. Stimson, C. L. Esteves, J. R. Seckl, K. E. Chapman, R. Andrew, B. R. Walker. Salicylate downregulates 11B-HSD1 expression in adipose tissue in obese mice and in humans, mediating insulin sensitization. Diabetes 61, 790-796 (2012).

21. R. Yamazaki, N.Kusunoki, T. Matsuzaki, et al. Aspirin and sodium salicylate inhibit proliferation and induce apoptosis in rheumatois synovial cells. Journal of pharmacy and pharmacology 54, 24-32 (2002).

22. R. C. Schmeltzer, T.J.Anastasiou, K. E. Uhrich. Optimized synthesis of salicylate-based poly(anhydride-esters). Polymer bulletin 49, 441-448 (2003).

23. A. S. Prudencio, R. C. Schmeltzer; Uhrich, K. E. Effect of Linker Structure on Salicylic Acid-Derived Poly(anhydride-esters). Macromolecules 38, 6895-6900 (2005).

24. B. Demirdirek, K.Uhrich. Salicylic acid-based pH-sensitive hydrogels as potential oral insulin delivery systems. Journal of drug targeting (2015).

25. E. Henin, M.Bergstrand, J. Standing, M. O. Karlsson. A mechanism-based approach for absorption modeling: the gastro-intestinal transit time (GITT) model. The AAPS journal 14, 150-163 (2012).

26. D. Mudie, G.Amidon, G. Amidon. Physiological parameters for oral delivery and in vitro testing. Molecular pharmaceutics 7, 1388-1405 (2010).

27. K. Nakamura, R.Murray, J. Joseph, N. Peppas, M. Morishita, A. Lowman. Oral Insulin delivery using P(MAA-g-EG) hydrogels: Effect of network morphology on insulin delivery characteristics. Journal of controlled release, 589-599 (2004).

28. X. Gao, Y.Cao, X. Song, Z. Zhang, C. Xiao, C. He, X. Chen. pH and thermo-responsive poly(N-isopropylacrylamide-co-acrylic acid derivative) copolymers and hydrogels with LCST dependent on pH and alkyl side groups. Journal of materials chemistry B 1, 5578-5587 (2013).

29. L. Yin, L.Fei, F. Cui, C. Tang, C. Yin. Superporous hydrogels containing poly(acrylic acid-co-acrylamide)/ O-carboxymethyl chitosan interpenetrating polymer networks. Biomaterials 28, 1258-1266 (2007).

30. X. Xu, Y.Shen, W. Wang, C. Sun, C. Li, Y. Xiong, J. Tu. Preparation and in vitro characterization of thermosensitive and mucoadhesive hydrogels for nasal delivery of phenylephrine hydrochloride. European journal of pharmaceutics and biopharmaceutics 2014, 998-1004 (2014).

31. E. Hagesaether, S.A.Sande. In vitro measurements of mucoadhesive properties of six types of pectin. Drug development and industrial pharmacy 33, 417-425 (2007).

32. R. C. Schmeltzer, T.J.Anastasiou, K.E. Uhrich. Optimized synthesis of salicylate-based poly(anhydride-esters). Polymer bulletin 49, 441-448 (2003).

33. T. Betancourt, J.Pardo, K. Soo, N. Peppas. Characterization of pH responsive hydrogels of poly(itaconic acid-g-ethylene glycol) prepared by Uv-initiated free radical polymerization as biomaterials for oral delivery of bioactive agents. Journal of biomedical materials research part A, 175-188 (2009).

34. Y. Qiu, K. Park. Enviromental-sensitive hydrogels for drug delivery. Advanced drug delivery reviews 64, 49-60 (2012).

35. K. Watkins, R.Chen. pH-responsive, lysine-based hydrogels for the oral delivery of a wide size range of molecules. International journal of pharmaceutics 478, 496-503 (2015).

36. J. Yu, X.Xu, F. Yao, Z. Luo, L. Jin, B. Xie, S. Shi, H. Ma, X. Li, H. Chen. In situ covalently cross-linked PEG hydrogel for ocular drug delivery applications. International journal of pharmaceutics 470, 151-157 (2014).

37. K. S. Anseth, C.N.Bowman, L. Brannon-Peppas. Mechanical properties of hydrogels and their experimental determination. Biomaterials 17, 1647-1657 (1996).

38. J. M. Zuidema, C.J.Rivet, R. J. Gilbert, F. A. Morrison. A protocol for rheological characterization of hydrogels for tissue engineering strategies. Journal of biomedical materials research part a 102, 1063-1073 (2014).

39. F. Madsen, K.Eberth, J.D. Smart. A rheological examination of the mucoadhesive/mucus interaction, the effect of the mucoadhesive type and concentration. Journal of controlled release 50 (1998).

40. G. Bonacucia, S.Martelli, G. F. Palmieri. Rheological, mucoadhesive and release properties of carbopol gels in hydrophilic cosolvents. International journal of pharmaceutics 282, 115-130 (2004).

41. H. Jiang, W.Su, P.T. Mather, T.J. Bunning. Rheology of highly swollen chitosan/polyacrylate hydrogels. Polymer 40, 4593-4602 (1999).

42. D. M. Devine, C.L.Higginbotham. Synthesis and characterisation of chemically crosslinked N-vinyl pyrrolidinone (NVP) based hydrogels. European polymer journal 41, 1272-1279 (2005).

43. N. A. Peppas. Devices based on intelligent biopolymers for oral protein delivery. International journal of pharmaceutics 277, 11-17 (2004).

44. M. Morishita, T.Goto, K. Nakamura, A. Lowman, K. Takayama, N. Peppas. Novel oral insulin delivery systems based on complexation polymer hydrogels: single and

multiple administration studies in type 1 and 2 diabetic rats. Journal of controlled release 110, 587-594 (2006).

45. H. Park, J.R.Robinson. Mechanisms of mucoadhesion of poly(acrylic acid) hydrogels. Pharmaceutical research 4, 457-464 (1987).

5. FUTURE WORK

In Chapter 4, salicylic acid was chemically incorporated to develop cross-linked hydrogels systems. These systems were developed as pH-sensitive systems to deliver intestine-targeted proteins or the small molecule, SA; these systems could deliver SA within 24 hours.

As previously described, SA is an anti-inflammatory agent that may be used to prevent diseases such as cancer[1] and diabetes[2]. The active compounds, currently used to cure these diseases can be physically incorporated and delivered in combination with SA. Insulin, the main protein given to diabetes patients, can be incorporated to SA-based chemically cross-linked hydrogels via the swelling-diffusion technique described in **Section 3.2**.[3] In addition to swelling-diffusion technique, alternative published procedures[4, 5] can be used to incorporate insulin. For example, monomers (SA-based diacid and acrylic acid), crosslinker, (poly(ethylene glycol)-diacrylate), and initiator (irgacure) could be dissolved in acetone:water mixture along with a small amount of insulin solution (80μL of 20 mg/mL). The mixture could be poured into teflon beaker and cross-linked under nitrogen. Cross-linking time may be shortened to the possible effect of UV light on proteins. Insulin and SA-based monomer amount can be adjusted according to desire dosage.

As a second project, SA has shown promising results in colon cancer treatment. Capecitabine is one of the active compounds used for treating colon cancer. [6] Capecitabine can be incorporated into hydrogel systems via the two techniques described for insulin incorporation and then delivered specifically to the colon for treatment. As shown in

Chapter 4, these hydrogels systems behave differently in stomach-simulated pH (pH 1.2) and intestine-simulated pH (pH 7.4) conditions. These results suggested that the systems can be used for colon specific delivery.

Third, SA release can be extended in chemically cross-linked hydrogel systems using alternative synthesis techniques using the synthesis proposed below, **Scheme 6.1**. Briefly, diacid synthesis can be followed by solution polymerization, and then cross-linked using poly(ethylene glycol)-diacrylate. Extended release (i.e., longer than 24 h) can be achieved using these systems for tissue engineering and wound dressing applications.

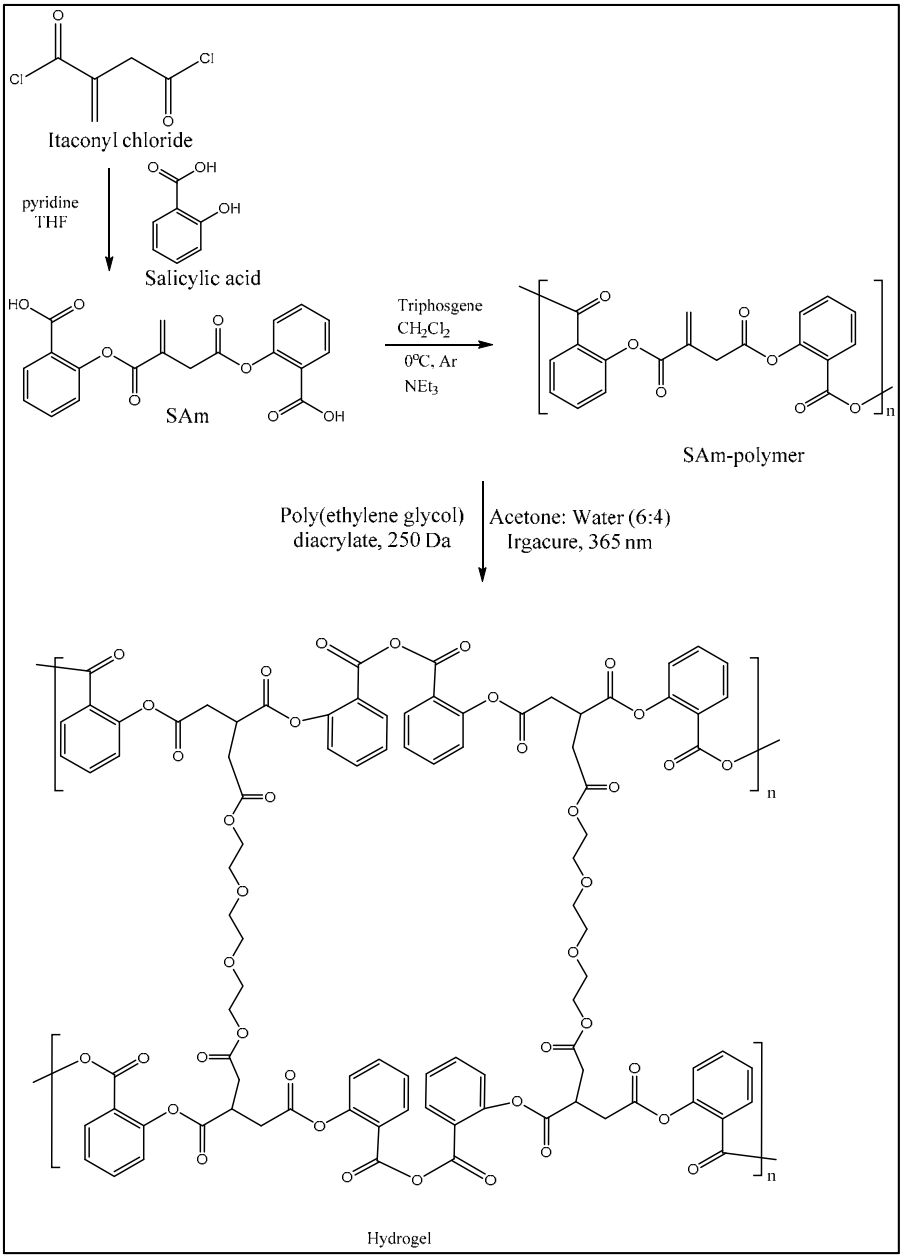

Scheme 5.1: Suggested synthesis scheme of chemically cross-linked extended SA release hydrogel system.

Fourth, chemically cross-linked SA-based injectable hydrogel systems can be developed using SAm diacid. Briefly, these SAm can be combined with NIPAM monomer

and then cross-linked via low percentage of cross-linked, poly(ethylene glycol)-diacrylate and SAm. A proposed synthetic scheme is shown in **Scheme 6.2**.

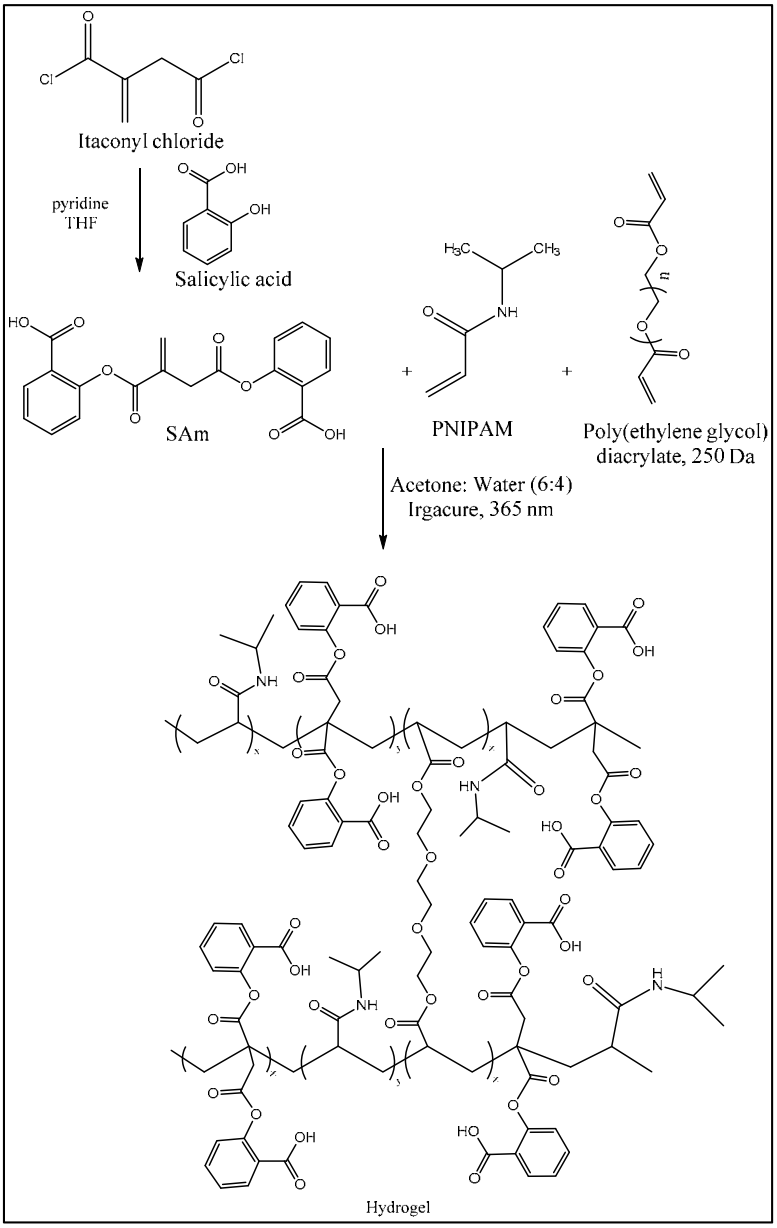

Scheme 5.2: Suggested synthesis scheme of chemically cross-linked temperature-sensitive hydrogel system.

Physically cross-linked pH sensitive hydrogel systems are discussed in Chapter 3. Insulin was successfully incorporated into hydrogel system and could like be protected in GI-mimicking conditions. Further, insulin, physical and chemical stability was evaluated using SEC and iCIEF, respectively. The results showed that insulin was stable after releasing from hydrogel systems. Furthermore, these systems showed promising mucoadhesion behavior. Literature shows that mucoadhesive systems improve protein bioavailability[7] and often contain acrylic acid and/or itaconic acid to yield promising results. [8-10] As an example, acrylic acid-based insulin incorporated systems were evaluated in diabetic rats and shown to lower glucose levels.[11, 12] Salicylic acid-based physically cross-linked hydrogels should be evaluated *in vivo* after incorporating insulin. The following published procedure can be used to evaluate *in vivo* behavior of insulin incorporated pH-sensitive hydrogel systems. Briefly, male rats will be injected with streptozotocin (40 mg/kg body weight) once daily for 3 days to achieve diabetic conditions, which should be confirmed by checking glucose levels. Once the diabetic conditions are achieved, hydrogels can be placed in a gelatin capsule and orally administered to rats at 50 IU/kg of animal body weight. Blood samples should be taken at specific times over 24 h to analyze glucose levels, which can be measured via glucose oxidase kit.[11]

Fifth, in chapter 2, BSA was incorporated as a model compound into temperature-sensitive hydrogel systems. These systems are unique as they have extended SA and BSA release profiles. Other active compounds such as insulin should be incorporated into these systems and the release profiles evaluated. Furthermore, *in vivo* studies should be performed to evaluate combination delivery of SA and insulin in diabetic's rats.

5.1. References

1. E. Bastiannet, K.Sampieri, O. Dekkers, A. de Craen. et al. Use of aspiring postdiagnosis improves survival for colon cancer patients. British journal of cancer 106, 1564-1570 (2012).

2. G. Jiang, Q.D.Yang, F. Liu, D.vMoller, B. Zhang. Salicylic acid reverses phorbol 12-myristate-13-acetate (PMA)- and tumor necrosis factor alpha (TNFalpha)-induced insulin receptor substrate 1 (IRS1) serine 307 phosphorylation and insulin resistance in human embryonic kidney 293 (HEK293) cells. Journal of biological chemistry 278, 180-6 (2003).

3. B. Demirdirek, K.Uhrich. Salicylic acid-based pH-sensitive hydrogels as potential oral insulin delivery systems. Journal of drug targeting (2015).

4. J. Jansen, M.Tibbe, G. Mihov, J. Feijen, D. Grijpma, . Photo-crosslinked networks prepared from fumaric acid monoethyl ester-functionalized poly(D,L-lactic acid) oligomers and N-vinyl-2-pyrrolidone for the controlled and sustained release of proteins. Acta biomaterialia 8, 3652-3659 (2012).

5. R. Censi, T.Vermonden, M.J. van Steenbergen, H. Deschout, K. Braeckmans, S.C. De Smedt, C.F. van Nostrum, P.di Martino, W.E. Hennink. Photopolymerized thermosensitive hydrogels for tailorable diffusion-controlled protein delivery. Journal of controlled release 140, 230-236 (2009).

6. C. Twelves, A.Wong, M. Nowacki, M. Abt, H. Burris, A. Carrato, J. Cassidy, A. Cervantes, J. Fagerberg et al. Capecitabine as adjuvant treatment for stage III colon cancer. The new england journal of medicine 352, 2696-2704 (2005).

7. J. Renukuntla, A.D.Vadlapudi, A. Patel, S. H. S. Boddu, A. K. Mitra. Approaches for enhancing oral bioavailability of peptides and proteins. International journal of pharmaceutics 447, 75-93 (2013).

8. H. Park, J.R.Robinson. Mechanisms of mucoadhesion of poly(acrylic acid) hydrogels. Pharmaceutical research 4, 457-464 (1987).

9. C. Eouani, P.Piccerelle, P. Prinderre, E. Bourret, J. Joachim. In-vitro comparative study of buccal mucoadhesive performance of different polymeric films. European journal of pharmaceutics and biopharmaceutics 52, 45-55 (2001).

10. T. Betancourt, J.Pardo, K. Soo, N. Peppas. Characterization of pH responsive hydrogels of poly(itaconic acid-g-ethylene glycol) prepared by Uv-initiated free radical polymerization as biomaterials for oral delivery of bioactive agents. Journal of biomedical materials research part A, 175-188 (2009).

11. A. Foss, T.Goto, M. Morishita, N. Peppas. Development of acrylic-based copolymers for oral insulin delivery. European journal of pharmaceutics and biopharmaceutics 57, 163-169 (2004).

12. M. Morishita, T.Goto, K. Nakamura, A. Lowman, K. Takayama, N. Peppas. Novel oral insulin delivery systems based on complexation polymer hydrogels: single and multiple administration studies in type 1 and 2 diabetic rats. Journal of controlled release 110, 587-594 (2006).

6. APPENDIX 1: CYTOCOMPATIBILITY STUDIES OF KOJIC ACID-BASED POLY(ANHYDRIDE-ESTERS)

6.1. Introduction

Melanogenesis is a process which occurs inside the epidermal later of the skin cells and produce a dark pigment called melanin.[1] Extensive level of melanin pigmentation cause hyperpigmentation, which is usually seen in elderly people.[1] Hyperpigmentation can be prevented using tyrosinase enzyme inhibitors and the antityrosinase agent, kojic acid, has been used for skin-lightening applications.[2, 3] In this research, kojic-acid based polymers were synthesized for extended release.

Kojic acid-based poly(anyhdride esters) shown in ***Figure 5.1*** *were synthesized by Jonathan Faig.*

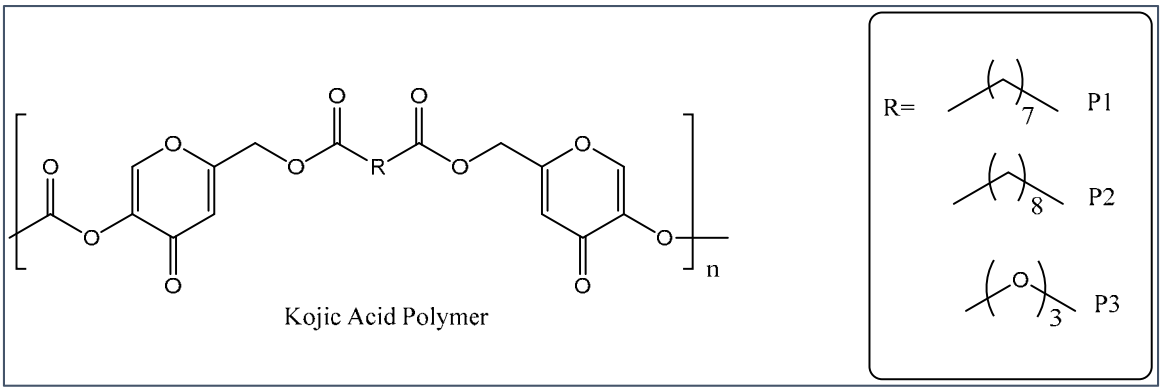

Figure 6.1: Kojic acid-based poly(anhydride-esters)

6.2. Cytotoxicity: Method

Kojic acid polymer cytocompatibility was performed by culturing 3T3 mouse fibroblast cells in polymer-containing media. Three different polymers were first sterilized under UV at 254 nm for 900 s (Spectronics Corporation, Westbury, NY), then dissolved in DMSO as a stock solution to yield 10 mg/mL and serially diluted to 0.1 mg/mL, 0.01 mg/mL and 0.001 mg/mL with cell culture media. Cell culture media consisted of Dulbecco's Modified Eagle's Medium (DMEM), 10 % v/v fetal bovine serum, 1 % L-glutamate and 1 % penicillin/streptomycin. The cells were seeded in 96-well plate at 2,000 cells per well in 100 μL media. After incubation for 1 h, the polymer-containing media at various concentrations were added to wells. The media with dissolved polymer was compared to DMSO-containing media (1 % v/v). For the fibroblasts, cell viability was determined by using MTS (3-(4,5-dimethylthiazol-2-yl)-5-(3-carboxymethoxyphenyl)-2-(4-sulfophenyl)-2H-tetrazolium) assay. After 24 h, 48 h, and 72 h incubation, MTS reagent was added to each well and further incubated for 3 hours at 37 °C, the absorbance was recorded with a microplate reader (Coulter, Boulevard Brea, CA) at λ = 490 nm.

6.3. Cytotoxicity: Results

Cytocompatibility was tested *in vitro* by the MTS assay using 3T3 cells was determined as a function of three different concentration of the polymer solution, 0.1 mg/mL, 0.01 mg/mL and 0.001 mg/mL. As shown **Figure 5.2**, cell viability was not

statistically different from the DMSO controls at the concentrations in which a therapeutic effect was observed (0.01 mg/mL and 0.001 mg/mL).

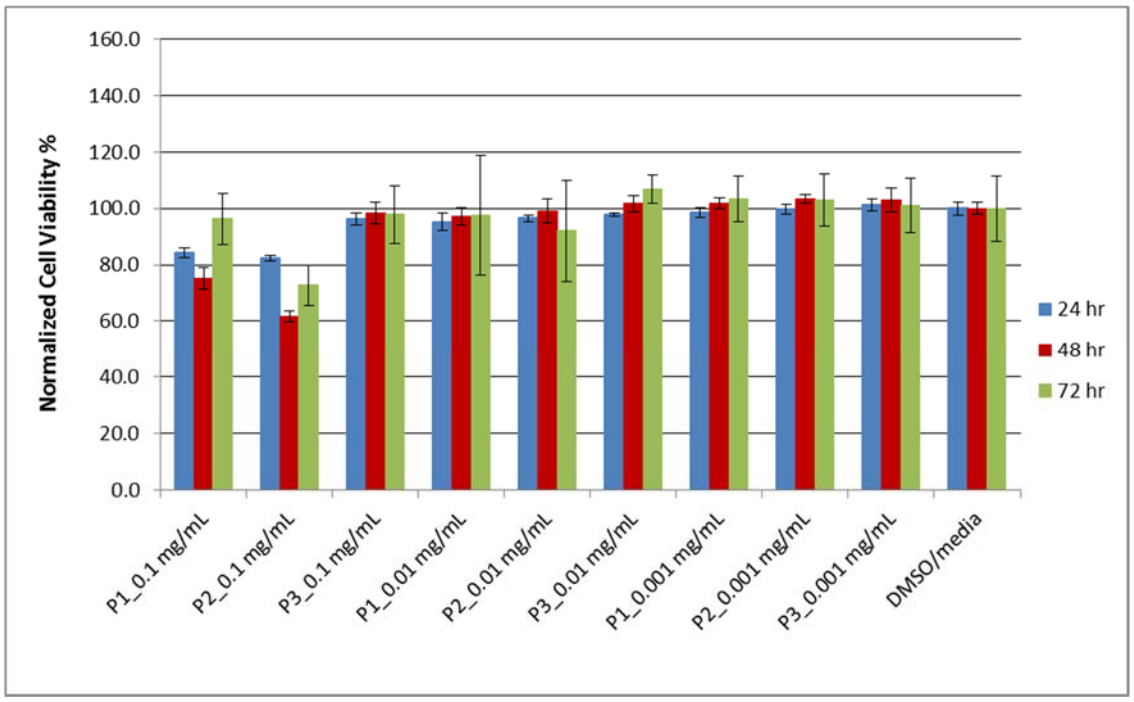

Figure 6.2: Cytotoxicity profile of the different concentrations of the hydrogels after 24 h, 48 h and 72 h incubation. Absorbance at 490 nm after MTS treatment is proportional to cell viability. Data presented as mean ± standard deviation, n=6 in each group.

6.4. References

1. M. L. Gonçalez, M.A.Correa, M. Chorilli. Skin delivery of kojic acid-loaded nanotechnology-based drug delivery systems for the treatment of skin aging. Biomedical research international 2013, 1-9 (2013).

2. M. D. Aytemir, G.Karakaya. Kojic acid derivatives. Medicinal chemistry and drug design (2012).

3. T. Raku, Y.Tokiwa. Regioselective synthesis of kojic acid esters by bacillus subtilis protease. Biotechnology letters 25, 969-974 (2003).

7. APPENDIX 2: PHYSICALLY CROSSLINKED SALICYLIC ACID-BASED POLY(*N*-ISOPROPYLACRYLAMIDE-*CO*-ACRYLIC ACID) HYDROGELS INJECTABILITY

7.1. Method and Results

Injectability test performed using a previously published procedure.[1] BSA, model protein was loaded to PN:SAPAE hydrogels using the procedure discussed in **Chapter 2**. 10 mg of BSA-loaded PN:SAPAE gels were ground and placed in 10 mL of PBS buffer and incubated at 5 ˚C for 2 h. After 2 h, 2 mL of the formulation was transferred to 5 mL syringe with 22 gauge needle and placed in syringe pump and set at a rate of 2.0 mL for 1h. The amount of formulation dropped from syringe was collected in graduate cylinder.

The amount of water was measured using graduate cylinder, both of the hydrogel systems (7:3 and 6:4 PN:SAPAE hydrogels) were delivered 1.9 ± 0.1 mL of formulation within 1h. These results suggest that these systems can be used as injectable.

7.2. Reference

1. D. F. Driscoll P. Ling, B. R. Bistrian: Physical stability of 20% lipid injectable emulsions via simulated syringe infusion: Effects of glass vs plastic product packaging. Journal of parenteral and enteral nutrition 31, 148-153 (2007).

8. COPYRIGHT PERMISSION

11/9/2015 Rightslink® by Copyright Clearance Center

Copyright Clearance Center RightsLink®

Home | Create Account | Help | Live Chat

informa healthcare

Title: Salicylic acid-based pH-sensitive hydrogels as potential oral insulin delivery systems

Author: Bahar Demirdirek, Kathryn E. Uhrich

Publication: Journal of Drug Targeting

Publisher: Taylor & Francis

Date: Sep 14, 2015

Copyright © 2015 Taylor & Francis

LOGIN

If you're a copyright.com user, you can login to RightsLink using your copyright.com credentials. Already a RightsLink user or want to learn more?

Thesis/Dissertation Reuse Request

Taylor & Francis is pleased to offer reuses of its content for a thesis or dissertation free of charge contingent on resubmission of permission request if work is published.

BACK CLOSE WINDOW

Copyright © 2015 Copyright Clearance Center, Inc. All Rights Reserved. Privacy statement, Terms and Conditions.
Comments? We would like to hear from you. E-mail us at customercare@copyright.com

https://s100.copyright.com/AppDispatchServlet#formTop 1/1